TREE MORTALITY AND DECOMPOSITION DYNAMICS FOLLOWING AN EXTREME DROUGHT IN EAST TEXAS, USA

A Dissertation

by

PAUL ALAN KLOCKOW

Submitted to the Office of Graduate and Professional Studies of
Texas A&M University
in partial fulfillment of the requirements for the degree of

DOCTOR OF PHILOSOPHY

Chair of Committee,	Jason G. Vogel
Co-Chair of Committee,	Georgianne W. Moore
Committee Members,	Christopher B. Edgar
	Sorin C. Popescu
	David M. Cairns
Head of Department,	G. Cliff Lamb

August 2019

Major Subject: Ecosystem Science and Management

Copyright 2019 Paul Klockow

ABSTRACT

Throughout 2011, the state of Texas, USA, experienced an extreme drought that broke statewide temperature and precipitations records, causing extensive tree mortality. No study comprehensively examined impacts to the heavily forested and important economic and ecologic region of east Texas. This dissertation aimed to fill that knowledge gap by: 1) examining tree species mortality responses multiple years post-drought; 2) evaluating the impacts of management and stand structure on pine species mortality; 3) quantifying and describing the dynamics of standing dead trees; and 4) refining understanding and estimation of structural volume changes in standing dead pine trees using terrestrial light-detection-and-ranging (LiDAR). The first three objectives made use of U.S. Forest Service Forest Inventory and Analysis data for east Texas. The final objective was accomplished using LiDAR and a novel volume calculation algorithm.

Oak species experienced significant immediate mortality, presumably crossing a threshold by which they could not continue transpiring. Pine species mortality was the lowest of all examined and did not increase significantly until two years post-drought, suggesting pines successfully employed physiological strategies to avoid rapid mortality. Planted loblolly pines were generally maintained at lower densities and moderate tree sizes than naturally-regenerated loblolly and shortleaf pines. This management effect appeared to offer favorable competitive conditions allowing planted loblolly pine to resist drought mortality. Standing dead trees experienced high probability of falling

within five-years, driven primarily by stem size and decay class. Reconstructed standing dead tree volumes derived from LiDAR produced robust allometric models for volume estimation and provided for empirical assessment of structural changes across decay classes.

These findings highlight the resistant nature of managed pines to extreme drought mortality and the vulnerability of oaks to die-off in future extreme droughts. Future work should strive to identify the physiological mechanisms driving drought mortality and specific silvicultural targets for mitigating extreme drought mortality. Biomass and carbon that transitions to the standing dead wood pool following mortality becomes downed dead wood very rapidly in east Texas. Tools developed herein for predicting fall rates and quantifying standing dead wood via LiDAR will help to refine future understanding of carbon dynamics, wildfire risk, and habitat management.

DEDICATION

I dedicate this dissertation to my parents and family for your love, support, humor, and for that trip out West in 1992.

ACKNOWLEDGEMENTS

I would like to thank my committee co-chairs, Dr. Jason G. Vogel and Dr. Georgianne W. Moore. I am truly grateful for the support and opportunities you provided to me throughout my four years at Texas A&M, from being a sounding board for ideas to funding my way to various workshops and conferences all of which helped me grow professionally and personally. I'll never forget the first time I spoke with you about this position over the phone. I was at a coffee shop in Laramie, Wyoming taking a break from my job. At one point, you asked me what the weather was like and I said something like, '*Really* nice.' (that being dry and cool), not realizing the drastic change in climate I would experience moving to Texas…which was likely insinuated by asking me that question. I am grateful for the opportunity to pursue this Ph.D. and to experience life in Texas. Even though I still greatly miss life in Wyoming, I've come a long way since that phone call and have even come to appreciate aspects of the warm, humid, sunny climate in the Brazos Valley.

Thanks to Dr. Christopher B. Edgar for your patience and expert guidance in helping me understand forest resources and their associated quantitative tools. Thanks also to Dr. Sorin C. Popescu for your support and direction in all things remote sensing. Finally, thanks to Dr. David M. Cairns for agreeing to support my research and pursuit of a Ph.D. and for your expertise in applied statistics and great sense of humor. I am grateful to all of my committee for being approachable and for your down-to-earth attitudes which ultimately helped me remain focused on completing my degree.

I am grateful to my lab mates and field technicians over the last four years, Taylor Wilson, Marco Minor, Ignacie Tumushime, Yang Zhang, Trevor Reed, Luiza Aparecido, Caitlyn Cooper, Rosaleen March, Amelia Min-Venditti, Ajinkya Deshpande, Austin Zen, Aaron Trimble, Ashley Cross, Chris Adkison, Aline Jaimes, Tan Zhou, Eric Putman, Lana Narine, Jake Gaster, Chase Brooke, Kathryn Benson, and Sascha Lodge. I would also like to thank Rachel Short, Jeff Martin, Rachel Adams, Vincent Adams, Samantha Gaster, Hsiao-Hsuan 'Rose' Wang, Ryan Mushinski, Yong Zhou, and Ayumi Hyodo for your guidance, friendship, and humor. You've all been immensely helpful in many ways and I'm grateful to have had the chance to overlap with you at Texas A&M.

I am extremely thankful for folks from the Texas A&M Forest Service, particularly Jordy Nelson, Crockett Pagoda, and Justin Branch, as well as with the U.S. Forest Service Sam Houston National Forest, Warren Oja and Justin Seaborn, for your help with field activities including felling dead trees and allowing access to standing dead trees for this work. Additionally, this dissertation would not be possible without the continued efforts of the U.S. Forest Service Forest Inventory and Analysis program for collecting, managing, and making available immensely useful and relevant forest inventory data. I am extremely grateful to Dr. Michelle Masuda with the National Oceanic and Atmospheric Administration (NOAA) and Dr. Denis Valle at the University of Florida for your assistance with helping me understand Bayesian analyses.

I want to extend sincere thanks to the Department of Ecosystem Science and Management faculty, staff, and graduate students for your efforts and time spent helping me through my program. In particular, I'd like to thank Dr. David Briske, Dr. Bill

Rogers, Dr. Katy Kavanagh, Dr. Tom Boutton, Dr. X. Ben Wu, and Dr. Joe Veldman for your support during my time as co-chair of the seminar committee and also for being great people. You've all lent a friendly ear to hear my stories and deal with my questions and struggles and made me feel like a true colleague and friend.

I want to acknowledge folks from my recent past who truly helped prepare me for the rigors of a Ph.D. program and allowed me to hit the ground running when I started in June 2015. Specifically, I want to thank Dr. Tony D'Amato and Dr. John Bradford for giving me a chance to begin grad school as a M.S. student and for building the foundation for my success in research. I would also like to thank my supervisors, co-workers, and colleagues at Western Ecosystems Technology, Inc., where I held a position prior to beginning my Ph.D. program, for giving me the opportunity to strengthen and explore my technical skills and abilities.

Even though they may never see my thesis, I want to thank Rob and Rachel Goyen and the trail running community they support through their group Trail Racing Over Texas (TROT). It has been an absolute pleasure to partake in your trail races as a runner and volunteer and to meet the inspirational people that are part of the trail running community. You've helped me appreciate the beauty of the Texas landscape by getting me to visit places I may never have and, through your positive encouragement of running and pushing oneself, I've learned so much about what I can achieve and also how to clear my mind and appreciate the little things.

I am continually amazed at the unwavering support given to me by my parents, Jayne and Roland Klockow and my immediate family, Laura, Daniel, and Keira Black

and Jessie, Andy, and Olivia Hardy. You've inspired me, encouraged me to explore, helped feed my curiosity for how things work, and always have been there to listen and share a hearty laugh. I truly can't thank you enough for your love and support.

I thank my wife Sascha for always being by my side and being my best friend. I am so grateful to have you on this journey through my Ph.D. program as a friend and advisor, having gone through the process yourself. I could not have been as successful as I've been without your love and support. Thank you for coming with me to Wyoming, Texas (getting married in San Antonio), and wherever our next adventures take us. The same goes for my dog and true pal, Elwood Blues. Thanks for getting me off the couch and outdoors to play.

I want to offer thanks to God for all the blessings in my life, those being everyone mentioned above. I never thought I'd reach this milestone and I couldn't have done it without curiosity, strength, love, and faith provided through all my family, friends, colleagues, and life experiences.

CONTRIBUTORS AND FUNDING SOURCES

Contributors

This work was supervised by a dissertation committee consisting of Dr. Georgianne W. Moore (advisor) of the Department of Ecosystem Science and Management, Dr. Jason G. Vogel (co-advisor) of the School of Forest Resources and Conservation at the University of Florida, Dr. Sorin C. Popescu of the Department of Ecosystem Science and Management, Dr. Christopher B. Edgar of the Department of Forest Resources at the University of Minnesota, and Dr. David M. Cairns of the Department of Geography.

All work was designed in part by Paul Klockow, Dr. Jason G. Vogel, Dr. Georgianne W. Moore, Dr. Sorin C. Popescu, and Dr. Christopher B. Edgar. Paul Klockow conducted the field work, lab and data analyses, data interpretation, and writing of this dissertation. Dr. Christopher B. Edgar conducted a portion of data analyses for Chapter II and Eric B. Putman conducted a portion of the field work and data processing for Chapter V. Dr. Jason G. Vogel, Dr. Georgianne W. Moore, Dr. Christopher B. Edgar, Dr. Sorin C. Popescu, and Dr. David M. Cairns all provided feedback and advice.

Funding Sources

Paul Klockow was supported in part by a Graduate Merit Fellowship (2015-2019) from the Office of Graduate and Professional Studies at Texas A&M University, the National Aeronautics and Space Administration Rapid Response and Novel Research

in Earth Science program (grant number NNX14AN99G) (2015-2018), and a teaching assistantship (2018-2019) from the Department of Ecosystem Science and Management. The contents of this study are solely the responsibility and creation of the authors and do not necessarily represent the official views of the National Aeronautics and Space Administration.

TABLE OF CONTENTS

Page

LIST OF FIGURES

Page

LIST OF TABLES

CHAPTER I

INTRODUCTION

Globally, forests are expected to experience greater levels of tree mortality with increasing temperatures from climate change (Allen *et al.*, 2010) and may already be experiencing and responding to such changes (van Mantgem *et al.*, 2009; Woodall *et al.*, 2009; Peng *et al.*, 2011). A possible effect of climate change could be an increase in the extent and severity of future droughts (IPCC 2013). In particular, in 2011, the state of Texas experienced the most extreme drought on record with greater than 80% of the land area enveloped in the most severe drought classification (Palmer, 1965) and the remaining land area in some elevated level of drought (Nielsen-Gammon, 2012). Impacts of this far-reaching event were immediately evident with approximately nine-times greater tree mortality seen statewide than in previous years resulting in 301 million dead trees just one year post-drought (Moore *et al.*, 2016). Accurately describing and predicting tree and stand response to extreme drought events remains a prominent challenge for managers and researchers (Clark *et al.*, 2016; Vose *et al.*, 2016).

Following mortality, dead wood or woody debris provides an important component of terrestrial ecosystems, serving as habitat for wildlife and insects, a source and sink of nutrients, and as a modifier of fire dynamics (Harmon *et al.*, 1986). Efforts to understand dead wood have increased substantially in recent years (Russell *et al.*, 2015) with studies occurring across a range of ecosystems and scales (Laiho and Prescott, 2004; Harmon *et al.*, 2008; Radtke *et al.*, 2009; Harmon *et al.*, 2011; Oberle *et al.*, 2018). In particular, the U.S. National Greenhouse Gas Inventory (NGHGI), produced

annually by the U.S. Environmental Protection Agency and charged with accounting for national carbon (C) emissions and removals, recognizes dead wood as a unique and important component of the forest C pool (U.S. Environmental Protection Agency, 2019). Despite this attention, much is still unknown about the dynamics of this pool and estimation techniques for accurately quantifying biomass and C totals contain considerable variation (Weiskittel *et al.*, 2015). Moreover, with high prospects of widespread and significant disturbances to forests in the face of future climate change scenarios (Joyce *et al.*, 2014), forests could see dramatic increases in dead wood and fuels representing rapid live-to-dead shifts in biomass and C pools (Breshears and Allen, 2002). Given this, there is a need to understand which trees are most vulnerable to mortality in severe disturbances and the subsequent dynamics of dead wood to accurately estimate associated changes in biomass and C for informing future management, C cycling, and fire risk.

Many factors play a role in describing the risk of mortality for any particular tree. Under the decline-disease spiral (Manion, 1981), trees are exposed to static predisposing factors (e.g., climate, edaphic properties, genetic makeup) making them vulnerable to inciting factors (e.g., drought, fire, defoliating insects), followed by contributing factors (e.g., bark beetles, fungi, viruses), eventually resulting in mortality. Under this paradigm, drought increases tree vulnerability to other agents and the tree eventually dies, however this could be reversed such that drought becomes a contributing factor to weakened trees (Wang *et al.*, 2012). Franklin *et al.* (1987) describe a modified version of the decline-disease spiral highlighting that stand structure (e.g., competition, suppression,

dominance, release) can interact with other factors to result in the decline of a tree with possible opportunities for recovery. Dense stands undergoing self-thinning may be most susceptible to drought conditions given already elevated competition for limited available resources (Peet and Christensen, 1987). However, extreme drought events may negate the influence of density-dependent mortality causing increased vulnerability in trees across a range of densities (Floyd *et al.*, 2009). Mixed-species stands may experience lessened tree vulnerability to drought (Klos *et al.*, 2009) as neighboring trees of different species may show facilitation more than competition (Pretzsch *et al.*, 2013). Furthermore, recent evidence suggests that large, old trees may be most susceptible to extreme drought conditions and suffer disproportionate mortality (Lindenmayer *et al.*, 2012; Bennett *et al.*, 2015; Ryan, 2015). Speculation as to causes of this large tree drought mortality include greater hydraulic stress from height (McDowell and Allen, 2015), increased crown exposure to radiation and evaporative conditions (Roberts *et al.*, 1990), and preference by bark beetles (Pfeifer *et al.*, 2011). However, all these patterns regarding drought-related mortality can be variable and have proven difficult to confirm (Floyd *et al.*, 2009; Klos *et al.*, 2009; Ganey and Vojta, 2011). Yet, understanding how forest stand structure effects drought-caused mortality has important implications for describing which species may be more resistant and adaptable to a changing climate. Importantly, this knowledge can inform management objectives, such as thinning, which can be effective at mitigating drought effects if employed properly (D'Amato *et al.*, 2013; Giuggiola *et al.*, 2013).

Once a tree dies, whether by drought or other disturbance, it transitions to the dead wood pool representing a shift in the biomass and C cycle (Maser *et al.*, 1988). There are many pathways of decomposition for newly dead trees including remaining as a standing dead tree (SDT or 'snag') to snapping or fragmenting and becoming downed woody debris (DWD) (Harmon *et al.*, 1986). Collectively, snags and DWD are typically termed coarse woody debris (CWD) and include stems and larger branch material. Dynamics of this material typically vary with temperature and precipitation (Russell *et al.*, 2014; Garbarino *et al.*, 2015; Crecente-Campo *et al.*, 2016; Oberle *et al.*, 2018), among other factors (e.g., wind speed, ice storms, etc.) (Foster *et al.*, 1998; Hooper *et al.*, 2001; Harcombe *et al.*, 2009), but largely remain unknown for many ecosystems. National forest inventory (NFI) guidelines typically include classification systems for characterizing CWD decay (USDA Forest Service, 2017). These classifications are subjective, yet comprehensive, and make inventory of decaying material more efficient (Russell *et al.*, 2015). Many researchers have described CWD dynamics via fall-rates and transitions across decay classes using time-since-death data and NFI data, with particular focus in northern regions (Kruys *et al.*, 2002; Storaunet and Rolstad, 2004; Vanderwel *et al.*, 2006b; Aakala *et al.*, 2008; Aakala, 2010; Aakala, 2011; Angers *et al.*, 2011; Russell and Weiskittel, 2012; Russell *et al.*, 2013). Despite the availability of such tools, studies of CWD dynamics in southern forests have focused primarily on important pine species (e.g., *Pinus taeda* L.) (Radtke *et al.*, 2009; Mobley *et al.*, 2013; Zarnoch *et al.*, 2014) and habitat for cavity nesting wildlife (Moorman *et al.*, 1999; Conner and Saenz, 2005; Jones *et al.*, 2009; Zarnoch *et al.*, 2013). Given the potential for increased

tree mortality from climate change coupled with the prevalence of fire, hurricanes, and other disturbances in the south-central U.S. (Klepzig *et al.*, 2014; Guldin *et al.*, 2015), it is critical to understand the dynamics of CWD for this region in particluar to inform fire risk and fuels management, habitat management, and C implications.

In the United States, the U.S. Department of Agriculture Forest Service (USFS) quantifies dead wood via annual inventory data collected nationally through the Forest Inventory and Analysis (FIA) program. Accurate accounting of national forest biomass and C pools is necessary to meet stipulations for the U.S. NGHGI which tracks dead wood stocks as one of five key components of forest C (U.S. Environmental Protection Agency, 2019). However, accurate estimation of dead wood biomass and C remains a challenging task due to variability in woody material and scaling issues (Domke *et al.*, 2011; Weiskittel *et al.*, 2015). The FIA program uses regionally-developed allometric equations to calculate live and dead tree biomass (Woodall *et al.*, 2010). While such equations work relatively well for live trees, snags and DWD change in density and volume as decay progresses requiring correction for these changes (Fraver *et al.*, 2007; Harmon *et al.*, 2008; Harmon *et al.*, 2011; Fraver *et al.*, 2013). Density corrections for snags have only recently been developed (Harmon *et al.*, 2011) yet volume corrections for snags remain a prominent challenge (Weiskittel *et al.*, 2015) subsequently receiving little attention (Aakala, 2010; Domke *et al.*, 2011; Russell and Weiskittel, 2012). Difficulties in accurately measuring stems and branches in snags coupled with inherent differences in growth patterns makes accurate and broad scale assessment of volume in snags challenging. For example, conifers and hardwoods differ in their branching

structure with the former having a main stem the full length of the tree (excurrent structure) and the latter having a main stem that terminates at less than the full height of the tree (decurrent structure). Accounting for differences such as these could provide better estimates of volume, biomass, and C and improve our understanding of decomposition and nutrient cycling in dead wood.

One tool with potential to efficiently and non-destructively measure volume reduction in snags is light-detection-and-ranging or LiDAR. LiDAR is a form of remote sensing which produces a three-dimensional spatial grouping of points (i.e., point cloud) of an object by transmitting laser pulses which reflect off the object surface and subsequently record a point location at the distance and angle of the point of reflection (Lefsky *et al.*, 2002). Use of this technology has gained substantial traction in recent years for estimating fine- and broad-scale forest metrics via ground, aerial, and spaceborne platforms (Dassot *et al.*, 2011; Gobakken *et al.*, 2012; Narine *et al.*, 2019). Initial work with ground-based or terrestrial LiDAR (hereafter, terrestrial laser-scanning, TLS) has produced effective estimates of live tree volume and biomass (Kankare *et al.*, 2013; Srinivasan *et al.*, 2014) and subsequent allometric equations (Olagoke *et al.*, 2016; Stovall *et al.*, 2018), while some work has looked at estimating branch volume and biomass (Hauglin *et al.*, 2013). However, very little work has utilized TLS to quantify and explore the dynamics of dead tree volumes and reduction with decay (Putman and Popescu, 2018; Putman *et al.*, 2018). Terrestrial laser-scanning could provide an efficient and effective means of more accurately describing and accounting for volume, biomass, and C changes with decay. Importantly, such tools have strong potential for

increasing accuracy of volume, biomass, and C in large-scale forest inventories (e.g., FIA) through development of improved allometric equations derived from TLS data.

The 2011 drought in Texas presents a unique opportunity to address questions regarding extreme drought impacts on tree species mortality responses and forest stand structure. This event also provides impetus for filling knowledge gaps related to dead wood dynamics and accurate estimation of associated volume, biomass, and C. This dissertation aims to understand patterns of drought-related tree mortality and subsequent SDT dynamics across forests in east Texas through analysis of re-measured FIA plot data. Additionally, TLS will be used to develop and assess novel estimates of snag volume for improving estimates by understanding and accounting for structural volume changes with decay class.

Specifically, this dissertation addressed the following objectives each comprising an individual chapter:

1) Examine how tree mortality from drought (weather) and insects and diseases (pests) varied throughout a four-year period for key species from the four most common tree genera in east Texas following the 2011 drought.
2) Determine which individual tree- and stand-structural factors contributed to probability of individual tree mortality across three common pine species groups both pre-drought and after exposure to the 2011 drought in east Texas.
3) Develop models predicting the probability of a tree falling in the five-year measurement interval in which it dies and the five-year probability of a snag

falling in east Texas forests by examining common endogenous factors (e.g., tree and stand attributes) that drive the dynamics of this pool in east Texas.

4) Quantify and assess empirical volume and structural volume changes in loblolly pine SDT by decay class using TLS and a novel volume calculation algorithm, TreeVolX from Putman and Popescu (2018).

CHAPTER II

LAGGED MORTALITY AMONG TREE SPECIES FOUR YEARS AFTER AN EXCEPTIONAL DROUGHT IN EAST TEXAS*

Synopsis

In 2011, east Texas experienced the worst drought on record causing extensive tree mortality. Initial mortality estimates for 2012 varied among tree genera. A rapid damage assessment (RDA) estimated that 65.5 (± 7.3) million trees died as a result of the drought in this region one year post-drought. However, this estimate was untested against established monitoring networks. Moreover, pests and physiological damage can elevate tree mortality multiple years beyond a drought event. Since the RDA was unable to quantify multi-year trends, it remained unclear if these drivers caused increased tree mortality in east Texas beyond one year post-drought and how different species responded over time. To address these questions, we compared total 2012 standing dead tree (SDT) estimates (i.e., drought-killed plus all other SDT excluding harvested or salvaged trees) derived from the RDA and U.S. Forest Service Forest Inventory and Analysis (FIA) data for east Texas. Total SDT estimates did not significantly differ between the RDA (120.5 ± 8.5 million) and FIA (108.4 ± 8.7 million). Furthermore, total SDT estimates for the four most common genera (*Pinus*, *Quercus*, *Liquidambar*, *Ulmus*), which comprised over 80% of all species, did not significantly differ between the RDA and FIA. Additionally, we used logistic regression and FIA data from east

*Reprinted with permission from "Lagged mortality among tree species four years after an exceptional drought in east Texas" Paul A. Klockow, Jason G. Vogel, Christopher B. Edgar, and Georgianne W. Moore, 2018. *Ecosphere*, Volume 9(10):e02455, pp. 1-14, DOI: 10.1002/ecs2.2455. Copyright © 2018 The Authors.

Texas for 2011 through four years post-drought (2012-2015) to examine temporal trends in plot-level drought- and pest-driven tree mortality of seven key species (*Pinus taeda*, *Pinus echinata*, *Quercus nigra*, *Quercus stellata*, *Quercus falcata*, *Liquidambar styraciflua*, *Ulmus alata*) from the four most common genera. At the plot-level, drought-driven mortality was immediate for the three *Quercus* species (notably *Q. falcata*) and *L. styraciflua* which significantly increased in 2012 while *P. taeda* mortality was delayed, not increasing significantly until 2013. Pest-driven mortality increased from 2013-2015 for all species, with the highest rates observed in *Q. falcata* and lowest in *P. taeda* and *U. alata*. This study affirms the validity and value of independent sampling efforts to quantify mortality immediately following major disturbance and also demonstrates the need for longer term species-level assessments beyond the initial year post-drought to account for differential impacts from drought and pests.

Introduction

Globally, climate change is expected to increase the extent and severity of future droughts (IPCC 2013) having widespread ramifications on forested systems (McDowell *et al.*, 2018). Recent severe droughts have led to increased tree mortality in forests worldwide and are predicted to be more common and impactful in the future (Allen *et al.*, 2015). In North America, many forest ecosystems have been affected by these events including southwestern U.S. pine forests (Breshears *et al.*, 2005), aspen forests in south-central Canada (Michaelian *et al.*, 2011), and diverse angiosperm and gymnosperm forests of Texas (Moore *et al.*, 2016) and California (Young *et al.*, 2017). It is difficult to

generalize about regional vulnerability to extreme events in diverse forests with species varying in their strategy for surviving drought and sensitivity to insects and diseases (Anderegg *et al.*, 2016; Adams *et al.*, 2017). Moreover, established monitoring networks may be slow to capture immediate effects and remote sensing technologies may miss key details necessary for differentiating mortality.

National forest inventories (NFI) such as the U.S. Forest Service Forest Inventory and Analysis (FIA) program provide sound, detailed, statistically-defensible estimates of forest attributes over time (Bechtold and Patterson, 2005). FIA plots are re-measured every five to ten years depending on location yet annual subsets of plots (panels) can provide valuable documentation of broad disturbances such as droughts in forests (Shaw *et al.*, 2005). Despite this, plot measurements and data processing take time and must go through the proper channels before being made public (i.e., most recently available data is typically one to two years old) (Vogt and Smith, 2017), which can limit the ability to immediately assess widespread mortality effects from major disturbances. Remote sensing technologies such as airborne or spaceborne imagery and LiDAR can document broad-scale forest changes in near 'real-time' (McDowell *et al.*, 2015). However, these technologies are limited in their ability to capture detailed inventory measurements such as species, stem diameter, stem density, and understory effects (Norman *et al.*, 2016). Rapid, independent, broad-scale sampling initiatives (e.g., 'damage assessments') could provide clarity of immediate mortality effects from disturbances such as extreme drought than slower NFIs and remote sensing technologies that only capture overstory effects (Hartmann *et al.*, 2018). However, such initiatives are

rare given the amount of financial, material, and human resources needed for rapid implementation and have not been compared against baseline networks such as the FIA program to gauge their effectiveness at capturing the impacts of major mortality events.

From October 2010 to September 2011, the state of Texas experienced the most extreme drought on record with over 80% of the state land area enveloped in exceptional drought (Nielsen-Gammon, 2012). Statewide average precipitation for this 12-month period was 276 mm, the record driest 12-months for the state of Texas, approximately 60% less than (410 mm below) the 20th century 12-month average (686 mm) (NOAA 2018). Temperature increases during the drought were particularly extreme with statewide summer average temperature (June-August 2011) at 30.4 °C which was 2.9 °C greater than the long term average (i.e., nearly twice the largest deviation from average) (Hoerling *et al.*, 2013). This drought is an example of an acute, intense drought which could become commonplace in this region in the next few decades.

In their rapid damage assessment (RDA) of the 2011 drought, Moore *et al.* (2016) noted immediate tree mortality across statewide climate zones, with portions of central Texas most affected and the heavily forested east Texas least affected. Another comprehensive study of drought effects one to two years after this event utilized novel remote sensing methodologies to assess canopy loss as a surrogate for mortality (Schwantes *et al.*, 2016). Following this, Schwantes *et al.* (2017) developed drought-related canopy loss estimates for 2012 across a statewide climate gradient and noted, again, the highest loss in central Texas with east Texas least affected. Localized studies within central and western portions of the state highlighted variability in drought-related

mortality among species (Kukowski *et al.*, 2013; Poulos, 2014), soil types (Twidwell *et al.*, 2014), and elevation (Waring and Schwilk, 2014). However, these studies were focused on initial mortality, and used independent stratified or remotely sensed estimates, and may have missed the extent of mortality from this event, or later, continued mortality from physiological stress or insects and diseases. At the present time, multiple years of FIA data have become available since the drought thus, providing an important opportunity to validate initial mortality estimates from the RDA and examine differential impacts across species, particularly in the heavily forested and important economic region of east Texas.

Many frameworks exist for describing the mechanisms of decline and ultimate mortality of trees from drought (Manion, 1981; McDowell *et al.*, 2008; Anderegg *et al.*, 2013a). Physiologically, trees purportedly respond to water stress along a spectrum of isohydry to anisohydry. Under this paradigm, isohydric trees will regulate stomata to reduce the risk of xylem cavitation at the cost of reducing carbon intake most likely resulting in mortality via carbon starvation while anisohydric trees will maintain transpiration and respiration but operate at very small hydraulic safety margins most likely resulting in mortality via hydraulic failure (McDowell *et al.*, 2008). Recent evidence examining these mechanisms suggests that hydraulic failure is most important in driving drought mortality across a range of species with reductions in carbon playing a smaller role, more so in gymnosperms than angiosperms (Adams *et al.*, 2017). A recent global meta-analysis highlights these trends in that gymnosperms and drought-tolerant species typically experience long lasting growth declines following a drought

event prior to mortality (i.e., carbon starvation) while angiosperms may not show long or notable growth declines prior to mortality (i.e., hydraulic failure) (Cailleret *et al.*, 2017). Gymnosperms, such as loblolly pine (*Pinus taeda* L.) which dominates throughout east Texas, are capable of employing physiological adaptations to avoid drought stress by shedding needles and maintaining high leaf water potentials (Maggard *et al.*, 2016), falling more under the isohydric strategy. Angiosperms, such as oaks, are prevalent throughout Texas and the south-central U.S. and, oaks in particular, are generally drought tolerant having deeper roots, ring-porous xylem anatomy, and operating at higher hydraulic safety margins (Abrams, 1990; Hoffmann *et al.*, 2011; Klein, 2014). Evidence from recent decline events in the south-central U.S. suggests that white oaks (*Quercus* Section *Quercus*) are better adapted to drought than red oaks (*Quercus* Section *Lobatae*; (Fan *et al.*, 2012; Haavik *et al.*, 2012). Moreover, evidence from central Texas following the 2011 drought suggests that trees did not follow expected patterns of iso/anisohydry in their mortality response (Johnson *et al.*, 2018). Despite growing knowledge on mechanisms of drought-related mortality, evidence is still lacking in how individual species respond to extreme events such as the 2011 drought.

Drought often results in elevated tree mortality rates and decreased productivity beyond the timeframe of the event (van Mantgem *et al.*, 2009). The duration and timing of drought can be important for predicting which trees will die and at what time (Bigler *et al.*, 2007; Anderegg *et al.*, 2013a). For example, a shorter, acute drought of high intensity may lead to immediate mortality in anisohydric trees via hydraulic failure while longer, chronic drought of low intensity might cause lagged mortality in isohydric trees

as carbon reserves become depleted (Cailleret *et al.,* 2017). Trees that survive the drought event become stressed and ultimately run a higher risk of attack from insects and diseases, resulting in lagged or multi-year mortality events (Desprez-Loustau *et al.*, 2006; Raffa *et al.,* 2008; Anderegg *et al.,* 2015). Drought stressed trees have weakened defenses (e.g., reduced or limited carbohydrate reserves, compromised xylem conductivity) and become unable to fend off attacking insects and diseases (Gaylord *et al.*, 2013). Bark beetles can be particularly virulent following drought events depending on a host of interacting factors (Raffa *et al.,* 2008). Limited knowledge exists on the impacts of drought on insect and disease populations and how these may interact with drought to drive continued mortality (Kolb *et al.,* 2016). Initial estimates of drought-related impacts (e.g., tree mortality, carbon cycling, economic losses, etc.) could be drastically underestimated if lagged mortality and productivity effects are not effectively quantified across large regions (McDowell *et al.,* 2018). Evidence of immediate and lagged drought mortality could foster future work pinpointing which species are more resistant or resilient to extreme events, ultimately informing models predicting future forest composition.

In this paper, we aimed to accomplish two main objectives 1) assess the validity of a rapid, independent, broad-scale sampling effort quantifying tree mortality following the 2011 drought (i.e., RDA from Moore *et al.* (2016)) by comparing it to baseline FIA results and 2) move beyond initial impacts by examining how tree mortality from drought (weather) and insects and diseases (hereafter, pests) varied throughout a four-year period for key species from the four most common tree genera in east Texas

following the 2011 drought. We focused on this region of Texas due to its economic and ecological importance, because past findings suggest it suffered relatively modest immediate mortality and dieback from the 2011 drought (Moore *et al.*, 2016; Schwantes *et al.*, 2017), and because it has received little attention in the literature in regards to detailed impacts following the 2011 drought. To our knowledge, this study provides the first assessment of a broad-scale, independent, ground-based sampling effort (RDA) compared to the well-established, statistically-defensible FIA sampling program for quantifying major disturbance effects.

Methods

Study Area

The study area includes the eastern portion of Texas, USA (Figure II.1), encompassing the western edge of the Western Gulf Coastal Plain and the Pineywoods ecoregion extending south to the Gulf of Mexico, bounded approximately by 29° 17’ to 33° 57’ N and 93° 30’ to 96° 27’ W. This region contains a diversity of tree species and is heavily dominated by southern pine, primarily loblolly pine, representing the southwestern range limit for many eastern tree species (Burns and Honkala, 1990). Climate in this region is characterized by hot, humid summers and short, mild winters. An east-to-west decreasing rainfall gradient exists as does a slight north-to-south increasing temperature gradient. Mean annual precipitation and temperature typically vary between ~990-1600 mm and ~16-23 °C, respectively (USDA NRCS 2006). During the drought period from October 2010 to September 2011, average precipitation in east

Texas was 619 mm, a record driest in this region, approximately 47% less than the 20th century average for this 12-month period (1159 mm) (NOAA 2018). Summer average temperature (June-August) in east Texas was also the record warmest at 30.7 °C which was 3.1 °C greater than the 20th century average for this summer period (27.6 °C) (NOAA 2018). During the study period of 2011-2015 in east Texas, mean annual (January - December) temperatures were 19.9, 20.1, 18.7, 18.1, and 19.3 °C (20th century average of 18.6 °C), respectively, and annual precipitation was 769, 1161, 1199, 1067, and 1737 mm (20th century average of 1162 mm), respectively (NOAA 2018). Topography in this region changes gradually with the highest upland areas approximately 200 m above sea level. Soils predominantly consist of well-drained to poorly-drained Alfisols and Ultisols with loamy to clayey textures (USDA NRCS 2006).

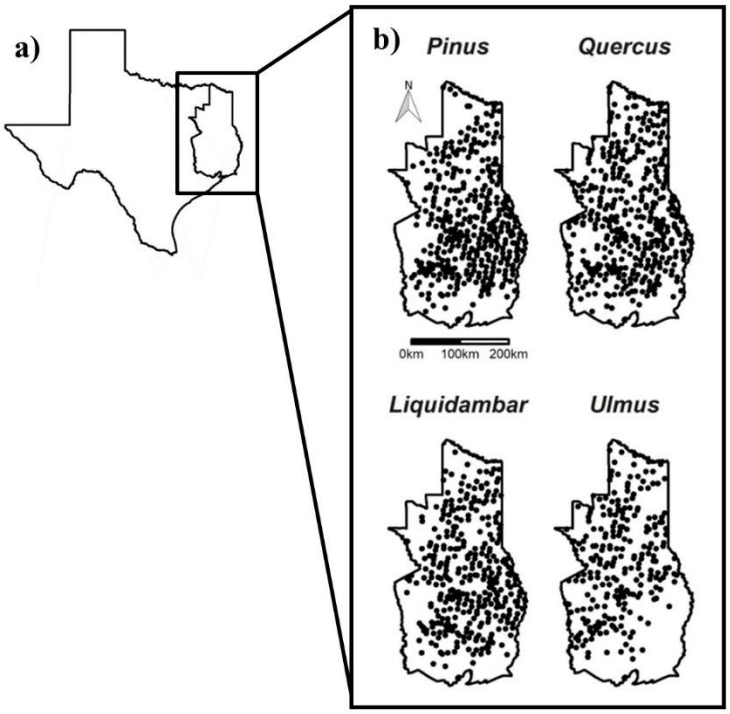

Figure II.1 State of Texas with (a) study area (east Texas) as inset and (b) FIA plot locations having presence of each of the four most common genera in 2011. Reprinted with permission from Klockow *et al.*, (2018).

Data

We examined data from FIA plots located throughout east Texas (Figure II.1). Plot measurements and re-measurements were carried out on a five year panel inventory as described in Bechtold and Patterson (2005). Due to logistical constraints, a small proportion of plots were measured just prior to or just following the scheduled inventory

year (~15% measured in the year before and ~1% measured in the year after inventory year for 2011-2015 data). Thus, inventory year refers to the scheduled panel year in which a plot is supposed to be measured and measurement year reflects the actual year in which the plot was measured. These typically coincide, but the operational schedule of the inventory has the measurements of a selected inventory year beginning in the latter months of the preceding year. For both objectives, trees were defined following FIA protocols as being ≥ 12.7 cm diameter at breast height (DBH) and located in forested plot conditions. Standing dead trees (SDT) had an unbroken height ≥ 1.37 m and a lean angle from vertical < 45 degrees. All harvested or salvaged trees were excluded from calculations. The four most common genera in the study area were *Pinus*, *Quercus*, *Liquidambar*, and *Ulmus*, representing over 80% of all live individuals (52%, 18%, 9%, and 4%, respectively). The predominant species from each of the four most abundant genera were analyzed separately to provide more resolution on species-specific effects of the drought. This included those species which together comprised approximately two-thirds of the total stem count in each genus for the years 2011-2015 (i.e., *Pinus taeda* (loblolly pine) - 89%, *Pinus echinata* (shortleaf pine) - 8%; *Quercus nigra* (water oak) - 28%, *Quercus stellata* (post oak) - 24%, *Quercus falcata* (southern red oak) - 15%; *Liquidambar styraciflua* (sweetgum) - 100%; *Ulmus alata* (winged elm) - 68%). Agents of mortality (weather, pests) as determined by field crews were used for assessment of trends in the causes of SDT mortality. Data uploaded to the FIA DataMart on December 14, 2017 were used for all analyses.

Analyses

In order to address our first objective, we used 2012 tree mortality data from the RDA reported in Moore *et al.* (2016) and SDT population estimates from FIA inventory years 2011 and 2012 for the study region. The RDA employed design-based estimation. East Texas was divided into four strata and within each stratum a two-stage unequal probability sample with replacement was conducted. Primary sample units (10 km x 10 km areas) were selected with probability proportional to forest area. In each primary sample unit, seven secondary sample units (0.16-ha circular plots) were randomly selected. A total of 238 plots were established in the study and tallies of drought-killed trees were made with genus and diameter at breast height (DBH) recorded. FIA definitions of trees (qualifying species and size at least 12.7 cm DBH) were used in the RDA. The reader is referred to Lohr (1999) for more information on the general design and estimation and Moore *et al.* (2016) for specific application of the design in the RDA.

FIA also employs design-based estimation in the national forest inventory, although the specific design is considerably different from that employed in the RDA. FIA is an annual inventory and in east Texas 20 percent of the plots are measured each year such that a complete inventory cycle is completed every five years (i.e., as described above). At the core of FIA is a quasi-systematic grid of plots at spatial resolution of one plot per 2400 ha. FIA uses stratification, which was also employed in the RDA. Within strata, the sample is assumed to be a simple random sample. An FIA plot consists of a cluster of four subplots each 7.31 m in radius. One subplot forms the center point of the plot and the remaining three subplots are located at azimuths of 0,

120, and 240 degrees and 36.58 m distance from the central subplot center point. Bechtold and Patterson (2005) document the FIA survey design and estimation procedures. The 2011 and 2012 FIA data included 797 and 791 plots, respectively, considerably more than the 238 plots measured in the RDA. The difference between the two surveys was not as large as it appears because the RDA plot was 2.4 times the size of the FIA plot and the FIA plot counts included all plots, forested and non-forested. Total forest area measured in the RDA was about 38 ha and in FIA was 29.9 ha in 2011 and 29.5 ha in 2012.

The post-stratified estimation approach used by FIA (Bechtold and Patterson, 2005) was employed for calculating estimates of our first objective in this study. Estimates were calculated using data for individual inventory years of 2011 and 2012, which differs from FIA's standard approach of combining data across multiple inventory years when producing population estimates. Estimates for these individual inventory years were expected to provide more temporal resolution but at the cost of reduced sample size and thus higher standard errors when compared to the standard FIA approach. Population estimates for the RDA and FIA were compared using two-tailed *Z*-tests since they both represented independent samples of the study area. Significant differences were assessed at the $\alpha = 0.05$ level.

In order to inform our second objective, plot-level mortality estimates by species and agent of mortality were calculated across measurement years spanning 2011-2015 using plot stem counts from FIA data. Thus, plot-level mortality estimates represented an annual proportion of total SDT mortality across the study region in a given year and

not a rate. Plot-level mortality estimates comprised total SDT stem count for a particular species and agent divided by total (i.e., live and standing dead) stems for that same species in a given plot and measurement year (excluding harvested or salvaged trees). A total of 1882 plots were used for determining plot-level mortality estimates.

We employed generalized linear fixed effects modeling to determine differences in plot-level mortality estimates across measurement years and species. Specifically, we assumed that our data followed a binomial distribution such that total live and standing dead trees of each species in each plot represented *n* individual trials with probability of mortality *p* for each agent of mortality (i.e., weather, pests) and the number of SDT *y* for each agent in each plot represented trial 'successes'. For example, if a plot contained ten loblolly pines (i.e., ten trials) and three were denoted as killed by weather (i.e., three weather-related 'successes') and two were killed by pests (i.e., two pest-related 'successes'), their observed probabilities of mortality would be 0.3 and 0.2 respectively. Following this, we modeled the probability of mortality *p* with fixed effects of species and measurement year using a logistic regression approach and maximum likelihood estimation.

$$y_{ij} \sim Binom(n_{ij}, p_{ij}) \tag{II.1}$$

$$logit(p_{ij}) = SPP_{ij} + YEAR_{ij} + SPP_{ij} \times YEAR_{ij} \tag{II.2}$$

Where, *i* is plot, *j* is species, *SPP* is the fixed effect for species, and *YEAR* is fixed effect for year (*n*, *p*, and *y* are explained above). Individual plots were not re-measured on an annual basis (i.e., five year re-measurements per FIA protocol) thus, these data did not represent repeated measurements and, subsequently, measurement year was treated as a

fixed effect. Two models were built and assessed, one for weather-related mortality and the other for pest-related mortality. Main effects of species and measurement year and their interaction were tested for significance using likelihood ratio tests. If the *p*-value for a term was < 0.05, the term was deemed significant and included in the model. Overall goodness-of-fit was assessed using likelihood ratio tests between the final model and a null model and by examining the log likelihood and McFadden's pseudo-R^2 (Agresti, 2013). Meaningful post hoc contrasts between levels of each fixed effect were carried out using Tukey tests assessed at the $\alpha = 0.05$ level. All calculations and analyses of mortality estimates were conducted using R 3.3.1 software (R Core Team, 2016).

Results

Population estimates of SDT were compared between 2012 FIA data and the RDA conducted in 2012 by (Moore *et al.*, 2016) which used an independent survey to provide a rapid initial estimate of drought-killed SDT in 2012 (Table II.1). Both surveys included estimates of SDT of all species in east Texas. The RDA produced an estimate of 65.5 (± 7.3) million SDT in 2012, which pertained to drought-killed stems only (Table II.1). Thus, it was combined with the 2011 FIA SDT estimate of 55.0 (± 4.4) million to account for all other SDT existing on the landscape (Table II.1). This was done under the assumption that changes in SDT between 2011 and 2012 FIA data primarily consisted of drought-killed trees with some natural attrition of older SDT and sampling error. This resulted in an RDA (+ 2011 FIA) estimate of 120.5 ± 8.5 million total SDT from all causes (except harvest or salvaged stems) in 2012 (Table II.1). Forest land area has

remained fairly constant in east Texas at about 4.9 million ha producing a per unit area estimate of 24.7 ± 1.7 SDT ha^{-1}. The 2012 FIA estimate was 108.4 ± 8.7 million total SDT (Table II.1) from all causes (except harvest or salvaged stems) and 22.2 ± 1.8 SDT ha^{-1}. The estimates of FIA and RDA total SDT in 2012 did not significantly differ from each other (*p*-value = 0.318) having a difference of 12.2 ± 12.2 million SDT (Table II.1). In addition to the all-species estimates, comparisons of FIA and RDA total SDT estimates in 2012 for the four most common genera (*Pinus*, *Quercus*, *Liquidambar*, and *Ulmus*) produced no significant differences (*p*-value = 0.155, 0.270, 0.507, 0.398, respectively) having differences of 9.7 ± 6.8, 7.4 ± 6.7, 1.9 ± 2.8, 1.9 ± 2.3 million SDT for *Pinus, Quercus, Liquidambar,* and *Ulmus,* respectively (Table II.1). This suggests that the RDA conducted by Moore *et al.* (2016) provided a reasonable initial estimate of drought-killed trees in east Texas.

Table II.1 Standing dead tree (SDT) population estimates and standard errors (in parentheses) based on U.S. Forest Service Forest Inventory and Analysis (FIA) data from 2011 and 2012 and rapid damage assessment (RDA) data collected in 2012 from Moore et al. (2016). Reprinted with permission from Klockow *et al.*, (2018).

Genus	Pre-drought 2011 (2011 FIA)		Drought-killed 2012 (RDA)		Post-drought 2012 (2011 FIA+RDA)		Post-drought 2012 (2012 FIA)		Difference		*Z*-score	*p*-value
Pinus	18.4	(2.4)	16.4	(5.0)	34.8	(5.5)	25.1	(3.9)	9.7	(6.8)	1.422	0.155
Quercus	20.6	(3.2)	24.8	(3.9)	45.4	(5.0)	38.0	(4.5)	7.4	(6.7)	1.103	0.270
Liquidambar	4.3	(1.0)	6.3	(1.7)	10.6	(2.0)	12.5	(2.0)	-1.9	(2.8)	-0.663	0.507
Ulmus	1.1	(0.5)	5.2	(1.8)	6.3	(1.9)	4.4	(1.2)	1.9	(2.3)	0.845	0.398
All spp.	55.0	(4.4)	65.5	(7.3)	120.5	(8.5)	108.4	(8.7)	12.2	(12.2)	0.999	0.318

Notes: SDT population estimates are listed as number of stems times 10^6. No significant differences were observed based on *Z*-tests between independent samples of post-drought 2012 estimates (i.e., 2011 FIA + RDA vs. 2012 FIA).

Plot-level mortality models showed variability among species and measurement years highlighting differing species responses to the drought and pests over time (Figures II.2 and II.3, Appendix A: Tables A.1 and A.2). In particular, weather mortality showed a significant interaction between species and measurement year based on results of the likelihood ratio tests (χ^2 = 92.41 with 24 degrees of freedom, *p*-value = << 0.001). Pest mortality did not show a significant interaction (χ^2 = 35.40 with 24 degrees of freedom, *p*-value = 0.063) suggesting the main effects-only model was sufficient. However, the low *p*-value for this interaction term suggests potentially weak interaction between species and measurement year for pest mortality. Overall goodness-of-fit via the likelihood ratio test for each model was far superior to its respective null model (weather mortality model: deviance = 700.69 with 34 degrees of freedom, *p*-value = << 0.001; pest mortality model: deviance = 261.94 with 10 degrees of freedom, *p*-value = << 0.001). McFadden's pseudo-R^2 values for each model suggest moderate and reasonably low explanatory power (R^2 = 0.144 and 0.089) for the weather model and pest model, respectively.

Noteworthy post hoc comparisons of species and measurement year mortality predictions are presented in Figures II.2 and II.3. All coefficient estimates are listed fully in the supplementary material (Appendix A: Tables A.1 and A.2) along with observed vs. predicted mortality estimates (Appendix A: Figures A.1 and A.2). In general, weather mortality was highest in oaks and lowest in loblolly pine (Figure II.2). All oaks and sweetgum experienced significant immediate weather mortality in 2012 while loblolly pine mortality was delayed, significantly increasing in 2013 (Figure II.2). Sweetgum

showed continued mortality into 2013, also suggesting some delayed mortality, but this effect was not significant (Figure II.2). Both shortleaf pine and winged elm showed increases in weather mortality in 2013, suggesting some delayed mortality, but ultimately had no significant changes in mortality across all years (Figure II.2). Pest mortality was delayed, increasing significantly in 2013 and continuing a general increasing (but not significantly differing) trend into 2014 and 2015 for all species analyzed (Figure II.3). Pest mortality was highest in southern red oak and lowest in loblolly pine and winged elm (Figure II.3).

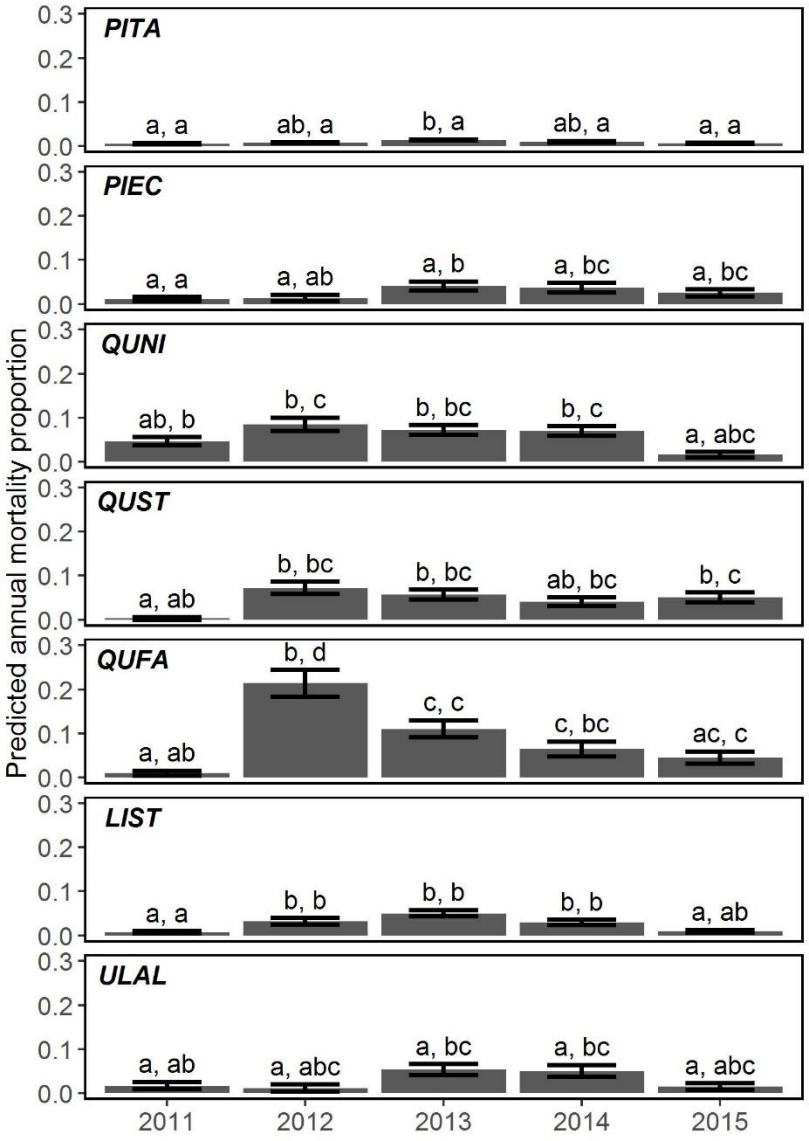

Figure II.2 Mean annual predicted probability of weather mortality in a plot for each species and measurement year across east Texas derived from logistic regression results. Bars denote standard errors for each estimate. Different letters above each bar denote significant differences ($p < 0.05$) derived from post hoc comparisons using Tukey tests. Letters to the left of commas correspond to differences among years for each individual species (i.e., read in rows, left-to-right). Letters to the right of commas correspond to differences among species within each year (i.e., read in columns, top-to-bottom). Species codes are as follows: PITA = *Pinus taeda*, PIEC = *Pinus echinata*, QUNI = *Quercus nigra*, QUST = *Quercus stellata*, QUFA = *Quercus falcata*, LIST = *Liquidambar styraciflua*, ULAL = *Ulmus alata*. Reprinted with permission from Klockow *et al.*, (2018).

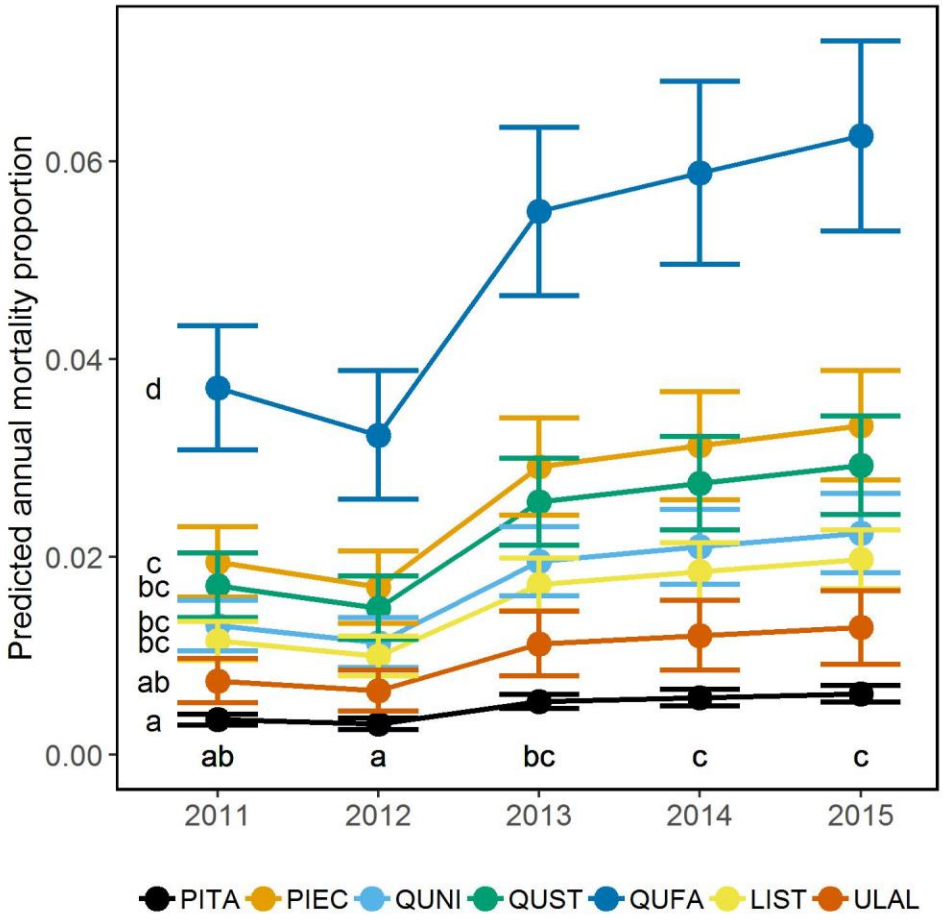

Figure II.3 Mean annual predicted probability of pest mortality in a plot with standard errors for each species and measurement year across east Texas derived from logistic regression results. Different letters along the x- and y-axes denote significant differences ($p < 0.05$) from post hoc comparisons using Tukey tests. Letters along the x-axis correspond to differences among years across all species while, letters along the y-axis correspond to differences among species across all years. Species codes are as follows: *PITA = Pinus taeda, PIEC = Pinus echinata, QUNI = Quercus nigra, QUST = Quercus stellata, QUFA = Quercus falcata, LIST = Liquidambar styraciflua, ULAL = Ulmus alata*. Reprinted with permission from Klockow *et al.*, (2018).

Discussion

To our knowledge, this study is the first comparison between a rapid, independent sampling effort (RDA) and a baseline, established inventory such as FIA for quantifying mortality from a major disturbance event. The rapidity and effectiveness of the RDA, aided by an established agency in the Texas A&M Forest Service which had the infrastructure and personnel to carry out the sampling, provided crucial knowledge about the initial impacts of an extreme drought on tree mortality approximately nine months before the first post-drought data from FIA were available, ultimately influencing forest management and policy decision-making. This comparison to FIA provides assurance that those decisions were grounded on correct information. The sampling schemes for the RDA and FIA differ in significant areas yet both adhere to sound theory and ultimately provide viable quantification of tree mortality in east Texas. Differences in the designs of the two surveys can be traced back to their primary purpose. Monitoring of trends over time is a major objective of FIA and the design is set up for re-measurement of plots and efficient estimation of change. The purpose of the RDA was to estimate the number of drought-killed trees at one point in time, i.e., monitoring over time and re-measurement were not considered as survey objectives. As a one-point-in-time survey, the RDA was able to utilize design features for the purpose of achieving variance reduction (i.e., stratification, unequal probability sampling) and cost savings (i.e., two-stage sampling) without consideration for implications on change estimation. Where resources permit, independent sampling efforts based on sound sampling theory aimed at rapidly quantifying disturbances can provide an effective

critical first look into how forests and ecosystems respond to a changing climate. Interest has necessarily shifted with time from the initial impacts of the drought to longer-term trends and forest response, and for that the FIA data is ideally suited.

Making appropriate use of FIA data, here we moved beyond initial estimates and examined temporal and species-level mortality impacts in east Texas following the 2011 drought. Models of predicted weather and pest mortality showed that species differed quite widely in their response to the drought. Generally speaking, the models provide decent predictions of plot-level mortality yet certain species and years matched observations more closely than others. For the most part, results follow observed trends but may under- or over-estimate mortality in some cases (Appendix A: Figures A.1 and A.2). The impact of the drought on SDT in east Texas was plainly apparent in the FIA data, specifically in the weather mortality model predictions. Clear increases in mortality were evident in 2012, one year post-drought, and even into 2013. Increases in mortality from one year to the next generally correlate well with disturbance events given the nature of the observations (i.e., proportion of SDT in a plot in a year). However, if mortality does not change or drops from one year to the next, it is difficult to assess how much new mortality has occurred in that time span. This is because these mortality estimates represent net effect of mortality (e.g., disturbance) and decomposition (e.g., falling of trees). Thus, no change in mortality between years suggests that any new mortality and the falling of SDT are roughly similar whereas a decrease in mortality suggests that the falling of SDT has exceeded any new mortality. Interestingly, all species showed fairly rapid turnover of SDT within the timeframe examined ultimately

returning to pre-drought (2011) mortality levels within three or four years. In particular, oaks experienced significant decreases in mortality on an annual basis indicating rapid decomposition for this genus. Trees in east Texas tend to decompose rapidly (Conner and Saenz, 2005; Putman *et al.*, 2018) given the hot, humid, and moist conditions that generally persist year round (USDA NRCS 2006). Moreover, unlike other parts of the U.S., east Texas has termite populations as part of the biotic decomposer community that greatly increase decomposition (Zhang *et al.*, 2016). In tandem, these abiotic and biotic factors create a prime scenario for rapid turnover of dead wood. This observation has important implications for carbon accounting as massive mortality events such as the 2011 drought could drastically alter carbon budgets by turning forests into a carbon source rather than sink.

We observed that loblolly pine, the predominant tree species in east Texas, suffered very little weather mortality from the 2011 drought, as past studies have suggested (Moore *et al.*, 2016; Schwantes *et al.*, 2017). Loblolly pine maintained the lowest predicted weather mortality from 2011 to 2015 of all species analyzed. One caveat to this is that mean predicted loblolly weather mortality was consistently underestimated each year (i.e., observations were 29-66% greater than predictions across all years; Appendix A: Figure A.1). Despite this, observed mean loblolly pine weather mortality and standard errors were consistently lower than other species. Thus, predictions are underestimates but still highlight general trends for this species. Shortleaf pine also maintained low weather mortality but remained consistently higher than loblolly pine. Both pine species experienced immediate but small increases in weather

mortality which continued increasing into 2013 (significantly so for loblolly), two years post-drought, suggesting that mortality for pines was lagged. However, the lack of any significant difference in shortleaf pine weather mortality is likely due to the small numbers of this species on the landscape reflected by the high variability in mortality estimates. These general trends in pines could relate to both the widespread, active management of loblolly pine and the ability of this species to thrive in a wide range of conditions (Fox *et al.*, 2007). Extensive and intensive actions such as thinning, fertilizing, prescribed burning, and other means of competition-control may have provided favorable conditions for pine allowing it to resist drought more effectively. Recent tree-ring studies of pine species across the U.S. highlight the effectiveness of thinning and reduced stand densities at mitigating water stress (D'Amato *et al.*, 2013; Bottero *et al.*, 2017; Gleason *et al.*, 2017) lending support to our observations in east Texas. At a finer scale, loblolly pine employs morphological water conservation strategies under moderate drought by reducing leaf area and maintaining leaf water potential high enough to avoid mortality (Maggard *et al.*, 2016), representing an isohydric water conservation strategy. These physiological strategies also may have allowed many pines to avoid immediate mortality under the severe 2011 drought conditions. However, given the continued increase in mortality for pines into 2013, it seems plausible that the intense, acute drought conditions may have been severe enough to cause terminal hydraulic damage or deplete carbon stores to the point that eventual recovery was not possible, particularly for trees suffering from low vigor prior to the drought (Anderegg *et al.*, 2013b; Berdanier and Clark, 2016).

Oaks appeared most vulnerable to extreme drought given the combination of the initial sharp increase in predicted weather mortality in 2012 and the generally higher predicted weather mortality relative to other species. It was clear that all oak species analyzed in this study experienced significant, immediate drought mortality. Not surprisingly, the red oak species (i.e., water oak and, in particular, southern red oak) had higher mortality in 2012, one year post drought, than post oak (i.e., a white oak species). When not under stress, red oaks can experience mortality rates three to six times that of other species (Fan *et al.*, 2006). Yet, in the south-central U.S., red oaks have been particularly vulnerable to decline events driven by multiple stressors including drought and pests (Fan *et al.*, 2012; Haavik *et al.*, 2012). Oaks, in general, tend to maintain stomatal conductance and transpiration even under very dry conditions (Pataki and Oren, 2003; Will *et al.*, 2013) and operate with very small hydraulic safety margins (Rodríguez-Calcerrada *et al.*, 2017) thus, following an anisohydric strategy. It appears the 2011 drought conditions may have surpassed a threshold by which sustained transpiration and increasingly negative water potentials could not be maintained resulting in rapid onset of mortality via hydraulic failure for the three oak species analyzed here, falling in line with global observations of anisohydric trees under drought (Adams *et al.*, 2017; Cailleret *et al.*, 2017). This finding has important implications for predicting future forest composition if severe droughts like that which occurred in 2011 become more frequent in the future. Oaks in general may suffer disproportionate loss of mature individuals in addition to regenerating seedlings and saplings under future

extreme droughts via immediate hydraulic failure and subsequent decline and dieback (Rodríguez-Calcerrada *et al.*, 2017).

Sweetgum and winged elm appeared to show lagged drought-related mortality ultimately reaching their peak predicted mortality by 2013. Interestingly, sweetgum experienced significant immediate mortality in 2012 which continued increasing into 2013 albeit not significantly. Winged elm weather mortality was highly variable resulting in the lack of significantly different mortality estimates across years, despite the notable increase in 2013. These two species are widespread in east Texas primarily occurring as intermediate or suppressed trees in the pine forests that dominate this region (Burns and Honkala, 1990). It is possible that competition for resources (i.e., light and water) with more dominant pines was exacerbated for sweetgum during the drought thus, resulting in significant initial mortality, likely via hydraulic failure. Physiologically, sweetgum will reduce stomatal conductance quite rapidly allowing it to avoid leaf desiccation (Pezeshki and Chambers, 1986) and may also undergo leaf senescence and abscission quite rapidly under water stress (Pataki and Oren, 2003; Esperon-Rodriguez and Barradas, 2015), generally following an isohydric strategy. It is possible that those more vigorous sweetgum successfully employed this strategy to avoid the initial drought effect but eventually sustained notable, but not significant, increased mortality two years post drought through potential carbon depletion and compromised xylem conductance.

While weather was the greatest factor attributed to tree mortality in the years following the drought, pests also contributed. As expected, mortality from pests was delayed following the drought, significantly increasing in 2013 with continued smaller

increases through 2014 and 2015. Pest-driven mortality following drought events are poorly understood and often depend on many factors including the extent and severity of a drought, tree species in the affected region, insect and disease species in the affected region, and interactions among these factors (Anderegg *et al.*, 2015; Kolb *et al.*, 2016). The acute, exceptional nature of the 2011 drought was broad and severe enough that many tree species remained physiologically weakened, making them susceptible to various pests. Regionally prevalent insects such as *Ips* beetle (*Ips grandicollis*, *I. avulsus*, and *I. calligraphus*) and diseases including hypoxylon canker (*Biscogniauxia atropunctatum*) and oak wilt (*Ceratocystis fagacearum*) appeared to facilitate continued tree mortality by attacking drought-stressed trees multiple years post-drought (Texas A&M Forest Service, U.S. Forest Service, Forest Health Highlights for Texas, 2012-2014). Notably, the southern pine beetle (*Dendroctonus frontalis*) had a minimal impact and did not erupt following the drought event (Asaro *et al.*, 2017) falling in line with a synthesis of past evidence (Kolb *et al.*, 2016). In fact, loblolly pine maintained the lowest predicted pest mortality through all years of all species analyzed. This is likely due in part to the non-effect of southern pine beetle and, as mentioned previously, the extensive management of loblolly pine in this region providing a favorable competitive environment (Fox *et al.*, 2007). The high predicted pest mortality in southern red oak follows observations from recent decline events further north in Arkansas and Missouri which resulted in substantial mortality in red oak species from red oak borer outbreaks following periodic drought events (Fan *et al.*, 2008; Fan *et al.*, 2012; Haavik *et al.*,

2012). Overall, pest mortality clearly added to the broader effect of the 2011 drought yet was relatively more muted than weather mortality.

Conclusions

The historically unprecedented drought event in 2011 caused immediate shifts in live-to-dead tree numbers and increased mortality up to three years after the event in east Texas. Species differed in immediate or delayed drought mortality impacts suggesting fundamental differences in sensitivity to drought. Specifically, oaks showed a near immediate drought mortality response in 2012 while pines, and somewhat for sweetgum and winged elm, had a delayed mortality response. The initial RDA of drought mortality in 2012 is supported by new estimates computed from 2012 FIA data highlighting the effectiveness of rapid, independent sampling efforts for quantifying the impacts of major disturbance events and informing management and policy decisions. Ultimately, the drought and subsequent pest effect on angiosperms was likely more severe than previous estimates in part because of continued mortality beyond 2012. This lagged effect in angiosperms may also affect efforts to remotely sense drought impacts because many of these species are found in the lower canopy while the more common overstory pines were relatively unaffected. Insect and disease characteristics played a role in driving differing and lagged responses among species two and three years beyond the drought event. Additionally, broad-scale factors such as active management of loblolly pine likely created favorable competitive environments which muted any substantial mortality impacts in this species. Future work should aim to identify the drivers of immediate

mortality in oaks (i.e., whether they crossed a physiological threshold of climate-related mortality) and the strategies or conditions that allowed pines to remain relatively unaffected (e.g., morphological adaptations, stand structure).

CHAPTER III

SOUTHERN PINE MANAGEMENT REINFORCES RESISTANCE TO EXTREME DROUGHT MORTALITY AT THE WESTERN EDGE OF ITS RANGE

Synopsis

Tree mortality is expected to increase as future droughts become more extensive and severe. Forest managers must cope with the effects of extreme droughts while continuing to provide valuable ecosystem services. In 2011, the state of Texas experienced an exceptional drought covering all forested areas, breaking statewide and regional temperature and precipitation records. In the eastern region of Texas, pine species are economically and ecologically important and are often managed, providing an opportunity to examine whether silvicultural strategies could mitigate extreme drought mortality. We used U.S. Forest Service Forest Inventory and Analysis data to construct Bayesian, logistic, mixed effects regression models describing individual tree mortality of three major pine groups (planted and naturally-regenerated loblolly pine, *Pinus taeda* (PL and NL, respectively), and shortleaf pine, *Pinus echinata*, (SL)) under pre-drought and drought periods for east Texas. Additionally, we built similar models for these pine groups and periods to assess how stand structure (i.e., tree size, relative density, and species dominance) affected individual tree mortality. Surprisingly, pine mortality did not increase significantly from pre-drought to drought periods but the group mortality rates did differ from one another as well as in response to stand structural characteristics. Planted loblolly was least affected as mortality increased 9.8%

between periods. In contrast, NL and SL pine mortality rates were significantly higher than PL but were relatively similar to each other, increasing 26.3% and 20.0%, respectively. Somewhat surprisingly, stand structure did not explain mortality in SL in either period. However, tree size and relative density were key factors explaining mortality in loblolly pine. The smallest and largest stems experienced elevated mortality, particularly for PL under extreme drought. As expected, loblolly pine in dense stands were more susceptible to drought mortality. Notably for NL, greater overstory diversity reduced the probability of pine mortality under extreme drought. Our results suggest that current practices in PL that manage relative density and tree size confers some resistance to extreme drought. In NL stands, drought resistance could be increased from thinning and management that encourages tree diversity.

Introduction

Future climate is predicted to become hotter and increase the extent and severity of future droughts worldwide (IPCC 2013). Forests may already be responding to climatic changes (van Mantgem *et al.*, 2009; Peng *et al.*, 2011) in part through increases in drought-related tree mortality (Allen *et al.*, 2015). Elevated mortality could have profound ramifications on forested systems (Anderegg *et al.*, 2013a) and represent a major challenge to resource managers tasked with maintaining healthy, productive forests in an uncertain future (Clark *et al.*, 2016; Vose *et al.*, 2016). Manipulating stand structure and composition through silvicultural practices could mitigate stressful conditions from future disturbances (Puettmann, 2011). However, it remains unclear as

to whether such tools could be effective under future extreme droughts. Knowledge of forest stand response to extreme drought is critical for guiding and adapting future management strategies aimed at mitigating the impacts of a changing climate on forests.

From October 2010 to September 2011, the state of Texas experienced the most extreme drought on record with over 80% of the land area under the most severe drought classification (Nielsen-Gammon, 2012). The heavily forested region of east Texas followed temperature and precipitation patterns seen statewide during the drought, having the hottest summer temperature deviation (+3.1 C) and lowest 12-month precipitation (619 mm; 47% lower than 20th century average of 1162 mm) (NOAA 2018). Regarding tree mortality within east Texas, *Pinus* fared better than other common genera such as *Quercus* and *Liquidambar* (Moore *et al.*, 2016; Klockow *et al.*, 2018). Given their economic importance and the high proportion of planted pine in the region, the drought provides an opportunity to assess which pines were most affected and to identify specific sources of vulnerability to be addressed by improved management practices that further mitigate risks of mortality from extreme drought.

Nearly 20% of all pine-dominated forest in the southeastern U.S. is comprised of intensively managed plantations (Chen *et al.*, 2017) often receiving competition control, fertilization, and planting of genetically improved seedlings at calculated densities (Fox *et al.*, 2007). In east Texas, loblolly pine (*Pinus taeda* L.) is an important economic species with large proportions of both heavily managed planted pine and unmanaged or minimally-managed, naturally-regenerated pine (Texas A&M Forest Service, Annual Forest Report 2017). This dichotomy in loblolly pine condition has led to questions

about the functionality of plantations compared to naturally-regenerated stands of this species under drought. Evidence from a comparison of physiological characteristics (i.e. root hydraulic conductivity, root:shoot ratios) suggested that plantation loblolly pine should be more drought-sensitive than naturally-regenerated pine in terms of productivity (Domec *et al.*, 2015) possibly driven by fertilization inputs affecting transpiration and root production (Ward *et al.*, 2015). However, fertilized plantation pine at the western edge of its range increased water use efficiency and sustained productivity under water-limited conditions (Maggard *et al.*, 2017; Bracho *et al.*, 2018) suggesting intensively managed pine could better cope with drought. Still, there has been no study contrasting planted and naturally-regenerated pine, particularly under extreme drought, informing whether their perceived differences translate into differential mortality response.

Species selection for planting may also play a role in the overall mortality response of regional pine to drought. Shortleaf pine (*Pinus echinata*) has a perceived potential to withstand drought given its historical occurrence across a range of site conditions including xeric sites and rocky outcrops (Mattoon, 1915). Under non-drought conditions, mature shortleaf pine sustained higher mortality and lower productivity than loblolly pine in southeastern Oklahoma (Dipesh *et al.*, 2015) yet, it remains unclear how they compare under extreme drought conditions. Shortleaf pine has seen drastically reduced dominance because of logging and subsequent fire suppression (Barrett, 1995) leading to widespread restoration initiatives to increase its prevalence in the southeastern U.S. (e.g., Shortleaf Pine Initiative). East Texas is one region in which this species could

be targeted for restoration efforts. Yet, limited information on growth and mortality responses to drought hinder management efforts aimed at successfully restoring this declining species, particularly in the face of an uncertain climate future.

Stand structure (e.g., tree size, stem density, and species composition) represents one set of conditions most easily manipulated by managers for mitigating negative drought effects (Clark *et al.*, 2016). It is well-documented that the smallest and largest trees tend to experience higher mortality rates, often termed 'U-shaped' or 'J-shaped' mortality curves (Lines *et al.*, 2010; Dietze and Moorcroft, 2011). Small stems typically comprise the regenerating component of early-successional forests and elevated drought mortality in this group could alter future forest composition (Thrippleton *et al.*, 2018). Large trees play important ecological roles in forested ecosystems (Lindenmayer *et al.*, 2012) yet, recent evidence suggests that they may be most susceptible to extreme drought and are suffering disproportionate mortality worldwide (Lindenmayer *et al.*, 2012; Bennett *et al.*, 2015). However, these patterns in large tree drought mortality can be variable and difficult to confirm (Floyd *et al.*, 2009; Klos *et al.*, 2009; Ganey and Vojta, 2011). Additionally, alleviating competition for limited resources by reducing stand density and basal area (cross-sectional stem area at 1.37 m height) has long been utilized by practitioners to improve growth and productivity. Reducing competition through silvicultural thinning has improved growth response to water stress (D'Amato *et al.*, 2013; Bottero *et al.*, 2017; Gleason *et al.*, 2017). However, extreme drought conditions that drive very low soil water potentials may negate any benefits gained from reduced competition resulting in increased tree mortality across a range of densities

(Floyd *et al.*, 2009). Finally, stand species composition can be an important factor in affecting drought mortality (Klos *et al.*, 2009; Cavin *et al.*, 2013) as interactions with water and nutrient pools may differ among species (Forrester, 2014). Neighboring trees of different species may show facilitation via hydraulic lift more than competition (Pretzsch *et al.*, 2013) or access different resource pools alleviating stressful conditions (Kramer and Holscher, 2010) which may be exacerbated in single-species-dominated stands.

The magnitude and widespread nature of the 2011 drought in east Texas provided a unique opportunity to address questions related to the mortality of pine species and associated stand structure in this region. Using national forest inventory (NFI) plots with complete and systematic coverage of east Texas, we addressed the following objectives, 1) compare mortality rates of three common pine species groups (i.e., planted loblolly pine, naturally-regenerated loblolly pine, and shortleaf pine) under exceptional drought conditions and pre-drought conditions, 2) determine how stand structure (i.e., tree size, stem density, and species composition) affected individual tree mortality in the same pine species groups under exceptional drought conditions and pre-drought conditions, and 3) provide targeted management suggestions based on predicted mortality trends for mitigating extreme drought mortality in southern pine. We address these objectives at the individual tree scale using extensive re-measurements of pine.

For objective 1, we hypothesize that pre-drought group mortality rates will be lowest in planted loblolly pine, given the extensive competition control and management actions in this group, and highest in the shortleaf pine group, given past evidence from

Dipesh *et al.* (2015) under non-drought conditions. Regarding objective 2, we hypothesize for each group that, under pre-drought conditions, smaller trees will have higher mortality given their limited rooting depth and access to deeper water. Larger trees will have higher mortality potentially due to greater hydraulic stress, increased crown exposure, and preference by bark beetles (Bennett *et al.*, 2015). Furthermore, under pre-drought conditions, the highest stem densities will show higher mortality following expected patterns of competition and the lowest stem densities will show higher mortality due to possible increased individual tree risk from maintenance of greater leaf area and root systems (Clark *et al.*, 2016). Finally, pure species mixtures will show higher mortality possibly through increased intra-specific competition (Klos *et al.*, 2009). We generally expect that mortality increased from pre-drought to drought period for each group and each stand structure factor given the extreme nature of the drought.

Methods

Study Area

Our study was located in eastern Texas (29° 17’ to 33° 57’ N and 93° 30’ to 96° 27’ W; Figure III.1), comprising the western extent of West Gulf Coastal Plain forests. Forests in this region are composed of a diverse species mix yet are heavily dominated by pine species, namely loblolly pine (*Pinus taeda* L.) followed by shortleaf pine (*Pinus echinata*). Hardwood species tend to comprise much of the mid- and under-story and include a diverse mix of oaks (e.g., *Quercus stellata*, *Quercus nigra*, etc.), sweetgum (*Liquidambar styraciflua*), and elm species (e.g., *Ulmus alata*). Climate is generally

humid sub-tropical with hot, humid summers and mild, wet winters. During the study period (2003-2016), mean annual precipitation and temperature ranged between 769-1737 mm and 18.1-20.1 °C, respectively (20th century averages of 1162 mm and 18.6 °C, respectively) with the lowest precipitation (769 mm) and second highest temperature (19.9 °C) during this period occurring in 2011 (NOAA 2018). Variation in topography is minimal with flat to rolling elevation changes ranging from sea-level near the coast to nearly 200 m above sea level. Soils are variable, ranging from poorly-drained to well-drained conditions predominantly comprised of loamy to clayey Alfisols and Ultisols (USDA NRCS 2006).

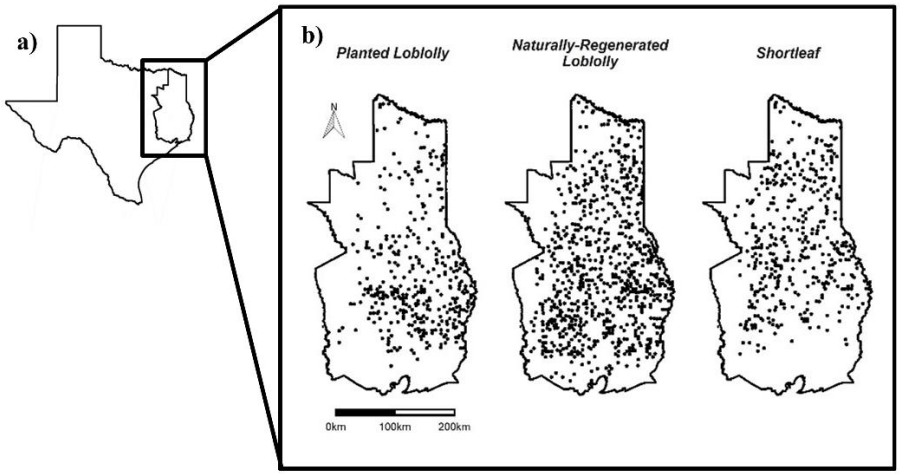

Figure III.1 State of Texas map with (a) study area (east Texas) as inset and (b) Forest Inventory and Analysis plot locations used for each pine group.

Dataset

Data were taken from the U.S. Forest Service Forest Inventory and Analysis (FIA) program for east Texas. The full dataset consisted of 1,640 forested (> 10% tree cover) plots. A plot consists of four subplots each covering 168.1 m^2 (~672.5 m^2 total plot area) with one central subplot and the three remaining subplots oriented ~36.6 m distance (central subplot-center to outer subplot-center) at 0, 120, and 240 degrees. Trees were classified as stems ≥ 2.54 cm diameter at breast height (DBH; 1.37 m stem height). Trees with DBH ≥ 2.54 cm and < 12.7 cm were measured on four microplots (13.5 m^2

each, ~54.0 m^2 total) located within subplots while trees with DBH ≥ 12.7 cm were measured on each full subplot. Species, DBH, status (live or dead) were all recorded at each plot measurement and used in this study.

We categorized trees within the dataset as planted loblolly pine (PL), naturally-regenerated loblolly pine (NL), and shortleaf pine (SL). Planted loblolly was identified by selecting plots originating from planted seedlings of loblolly pine and NL was identified by selecting plots of non-planted origin. There existed a few instances where a plot straddled both PL and NL conditions. We excluded these plots from our dataset to avoid the confounding effects of active or non-management at the interface of PL and NL conditions. Given the rare occurrence of shortleaf pine plantations coupled with their relatively low numbers in the dataset, shortleaf pine was categorized as one group. All harvested/salvaged trees were excluded from the dataset to avoid confounding effects of silvicultural activity on mortality.

We classified trees into two measurement periods, pre-drought and drought. The pre-drought period consisted of trees initially measured as being alive and subsequently re-measured as alive or dead prior to 2011 (i.e., 2003-2010). Thus, the mortality response of pre-drought trees was not affected by the 2011 drought. Drought period trees were initially measured as alive prior to 2011 and subsequently re-measured as alive or dead after 2011 (i.e., 2012-2016). Thus, the mortality response of drought period trees reflect exposure to the 2011 drought assuming any individual tree did not die after initial measurement and prior to the onset of the drought. All plots were re-measured over approximately a five-year period.

We selected and calculated stand structural variables prior to any analysis, including DBH, plot relative density (RD; after Ducey and Knapp (2010)), and plot species group dominance (SPD; basal area of a focal species group in a plot divided by total basal area of the plot). Variable selections were chosen based on their importance in describing individual tree size/age and local inter- and intra-specific competitive interactions. Moreover, the variables included in our analyses represent common metrics used by managers for manipulating forest conditions. All data were summarized and presented in Table III.1.

Table III.1 Summary information for the pine groups analyzed in the study. Pre-drought period (Pre) refers to trees measured prior to the 2011 drought and drought period (Drought) refers to trees initially measured prior to 2011 and re-measured after 2011. Diameter at breast height (DBH) is summarized across individual trees while relative density and species dominance are plot-level metrics. Median values and 2.5th and 97.5th quantiles are presented in parentheses.

Pine Group	Period	Plot Count	Tree Count	DBH (cm)	Relative Density	Species Dominance
Planted Loblolly	Pre	173	3347	17.0 (4.6, 31.6)	0.37 (0.03, 0.95)	0.88 (0.16, 1.00)
	Drought	282	5855	17.3 (4.8, 32.8)	0.38 (0.03, 1.00)	0.87 (0.11, 1.00)
Naturally-regenerated Loblolly	Pre	444	3992	18.0 (3.3, 54.6)	0.53 (0.03, 1.09)	0.40 (0.03, 0.95)
	Drought	612	5489	19.8 (3.3, 58.9)	0.57 (0.07 1.10)	0.40 (0.02, 0.96)
Shortleaf	Pre	231	871	22.6 (5.1, 50.0)	0.58 (0.14, 0.98)	0.12 (0.01, 0.69)
	Drought	316	1175	24.9 (6.9, 53.2)	0.59 (0.11, 1.10)	0.12 (0.01, 0.71)

Analysis

We analyzed the data for each objective using Bayesian logistic mixed-effects models. In all cases, the response variable was binary tree status (live = 1, dead = 0) modeled as a Bernoulli-distributed variable constrained by a probability of survival.

$$y_{ij} \sim Bernoulli(p_{Sij}) \quad \text{(III.1)}$$

Where, y_{ij} is the response for tree i in plot j and p_{Sij} is the probability of survival for tree i in plot j. To account for variability in plot re-measurement time, we used an approach first presented by Hamilton Jr. and Edwards (1976) and incorporated a random effect component.

$$p_{Sij} = \left[\frac{1}{1+ e^{-\left(X_{ij}^T \beta_k + \mu_j\right)}}\right]^{L_j} \quad \text{(III.2)}$$

Where, p_{Sij} is the same as described in equation 1, X^T_{ij} is the transposed matrix of covariates for tree i in plot j, β_k is the vector of length k of parameters to be estimated, u_j is the random effect of plot j, and L_j is the re-measurement interval for plot j. Using this approach, the estimated β_k's describe the annual log odds of survival for each tree as opposed to the log odds of survival for the specific re-measurement interval L_j. We included the random effect in each model to account for plot-level variability from site differences. Random effects were modeled as a normally-distributed variable with mean of zero and common variance.

$$\mu_j \sim Normal(0, \sigma^2) \quad \text{(III.3)}$$

Where, μ_j is the mean effect in log odds for plot j and σ^2 is the variance of the distribution of plot mean effects. For objective 1, a single model was constructed and

explanatory variables included the three pine groups (PG: PL, NL, SL), two measurement periods (MP: pre-drought, drought), and their interaction.

$$X = PG + MP + PG * MP \quad \text{(III.4)}$$

Where, X is the matrix of covariates from equation III.2. For objective 2, separate models were constructed for each pine group and measurement period (six total). Explanatory variables for each model included the three stand structural variables of DBH, RD, and SPD. All the explanatory variables were modeled as having a quadratic effect on predicted survival response.

$$X = DBH + DBH^2 + RD + RD^2 + SPD + SPD^2 \quad \text{(III.5)}$$

Where, X is the matrix of covariates from equation III.2. Variables for objective 2 were mean-centered and standardized to allow for more meaningful comparison of the effect sizes of each variable on predicted mortality within each model. For the presentation of results, we converted survival probabilities to mortality probabilities via $p_{Mij} = 1 - p_{Sij}$.

All models were fit using Hamiltonian Monte Carlo simulations implemented in the RStan package (Stan Development Team, 2017) accessed via R software (R Core Team, 2016). Vague priors were chosen for the estimated parameters. Specifically, priors for β_k followed a normal distribution of mean zero and standard deviation of 10^4 and μ_j followed a uniform distribution with mean zero and range 10^4. Use of vague priors meant that results of these analyses should be close to estimations from a maximum likelihood analysis. Chains were run for 100k iterations with a 50k warm-up and were thinned by 1/20 to reduce autocorrelation. Chain convergence to the posterior

distribution was assessed visually using traceplots and by the R-hat statistic (Gelman and Rubin, 1992). To evaluate the performance of our models, we used a mixed posterior predictive assessment as developed by Green *et al.* (2009) and employed by Masuda and Stone (2015). Broadly, posterior predictive model checking involves simulating replicated data under its modeled distribution using each MCMC simulated value of the estimated model parameters and comparing these new data with the observed data set (Hobbs and Hooten, 2015). In particular, the mixed posterior predictive assessment provides a more conservative assessment of model performance, being similar to the widely-accepted cross-validation technique, than a full posterior predictive assessment, particularly for hierarchical models (e.g., containing a random effect) (Green *et al.*, 2009). This is accomplished by first drawing a new random effect for each group from its modeled distribution, adding the new mean effect to the estimated linear model component, and using the resulting value to draw a new observation from its modeled distribution. In contrast, the fixed posterior predictive assessment uses the estimated random effect rather than drawing a new one which consistently results in a deceptively better fit between observed data and replicated data (Green *et al.*, 2009).

We used common management metrics to produce mortality curves from our resulting models and identified particular areas where management actions could be implemented when extreme drought is a concern. Specifically, we produced mortality curves for 35% and 65% relative densities, which represent the range of fully-stocked stands, and for merchantable stem diameters of 15, 25, and 35 cm, representing common

pulpwood, small sawtimber, and large sawtimber stem sizes, respectively, in the study area.

Results

Pine Group Mortality

Drought mortality increased relative to pre-drought mortality for all pine groups by 9.8%, 20.0%, and 26.3% for PL, SL, and NL, respectively, yet, none differed significantly from its pre-drought period (Figure III.2, Appendix B: Table B.1). Planted loblolly pine had the lowest overall group mortality for both periods being significantly lower than NL and SL. Shortleaf pine had the highest overall mortality for both periods and had the greatest variability. Naturally-regenerated loblolly pine had the greatest increase in mortality between periods suggesting it was the most sensitive to the drought conditions.

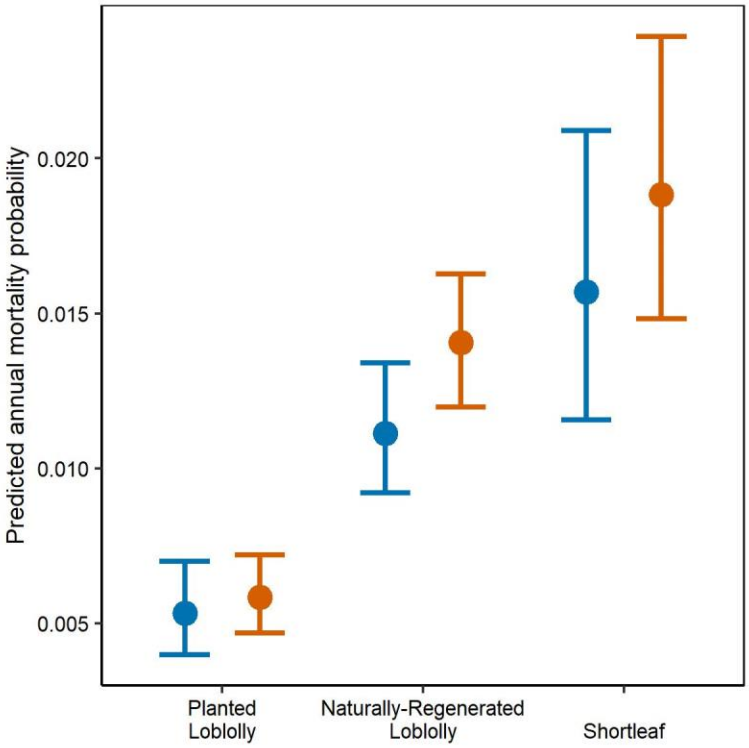

Figure III.2 Mortality probabilities for each pine group and measurement period with 95% credible intervals (blue = pre-drought, orange = drought). The R^2 for the mixed predictive assessment was 0.09. Prediction accuracy of live and dead trees was 0.999 and 0.132 for observed vs. predicted responses and 0.916 and 0.097 for replicated vs. predicted responses, respectively.

Stand Structure

Stand structure was most important for describing mortality in loblolly pine with differing effects across PL, NL, and measurement periods (Table III.2). Interestingly, stand structure did not describe mortality in SL under either period. Diameter at breast height followed the familiar 'U-shaped' or 'J-shaped' pattern, reflecting higher mortality in the smallest and largest stems, when examined in relation to mortality for both PL and NL in both periods (Table III.2). Drought accentuated this effect in the smallest and

largest stems of PL more so than in NL. Plot relative density significantly affected mortality in loblolly pine primarily causing greater mortality with increasing density, which was most pronounced in PL under drought (Table III.2). The effects of relative density on pre-drought NL mortality leveled off at the highest densities but, under drought, continued increasing at higher densities. Plot species dominance affected mortality among pre-drought PL causing lower mortality under more pure mixtures while drought-period NL experienced higher mortality with increasing NL dominance (Table III.2).

Table III.2 Model results for the effects of stand structure on pine group mortality for each measurement period with 95% credible intervals (DBH = diameter at breast height, RD = plot relative density, SPD = plot species dominance, Plot RE SD = estimated standard deviation from the random effect of plots). Bold estimates, intercepts, and Plot RE SDs are significantly different from zero. The bottom three rows provide metrics from model assessment including, proportion of explained variance from the mixed predictive assessment on observed vs. replicated data (R^2 MPA), accuracy of observed vs. predicted live and dead trees and, accuracy of replicated vs. predicted live and dead trees.

Estimated Parameters	Planted Loblolly		Naturally-regenerated Loblolly		Shortleaf	
Log Odds Mortality	Pre	Drought	Pre	Drought	Pre	Drought
Intercept	-5.617 (-6.183, -5.127)	-5.947 (-6.450, -5.498)	-4.924 (-5.291, -4.591)	-4.716 (-5.020, -4.417)	-4.848 (-5.789, -4.080)	-4.133 (-4.601, -3.705)
DBH	**-0.958 (-1.178, -0.748)**	**-1.082 (-1.234, -0.936)**	**-1.421 (-1.617, -1.239)**	**-1.130 (-1.272, -0.990)**	**-0.422 (-0.756, -0.098)**	-0.040 (-0.246, 0.173)
DBH^2	**0.188 (0.124, 0.249)**	**0.330 (0.274, 0.384)**	**0.451 (0.384, 0.517)**	**0.396 (0.341, 0.452)**	0.145 (-0.009, 0.286)	0.089 (-0.022, 0.192)
RD	**0.350 (0.031, 0.678)**	**0.831 (0.521, 1.169)**	**0.449 (0.251, 0.650)**	**0.233 (0.057, 0.414)**	0.257 (-0.096, 0.643)	0.098 (-0.106, 0.309)
RD^2	-0.128 (-0.357, 0.103)	0.017 (-0.191, 0.221)	**-0.160 (-0.312, -0.014)**	-0.037 (-0.161, 0.078)	0.024 (-0.260, 0.273)	0.075 (-0.037, 0.187)
SPD	**-0.587 (-1.075, -0.107)**	-0.071 (-0.520, 0.379)	0.130 (-0.064, 0.328)	**0.266 (0.074, 0.464)**	-0.094 (-0.567, 0.382)	0.061 (-0.186, 0.317)
SPD^2	**-0.221 (-0.439, -0.025)**	-0.176 (-0.383, 0.005)	0.006 (-0.162, 0.168)	-0.066 (-0.221, 0.086)	-0.016 (-0.484, 0.410)	0.037 (-0.231, 0.302)
Plot RE SD	-1.352 (-1.755, -1.016)	-1.715 (-2.087, -1.399)	-1.008 (-1.279, -0.762)	-1.458 (-1.657, -1.273)	-1.813 (-2.594, -1.205)	-1.067 (-1.417, -0.761)
R^2 MPA	0.38	0.25	0.71	0.20	0.07	0.07
Observed Pred. Acc. (live / dead)	0.999 / 0.014	0.997 / 0.330	0.996 / 0.144	0.991 / 0.315	1 / 0.144	0.997 / 0.070
Replicated Pred. Acc. (live / dead)	0.953 / 0.111	0.925 / 0.211	0.902 / 0.262	0.858 / 0.226	0.870 / 0.145	0.851 / 0.156

Management-Based Mortality Curves

Planted loblolly mortality curves for DBH highlight the vulnerability of the smallest and largest stem sizes under drought conditions (DBH of < 20 cm and > 40 cm; Figures III.3a, b). This effect was most pronounced in the largest stems at higher densities (65% RD; Figure III.3b). Merchantable stems of PL had very low mortality with very low variability regardless of period (Figures III.3a, b). Interestingly, smaller stems under pre-drought conditions did not significantly differ in mortality at 35% or 65% RD (Figure III.3c). However, smaller stems under extreme drought had significantly higher mortality at 65% RD than at 35% RD (Figure III.3d).

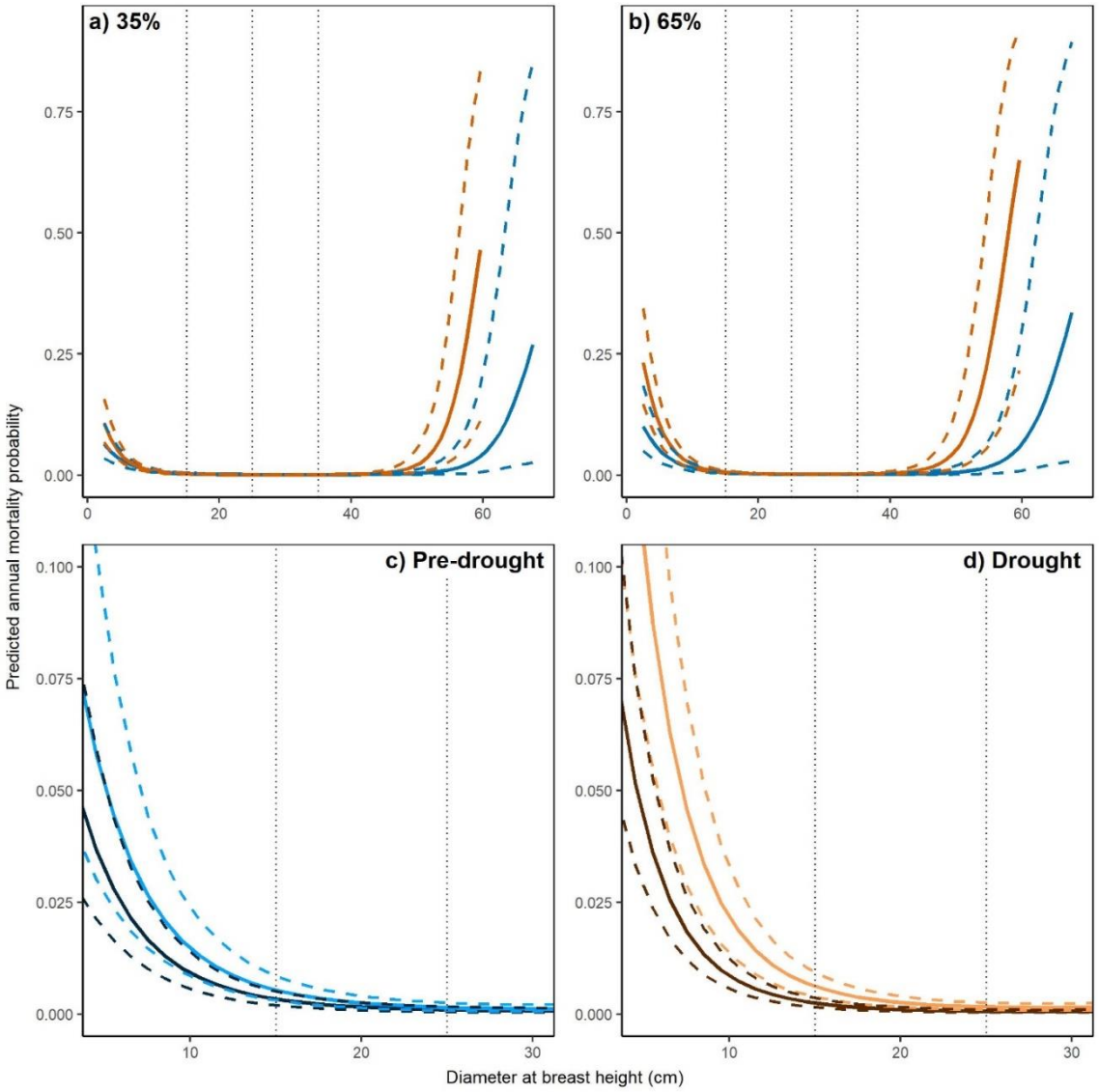

Figure III.3 Mortality curves (solid lines) for planted loblolly and diameter at breast height with 95% credible intervals (dashed lines). Relative density is held constant at the lower (35%) and upper (65%) limits of fully-stocked conditions while species dominance is held constant at its median values (~90%, see Table III.1). Dotted vertical lines highlight merchantable size classes (15, 25, and 35 cm DBH). Panels a) and b) show mortality curves across the full range of DBH values (panels a and b: blue = pre-drought, orange = drought) while panels c) and d) display notable differences which occur at smaller DBH values (panels c and d: 35% RD = dark blue, dark orange; 65% RD = light blue, light orange).

Naturally-regenerated loblolly pine had higher mortality in the smallest and largest stems but this effect did not differ between pre-drought and drought periods (Figures III.4a, b). As with PL, merchantable stems of NL had very low mortality with very low variability (Figures III.4a, b). However, merchantable stem mortality was significantly higher under extreme drought at 35% RD (Figure III.4c) whereas, at 65% RD, mortality did not differ between periods but was higher overall than at 35% RD (Figure III.4d). Interestingly, SPD mortality curves for NL indicated that drought mortality was significantly higher than pre-drought above ~50% loblolly dominance for all merchantable stem sizes (Figures III.5a, b, c). However, mortality was lower overall and did not differ significantly below ~50% loblolly dominance (Figures III.5a, b, c).

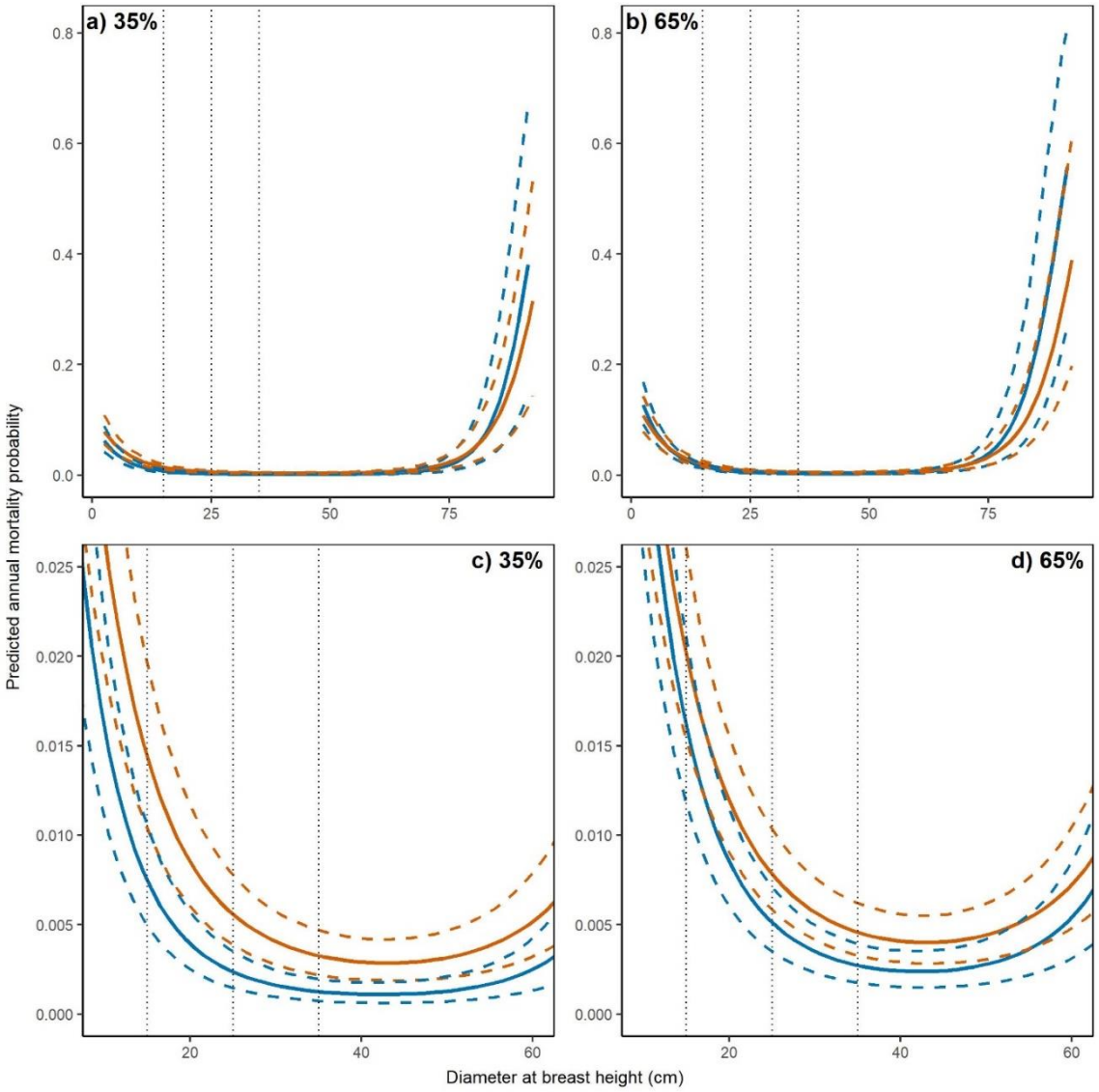

Figure III.4 Mortality curves (solid lines) for naturally-regenerated loblolly and diameter at breast height with 95% credible intervals (dashed lines) (blue = pre-drought, orange = drought). Relative density is held constant at the lower (35%) and upper (65%) limits of fully-stocked conditions while species dominance is held constant at its median values (~60%, see Table III.1). Dotted lines highlight merchantable size classes (15, 25, and 35 cm DBH). Panels a) and b) show mortality curves across the full range of DBH values in the dataset while panels c) and d) display notable differences which occur at small and mid-range DBH values.

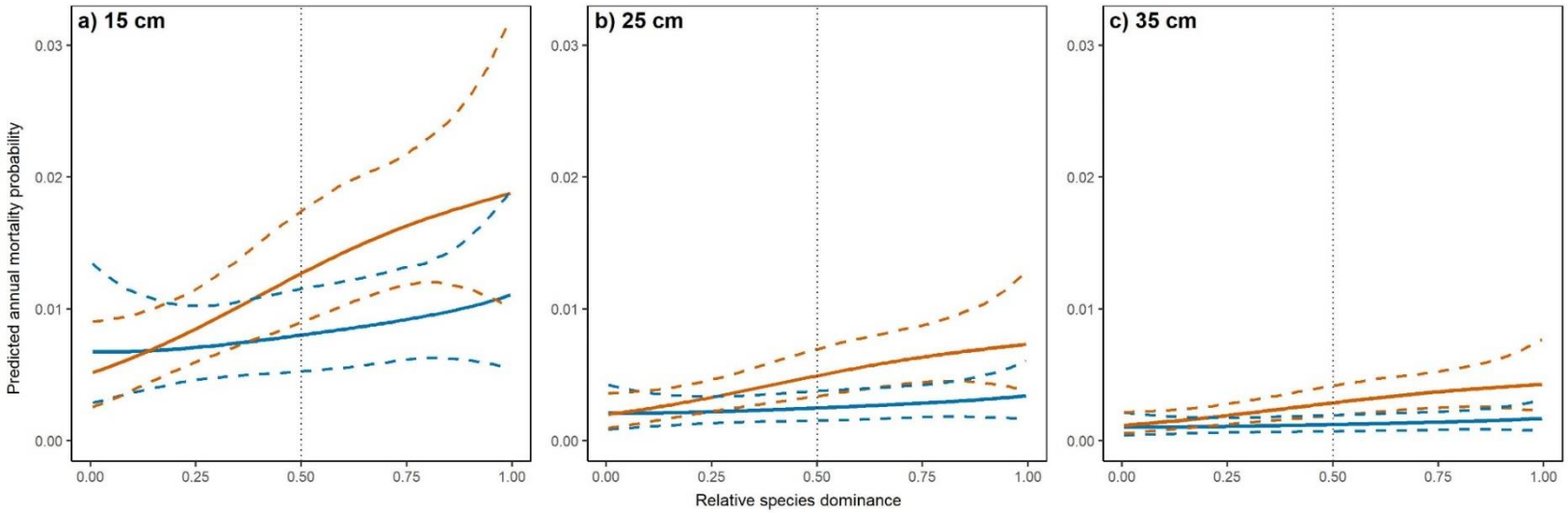

Figure III.5 Mortality curves (solid lines) for naturally-regenerated loblolly and species dominance with 95% credible intervals (dashed lines) (blue = pre-drought, orange = drought). Diameter at breast height is held constant at merchantable size classes (15, 25, and 35 cm) while relative density is held constant at the lower limit of fully-stocked conditions (35%). Dotted vertical lines highlight 50% dominance by naturally-regenerated loblolly.

Model Assessment

The mixed predictive assessment for the model based on equation 4 (i.e., pine groups and measurement periods) suggested that live trees were predicted accurately and mortality responses were not predicted well (Table III.2). This is likely attributable to the limited number of dead trees in the dataset for PL as it had low mortality during both periods and may also be attributable to the similarity in mortality estimates for NL and SL making differentiation between groups difficult. The mixed predictive assessment for the models based on equation 5 (i.e., stand structure) show that the PL and NL models performed fairly well while the SL models performed poorly (Table III.2). In all cases, live trees were predicted well while dead trees were predicted fairly (NL, PL) to poorly (SL). Since essentially none of the stand structural variables for SL significantly differed from zero and most were different from zero for PL and NL, it is not surprising that the SL models performed poorly and the PL and NL models provided better explanatory power for describing mortality.

Discussion

Pine Group Mortality

In this study, we provide a unique assessment of extreme drought mortality among both planted and naturally-regenerated pines. The effects of widespread and often intensive management actions in PL stands appears to play a critical role in mitigating mortality from extreme drought. Planted loblolly mortality was lowest of the three pine groups for both pre-drought and drought conditions, providing support for our

hypothesis for pre-drought PL. Interestingly, extreme drought exposure did not result in disproportionate vulnerability to drought in PL as has been hypothesized (Domec *et al.*, 2015). Klos *et al.* (2009) observed higher drought sensitivity (growth and mortality) in pine species of Alabama, Georgia, and Virginia; however, they did not separate out PL from NL. Also, pines in the Klos *et al.* (2009) study occur in the central reaches of their geographical distribution, whereas east Texas represents the western range margin of loblolly pine. It is possible loblolly pine genotypes in Texas are better adapted to drier, more variable climate than those further east (McNulty *et al.*, 2014; Rehm *et al.*, 2015). Recent examination of PL growth in the West Gulf Coastal Plain suggests that, even under water-limited conditions (albeit not as extreme as the 2011 drought), trees remained productive particularly when given fertilizer inputs (Maggard *et al.*, 2017), suggesting positive response of water-stressed PL under management. However, Maggard *et al.* (2017) addressed growth and not mortality response of PL. Critically, it appears the management actions associated with PL likely allowed these stands to endure the harsh water stress of the 2011 drought.

Of the groups examined, NL appeared the most vulnerable to extreme drought having the highest increase in mortality (26.3% increase). A challenge with examining this group as a whole across the region of east Texas is disentangling the multiple factors driving this mortality response. Often, NL stands remain unmanaged until harvest, however, many stands of NL still have active competition control to improve productivity (Nelson and Bragg, 2016) providing an advantage when exposed to water stress. The existence of some management activity in a portion of NL stands may have

muted the mortality response of unmanaged stands. Regardless, our data highlight that NL stands, as a whole, typically have higher densities across east Texas than PL (Table III.1) suggesting that density-dependent competition may be driving the higher mortality in this group.

Shortleaf pine maintained the highest group mortality rates under both measurement periods, providing some support for the hypothesis that this species experiences the highest pre-drought mortality of the pine groups examined. This agrees with a recent study conducted in forests of southeastern Oklahoma, which reported higher mortality in SL compared to PL (Dipesh *et al.*, 2015). The high variability in mortality estimates for SL can be attributed to the relatively small sample size in our dataset. Ultimately, SL is a relatively minor component of east Texas forests (~3% of all species measured by FIA) possibly occurring on sites less suitable for loblolly production. Thus, these high mortality rates may be more reflective of inherent site conditions than any particular physiological adaptations suited for drought.

Stand Structure

It is evident from our data that stand structure, particularly tree size and relative density, played an important role in driving mortality in loblolly pine. Our hypothesis of 'U-shaped' or 'J-shaped' tree size mortality was supported in both PL and NL confirming the vulnerability of the smallest and largest trees. Higher mortality in smaller stems is most likely driven by inter- and intra-specific competitive effects before reaching maturity. Increased mortality in larger stems could be driven by multiple effects

including senescence, preference by pests (Pfeifer *et al.*, 2011), windthrow (Harcombe *et al.*, 2009), and increased susceptibility to hydraulic failure (Zhang *et al.*, 2009). Interestingly, tree size appeared to have a greater effect on drought period mortality in the smallest and largest PL stems than NL. D'Amato *et al.* (2013) found that pine stands thinned at a young age and maintained at a low density exhibited lower growth resistance and resilience to drought at later ages likely due to difficulty maintaining high leaf area-to-sapwood ratios developed over time in the low-density conditions. It is possible this effect is occurring in intensively managed loblolly pine stands in east Texas which were thinned and maintained at low densities and slated for harvest beyond a typical rotation age (e.g., > 25 years) but were later abandoned.

Density-dependent mortality in PL and NL followed expected trends of increasing mortality with increasing density (linear trend) yet did not show increasing mortality at lower densities (quadratic trend). A growing body of literature has found density-dependent mortality occurs in pine species under increasingly water-limited conditions across temperature and precipitation gradients (D'Amato *et al.*, 2013; Bottero *et al.*, 2017; Gleason *et al.*, 2017). Resources inherently become limited as the number of trees occupying the potential growing space in a stand increases and this appeared to be exacerbated under extreme drought conditions for PL. Naturally-regenerated loblolly trees growing at low densities may have greater canopy area and root architecture than denser stands, given the increased growing space and access to resources (D'Amato *et al.*, 2013), and may be more prone to hydraulic failure possibly causing the elevated drought mortality in low density NL stands compared to pre-drought.

Under extreme drought, species dominance became a significant factor in describing NL mortality but did not play a substantial role in PL mortality. Planted loblolly predominantly occurs in monocultures and ~85% of all PL plots had > 50% of basal area as PL. In fact, mortality decreased as PL dominance increased under pre-drought conditions. This likely reflects that, as PL dominance reaches 100%, these plots occur in the most intensively managed plantations where competition control is most prevalent. Thus, pure stands of PL may be more buffered against mortality if they are primarily occurring in active plantations. Interestingly, intra-specific competition significantly increased mortality in NL-dominated stands under extreme drought, suggesting that more overstory diversity in NL stands allows for resource partitioning or facilitative effects between mature pine and other species, an effect also noted by Klos *et al.* (2009).

Management Implications

A critical finding of this study was that, broadly, the inherent management of PL stands appeared to play a key role in mitigating extreme drought stress. In general, PL stands were maintained at lower densities (i.e., within the range of fully-stocked conditions) and at smaller stem sizes compared to NL. These basic management-related effects may have provided the important buffer needed to keep mortality low in PL. Management suggestions for NL stands are comparable to those for PL with density of NL stems being a key driver of mortality risk. Maintaining stands in fully-stocked conditions and even understocked conditions could reduce overall mortality, particularly

from extreme drought. Importantly, promoting other species, ≤ 50% NL basal area, could provide a key advantage for reducing extreme drought mortality in NL stands, particularly at lower densities. Finally, it remains unclear as to what management strategies could benefit SL under extreme drought conditions. The general suggestions presented here are based on broad-scale modeling results from West Gulf Coastal Plain forests. Reduction of mortality risk depends on local conditions and, critically, overarching management objectives. However, these suggestions provide straightforward management actions that potentially could be implemented by resource managers concerned about extreme drought mortality.

CHAPTER IV

TREE- AND SNAG-FALL DYNAMICS IN WEST GULF COASTAL PLAIN FORESTS OF EAST TEXAS

Introduction

Standing dead trees, often termed ‘snags’, are an important structural component of forested ecosystems. Snags influence carbon and nutrient cycling (Mobley *et al.*, 2013), provide habitat for myriad wildlife species and other saproxylic organisms (Jones *et al.*, 2009), and impact fuel loads and wildland fire behavior (Collins *et al.*, 2012; Schoennagel *et al.*, 2012). Populations of snags within forested systems fluctuate based on the processes driving their creation (i.e., tree mortality) and transition (i.e., falling) to the downed wood pool (Harmon *et al.*, 1986; Vanderwel *et al.*, 2006b). In particular, large-scale disturbances can result in major shifts of biomass and carbon from the live tree pool to the dead wood pool (Breshears *et al.*, 2005; Moore *et al.*, 2016; Young *et al.*, 2017). Hurricane winds can snap and uproot large swaths of trees causing rapid transition from standing to downed dead wood or cause sufficient damage to kill trees that remain standing (Harcombe *et al.*, 2009; Edgar *et al.*, 2019). Future climate projections indicate that many regions will become hotter and drier within just a few decades, potentially increasing the number of snags in forested ecosystems via drought mortality (Allen *et al.*, 2015). As an example, the U.S. state of Texas experienced the worst drought on record from October 2010 to September 2011 resulting in 301 million newly dead trees statewide in just one year (Moore *et al.*, 2016) with more trees dying in

subsequent years (Klockow *et al.*, 2018). Understanding the dynamics of snags is therefore crucial for building quantitative tools to constrain carbon dynamics models as well as informing management objectives aimed at providing wildlife habitat and reducing wildland fire risk.

Climate and wood durability are key drivers of the decomposition and transition of snags to the downed wood pool (Oberle *et al.*, 2018). Many studies have examined the dynamics of snags in forested systems with particular emphasis in boreal and northern temperate forests where snags often persist for many decades (Cline *et al.*, 1980; Morrison and Raphael, 1993; Lee, 1998; Kruys *et al.*, 2002; Aakala *et al.*, 2008; Aakala, 2010; Angers *et al.*, 2012; Russell and Weiskittel, 2012; Yatskov *et al.*, 2019). In humid temperate forests of the southeastern U.S., dead wood studies are less common and tend to focus on dynamics of snags in relation to wildlife habitat, as many cavity-nesting species exist in this region (Jones *et al.*, 2009). However, the climate of this region and the unique decomposer community (i.e., presence of termites) (Zhang *et al.*, 2016) can make the longevity of snags quite ephemeral, often falling within 5-10 years (Moorman *et al.*, 1999; Conner and Saenz, 2005; Zarnoch *et al.*, 2013). Moreover, intensive management practices have been shown to reduce snag populations (Moorman *et al.*, 1999; Zarnoch *et al.*, 2014) making this resource more scarce on portions of the landscape. Smaller stems have generally been reported to fall faster than larger stems (Cain, 1996; Zarnoch *et al.*, 2013). However, some studies have reported no effect of stem size on fall rate (Moorman *et al.*, 1999; Radtke *et al.*, 2009). Stand density can influence fall rates, presumably by shielding trees from wind under increasingly greater

stem densities, yet, closely spaced stems could have a domino-effect, knocking over many stems despite only a few actually being blown over (Oberle *et al.*, 2018). In general, hardwood material tends to decay faster than softwood material when in contact with the ground (Weedon *et al.*, 2009; Zell *et al.*, 2009). However, limited studies have directly compared fall rates of wood types (i.e., hardwoods vs. softwoods) and tend to focus more on local species-level differences (Moorman *et al.*, 1999; Conner and Saenz, 2005). West Gulf Coastal Plain forests have received limited attention in regards to snag dynamics (Cain, 1996; Conner and Saenz, 2005). This region is characterized by intensive forest management, a warmer and more humid climate than other portions of the southeastern U.S., presence of termites, and potential for frequent large-scale disturbances, all of which impact snag dynamics. Subsequently, understanding snag dynamics in this region will provide the necessary tools for informing management of standing dead wood resources.

Transition of live trees to the downed wood pool follows relatively straightforward pathways. Specifically, live trees either die and fall simultaneously or they die and eventually fall after experiencing some level of decomposition (Vanderwel *et al.* (2006b), see their Figure 1, points A and B). Snags that remain standing continue to decompose and transition through decay classifications until eventually falling (Kruys *et al.*, 2002; Vanderwel *et al.*, 2006b). These scenarios continually iterate over time and have some probability of occurrence based on the time step between inventory re-measurements, often five-years (Kruys *et al.*, 2002; Vanderwel *et al.*, 2006a; Aakala *et al.*, 2008; Russell and Weiskittel, 2012). Many methods exist for representing the

dynamics of tree- and snag-fall (Storaunet and Rolstad, 2004), however, since these dynamics are a binary process (e.g., a stem either is standing or fallen at measurement), logistic regression methods provide a useful means for examining the probability of falling within a re-measurement period. Ultimately, these models can provide important utility by linking with models of tree mortality and snag decay class transitions to reveal patterns and drivers of biomass and carbon dynamics subsequently informing nutrient models and management objectives.

The goal of this study was to develop models predicting the probability of a tree falling in the five-year measurement interval in which it dies and the five-year probability of a snag falling in east Texas forests. Probabilities of tree- and snag- fall are delineated by examining common inventory metrics of size, stem density, height, wood type (i.e., hardwood, softwood) and decay class (i.e., for snags). Results from this study serve the purpose of better constraining models of decomposition and carbon dynamics in a region with rapid decay and potential for major future disturbances causing large-scale shifts in live-to-dead wood pools (e.g., hurricanes, extreme droughts). The specific objectives were to 1) develop models predicting five-year tree-fall and snag-fall probabilities for hardwood and softwood species in east Texas and 2) examine and assess differences in tree-fall and snag-fall processes by sizes, stem density, height, wood types, and decay classes. As a simple example of snag-fall model utility, Monte Carlo simulations were calculated representing the five-year transition of carbon in snags to downed dead wood following the 2011 Texas drought using models of snag-fall probability from objective 1.

Methods

Study Area

The focal study area was the eastern region of the state of Texas (Figure IV.1) which encompasses the western range margin of West Gulf Coastal Plain forests (29°17' to 33°57' N and 93°30' to 96°27' W). Climate in this region is generally hot and humid during the summer with mild and wet conditions during the winter. Temperature and precipitation have annual means of approximately 18.6°C and 1162 mm, respectively (NOAA 2019). Topography is flat to rolling with elevation ranging from sea-level up to around 200 m above sea level. Soils generally consist of the orders Alfisols and Ultisols with loamy to clayey textures (USDA NRCS 2006). This region encompasses the Pineywoods ecoregion which contains forests very similar to those throughout the Lower Coastal Plain of the southeastern U.S. Loblolly pine (*Pinus taeda* L.) is the dominant tree and dominant conifer, prevalent in both managed (e.g., plantations) and naturally-regenerated stands. Shortleaf pine (*Pinus echinata*) is the second most prevalent pine species and mostly occurs as naturally regenerated forests. Hardwood species are diverse and occur throughout the entire region in upland and lowland habitats. Oaks are most prevalent, particularly post oak (*Quercus stellata*) and water oak (*Quercus nigra*) followed by sweetgum (*Liquidambar styraciflua*) and winged elm (*Ulmus alata*). The region is characterized by a variety of disturbances at both small and large scales. Recent notable major disturbances have included hurricane Rita in September 2005, hurricane Ike in September 2008, and the worst drought on record from October 2010 to

September 2011 (Hoerling *et al.*, 2013) all of which resulted in substantial tree mortality in this region (Moore *et al.*, 2016; Klockow *et al.*, 2018; Edgar *et al.*, 2019).

Figure IV.1 Study area of a) east Texas region within state of Texas with b) plot locations containing at least one hardwood or softwood stem in each of the tree-fall and snag-fall datasets.

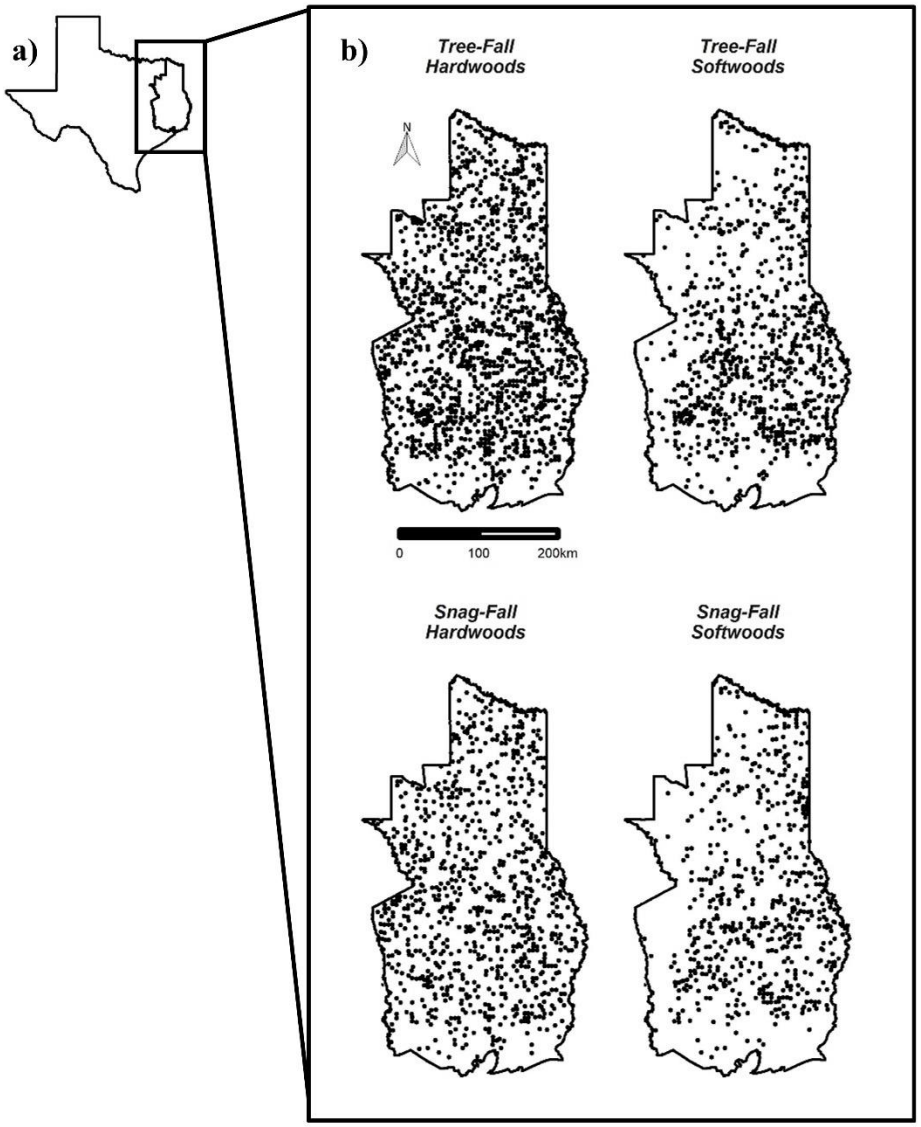

Data

Data used in this study were queried from the U.S. Forest Service Forest Inventory and Analysis (FIA) program database for the years 2004-2016 within the region of east Texas. The FIA program measures a systematic grid of plots each approximately 0.07 ha in area and representing approximately 2400 ha of the landscape (Bechtold and Patterson, 2005). Plots are laid out with one central and three radially-oriented circular subplots at 0, 120, and 240 degrees and 36.58 m distance relative to the central subplot center point each with a 7.31 m radius. Plots are organized into a series of five panels with each panel measured annually and representing a random sample of 20% of all plots. Plots are then re-measured starting with the first panel after all five panels have been completed. The years chosen for analyses in this study represent the first year the five panel inventory began (2004) and the most recently available data (2016). Data were downloaded from the FIA DataMart on February 15, 2018.

Trees and snags were selected from plots containing at least one forested condition within the plot. FIA defines forestland to have at least 10% canopy cover of live trees within an area approximately 0.40 ha and at least 36.58 m wide. Trees and snags ≥ 12.7 cm diameter at breast height (DBH) tallied on forested portions of plots were selected for analyses. The tree-fall dataset was defined such that trees were alive at the initial measurement and dead at re-measurement, approximately five years later. Status of dead trees at re-measurement was either as a SDT, defined as ≥ 1.37 m in height and leaning ≤ 45 degrees from vertical, or downed which did not meet these criteria. The snag-fall dataset was defined such that all stems were classified as SDT at

initial measurement and either SDT or downed at re-measurement. Tree-fall and snag-fall datasets were further split by wood type class (i.e., hardwoods and softwoods) as assigned by FIA based on field-assigned species. All harvested stems and ingrowth (i.e., a stem which first appeared as a dead tree in the dataset with no previous measurement as alive) were excluded from both datasets. A small portion of snag-fall stems (n = 168) reverted decay classes during re-measurement period, i.e., re-measurement decay class was a less-decayed status than the initial decay class, and were excluded from analyses. An even smaller portion of trees and snags (n = 10) were assigned different wood type classes (i.e., hardwood or softwood) at initial measurement and re-measurement. Subsequently, the initial wood type class assignment was used for classification given that it was likely more discernible at the earlier measurement than after some amount of decay at re-measurement.

While the two datasets, tree-fall and snag-fall, categorically represent distinct groups, we acknowledge that there is likely overlap between the processes occurring for either group. For example, a tree in the tree-fall dataset was measured as alive and may die one year later and spend the remaining four years as a SDT and either fall or remain standing before the next measurement. Likewise, a SDT in the snag-fall dataset may have been alive one year prior to initial measurement in which it was dead and be of very similar status to the previously described example tree in the tree-fall dataset. We were unable to discern and account for this perceived overlap in the two datasets which has been similarly analyzed in a previous study using five-year inventory data (Vanderwel *et al.*, 2006a). However, these categories represent an inherent challenge

with defining mortality processes in forest inventories that often utilize multi-year re-measurement intervals. Importantly, the tree-fall dataset accounts for two key processes, that being a tree that dies and falls simultaneously or a newly dead tree that spends a short time as a SDT and either remains standing or falls five years later. Whereas, the snag-fall dataset represents one general process in which SDT at various levels of decay either remain standing or fall after five years.

Common tree- and stand-level covariates were used in analyses for understanding the probability of tree- or snag-fall over a five-year period. These covariates included DBH (cm), height (m), and plot live stem density (stems/ha) and are often key parameters measured during an inventory and thus, readily available in most datasets. Values used in analyses pertained to those collected during the initial measurement representing the last known conditions of the tree or snag prior to re-measurement. Plot live stem density was calculated using all live stems for the entire plot (i.e., four subplots whether in FIA-defined forested or non-forested conditions). For the snag-fall dataset, decay class was included as a fixed effect to account for the general stage of decay of a particular stem at initial measurement. Variability in plot conditions as well as autocorrelation between stems in the same plot was accounted for by including plot as a random effect (Penner *et al.*, 1995). An additional random effect of physiographic class was also included to account for explicit differences in site conditions. FIA measures various subcategories of physiographic class conditions at each plot which are part of three major categories, xeric, mesic, and hydric conditions. For the tree-fall and snag-fall datasets, over 95% of the stems in each dataset occurred in

mesic class conditions. Following this, class groups were reassigned to aggregate some group sizes and help with interpretability. Specifically, all xeric conditions were grouped together into one class and all hydric conditions were grouped together into one class. Mesic subcategories were grouped into uplands, flatwoods, and bottomlands, generally representing a gradient of dry-to-wet conditions within the mesic category plus a fourth mesic category labeled 'other' which represented <1% of stems.

When FIA field crews encounter a newly dead tree during an inventory, they assign a perceived agent of mortality and estimated year of mortality. All stems in the tree-fall dataset were assigned such agents and an estimated mortality year given that they were newly dead trees. These classifications were used to discern unique processes occurring within the tree-fall dataset. Preliminary examination of these data revealed increased numbers of standing and downed trees for the years corresponding to hurricanes Rita (2005), Ike (2008), and the 2011 drought (2011 and 2012) (Appendix C: Figure C.1) which are described in further detail in Edgar *et al.* (2019). For this study, size of standing or fallen dead stems was examined further under different major disturbance events based on assigned agent of mortality and mortality year to provide further insight into the processes by which trees transition to downed dead wood. Weather-killed stems were classified into three groups, 'Hurricane' which contained all stems with estimated years of mortality in 2005 and 2008; '2011 Drought' which contained all stems with estimated years of mortality in 2011 and 2012, and 'Other Weather' which contained all remaining weather-killed stems. All other stems deemed killed by other agents excluding harvested stems were grouped into 'Non-Weather'.

Analyses

Generalized linear mixed models were built to predict five-year probabilities of both tree- and snag-fall for hardwood species and softwood species separately resulting in four separate models. Specifically, logistic regression was used with a binary response of 'success' being the tree or snag fell at re-measurement (fallen = 1, standing = 0). Fixed effects of size, live stem density, height, and decay class (for snag-fall stems) and random effects of plot and physiographic class were considered as covariates for each model. Re-measurement intervals generally occurred over a five-year period however, due to unforeseen logistical constraints (e.g., access) some plots were unable to be measured at exactly five-year intervals. This variability in re-measurement interval was accounted for by exponentiating the logistic model form by the re-measurement interval in years and dividing by five to constrain model parameters and predictions to a five year probability, generally following the compound interest formula (Flewelling and Monserud, 2002; Vanderwel *et al.*, 2006a).

$$p_{Fij} = \left[\frac{1}{1+ e^{-\left(X_{ij}^{T}\beta_k+\mu_j+\tau_l\right)}}\right]^{\left(t_j/5\right)} \quad \text{(IV.1)}$$

Where, p_{Fij} = five-year probability of falling, X^T_{ij} = the transposed matrix of covariates for stem i in plot j, β_k is the vector of length k of parameters to be estimated, u_j is the random effect of plot j, τ_l is the random effect of physiographic class l, and t_j is the re-

measurement interval for plot *j*. Using this approach, the estimated β_k's describe the five-year log odds of falling for each stem as opposed to the log odds of falling for the specific re-measurement interval t_j. Random effects were assumed to follow a normal distribution with mean of zero and common variance, σ^2, for each of the plot and physiographic class random effects.

Fixed and random effects were selected for each model by comparing iterations of nested models via likelihood ratio tests. Additional variables were added or excluded depending on whether they significantly contributed more explanatory power than a simpler model ($p < 0.05$). Model assessment was conducted by comparing the most parsimonious model to the null model (intercept plus random effect) via likelihood ratio tests ($p < 0.05$).

Average tree sizes (DBH) were calculated for standing and downed hardwood and softwood trees grouped into weather-killed ('Hurricane', '2011 Drought', and 'Other Weather') and non-weather-killed ('Non-Weather') groups in the tree-fall dataset. Differences between standing and downed dead tree mean DBH were analyzed by means of Welch's two-sample t-test on natural log-transformed data. Significant differences in mean tree sizes were denoted by $p < 0.05$.

All data manipulations and analyses were conducted using R software version 3.5.1 (R Core Team, 2018) with mixed modeling conducted using the 'lme4' package version 1.1.19 (Bates *et al.*, 2015).

Carbon Transition Simulations

Monte Carlo simulations were conducted in order to demonstrate the utility of models for predicting the five-year probability of snag-fall as a simple example. The 2011 drought in Texas killed millions of trees across the state resulting in a rapid transfer of carbon from the live tree pool to the SDT pool, roughly 24-30 Tg C in just one year (Moore *et al.,* 2016). To understand how quickly SDT carbon will transition from standing to downed dead wood in east Texas, all SDT (DBH ≥ 12.7 cm) were selected from the FIA database and the year 2012 for the region of east Texas. Models developed for objective 1 for hardwood and softwood snag-fall were applied to the SDT drought dataset to determine predicted probabilities of falling in five years. Monte Carlo simulations were subsequently carried out to determine whether each tree in the SDT drought dataset remained standing or fell after five years based on its predicted probability. Specifically, a random number was drawn from a uniform distribution ranging from 0 to 1 and assigned to each SDT. If the predicted probability of the SDT falling in five years was less than or equal to the random number, the SDT remained standing. If the predicted probability of the SDT falling in five years was greater than the random number, the SDT fell over. This scenario was repeated 1000 times and resulting metrics were summarized using these samples.

The FIA program calculates biomass of SDT using the Component Ratio Method (CRM) (Woodall *et al.*, 2010) adjusting for changes in density and structural reduction by decay class (Domke *et al.*, 2011) and assuming that carbon mass is half of the biomass. Using the carbon estimates for each SDT in the FIA dataset and the Monte

Carlo simulation results, the amount of carbon in measured SDT hardwoods and softwoods was calculated and summarized by decay class for the SDT drought dataset in 2012 (initial year post-drought) and as predicted five years later (2017) on a per-ha basis. All data manipulations and analyses for carbon transition simulations were conducted using R software version 3.5.1 (R Core Team, 2018).

Results

The tree-fall dataset contained 7116 stems in total measured across 2529 plots while the snag-fall dataset contained about half as many stems, 3722 in total, measured across 1950 plots (Table IV.1). Hardwoods were more numerous than softwoods in both datasets, being nearly double in both cases. Of the trees that were alive and subsequently died after five years (i.e., tree-fall dataset), approximately 50.2% of hardwood stems fell and 54.6% of softwood stems fell at re-measurement. Of the trees that were dead at initial measurement (i.e., snag-fall dataset), approximately 74.1% of hardwood stems fell and 81.4% of softwood stems fell at re-measurement.

Table IV.1 Summary of tree-fall and snag-fall datasets used for analyses (DBH = diameter at breast height). DBH, height, and plot live density are median values with 2.5th and 97.5th percentiles in parentheses.

	Class Type	# Plots	# Stems	# Standing	# Downed	DBH (cm)	Height (m)	Plot Live Density (stems/ha)
Tree-Fall	Hardwoods	1960	4772	2377	2395	19.1 (12.9, 54.8)	13.7 (4.9, 26.8)	297 (59, 669)
	Softwoods	1008	2344	1065	1279	20.1 (13.0, 57.3)	17.1 (7.9, 32.6)	372 (104, 976)
	Total	2529	7116	3442	3674	19.3 (13.0, 55.9)	14.6 (5.8, 29.9)	312 (59, 818)
Snag-Fall	Hardwoods	1354	2355	610	1745	20.3 (13.0, 54.1)	8.2 (2.1, 20.4)	297 (59, 654)
	Softwoods	802	1367	254	1113	20.1 (13.0, 52.2)	11.0 (1.8, 28.0)	342 (60, 936)
	Total	1950	3722	864	2858	20.3 (13.0, 54.1)	8.8 (2.1, 24.4)	297 (59, 788)

Variable selection for each of the developed models was conducted using likelihood ratio tests with associated parameter estimates based on log odds displayed in Table IV.2. Likelihood ratio tests indicated that the fixed effect of DBH was the best predictor of the five-year probability of falling for hardwoods in the tree-fall dataset (Table IV.2). For softwood tree-fall, both DBH and plot live stem density together produced the best model for predicting the five-year probability of tree-fall (Table IV.2). In addition, the random effect of plot contributed significantly to both the hardwood and softwood tree-fall models while the random effect of physiographic class contributed significantly only to the hardwood tree-fall model. The best-fit tree-fall models provided significantly more explanatory power for both hardwoods ($\chi^2 = 61.682$ with 1 degree of freedom, $p << 0.001$) and softwoods ($\chi^2 = 105.46$ with 2 degrees of freedom, $p << 0.001$) than the null models. For snag-fall hardwoods, DBH and decay class were the best predictors of the five-year probability of falling while, DBH, stem height, and decay class together were the best predictors of the five-year probability of falling for softwoods. Of the two random effects examined, only plot contributed significantly to explaining further variation in the data for both hardwood and softwood snag-fall models. The best-fit snag-fall models provided significantly more explanatory power for both hardwoods ($\chi^2 = 149.46$ with 5 degrees of freedom, $p << 0.001$) and softwoods ($\chi^2 = 72.84$ with 6 degrees of freedom, $p << 0.001$) than the null models.

Table IV.2 Summary of parameter estimates with standard errors from chosen models based on standardized covariates for log odds responses. Note that RE and SD refer to random effect and standard deviation, respectively.

Parameter	Tree-Fall		Snag-Fall	
	Hardwoods	Softwoods	Hardwoods	Softwoods
Intercept	0.059 (0.137)	0.065 (0.072)	na	na
DBH	-0.304 (0.040)	-0.633 (0.069)	-0.854 (0.093)	-1.132 (0.170)
Height	ns	ns	ns	0.422 (0.160)
Plot Density	ns	-0.178 (0.084)	ns	ns
Decay Class 1	na	na	1.022 (0.236)	2.388 (0.419)
Decay Class 2	na	na	1.366 (0.201)	2.406 (0.365)
Decay Class 3	na	na	1.922 (0.200)	2.860 (0.395)
Decay Class 4	na	na	2.125 (0.207)	3.601 (0.491)
Decay Class 5	na	na	3.431 (0.345)	3.637 (0.644)
Plot RE SD	1.240	1.238	2.525	2.945
Phys. Class RE SD	0.245	ns	ns	ns
AIC	6321.7	3047.2	2685.7	1273.4
Deviance	6313.7	3039.2	2671.7	1257.4

*na = not applicable to specific model
*ns = variable tested but no significant effect added to model via likelihood ratio tests ($p > 0.05$)

Trends for the selected variables in the tree-fall models are shown in Figures IV.2 and IV.3. For the tree-fall dataset, the probability of a tree falling in the five-year interval in which it dies was greatest for the smallest stems and decreased with increasing size for both hardwoods and softwoods (after holding plot live stem density constant at its median value for softwoods; Figure IV.2). These probabilities ranged

between approximately 0.5 to 0.75 for the smallest stems and dropped below 0.25 for the largest stems. In general, hardwoods had a higher probability of falling than did softwoods with the exception of the smallest softwoods, which tended to have a higher probability of falling than hardwoods. The significant effect of physiographic class on probability of tree-fall in hardwoods was relatively slight, ranging between roughly 0.43 to 0.54 (Figure IV.3). The mean effects of each physiographic class group representing the probability of falling in five years generally increased along a gradient of dry-to-moist sites for the mesic group. In particular, the most notable effects were in mesic uplands (lowest mean probability of falling in five years) and mesic bottomlands (highest mean probability of falling in five years).

Figure IV.2 Predicted probability of tree-fall in five years vs. tree size for hardwoods (solid line) and softwoods (dashed line). Probabilities for softwoods were calculated with plot density held constant at the median value.

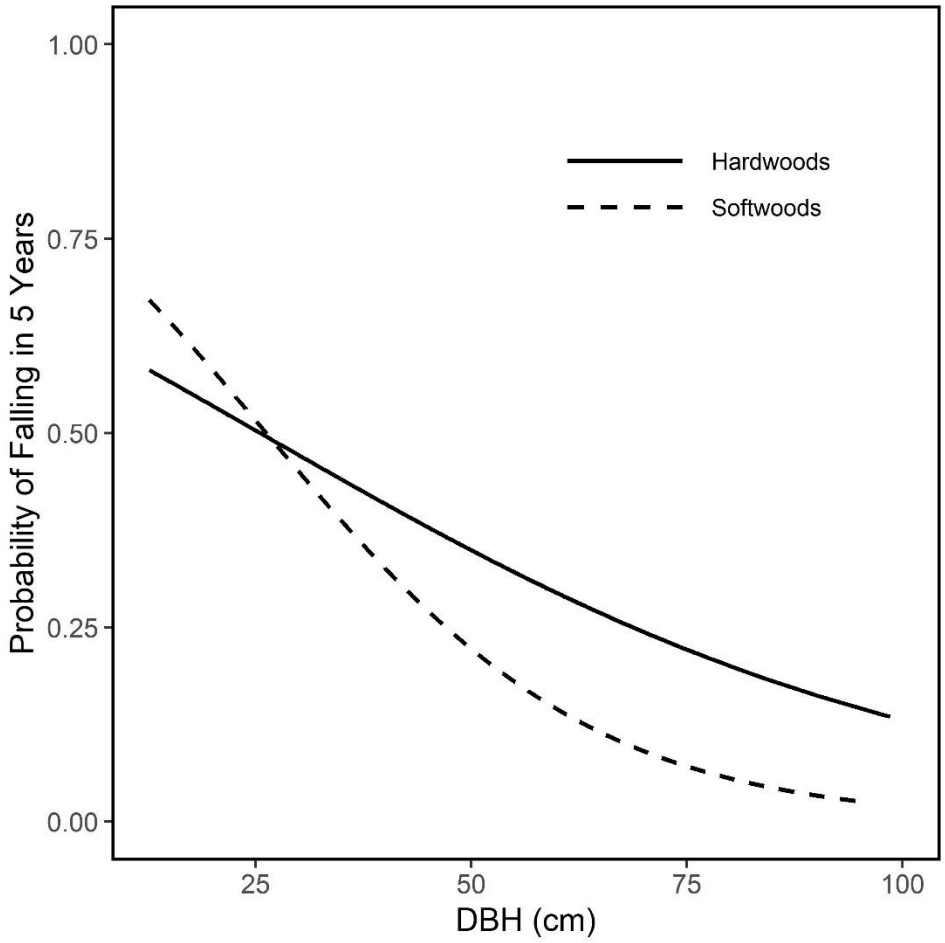

Figure IV.3 Physiographic class mean effects with standard deviation for hardwood tree-fall dataset converted from log odds to probabilities. Xeric and hydric groups encompass all subclassifications for that group. Asterisks above mean effects indicate that effect is different from 0.5 (i.e., log odds is different from 0). Vertical dotted lines separate xeric, mesic, and hydric groups.

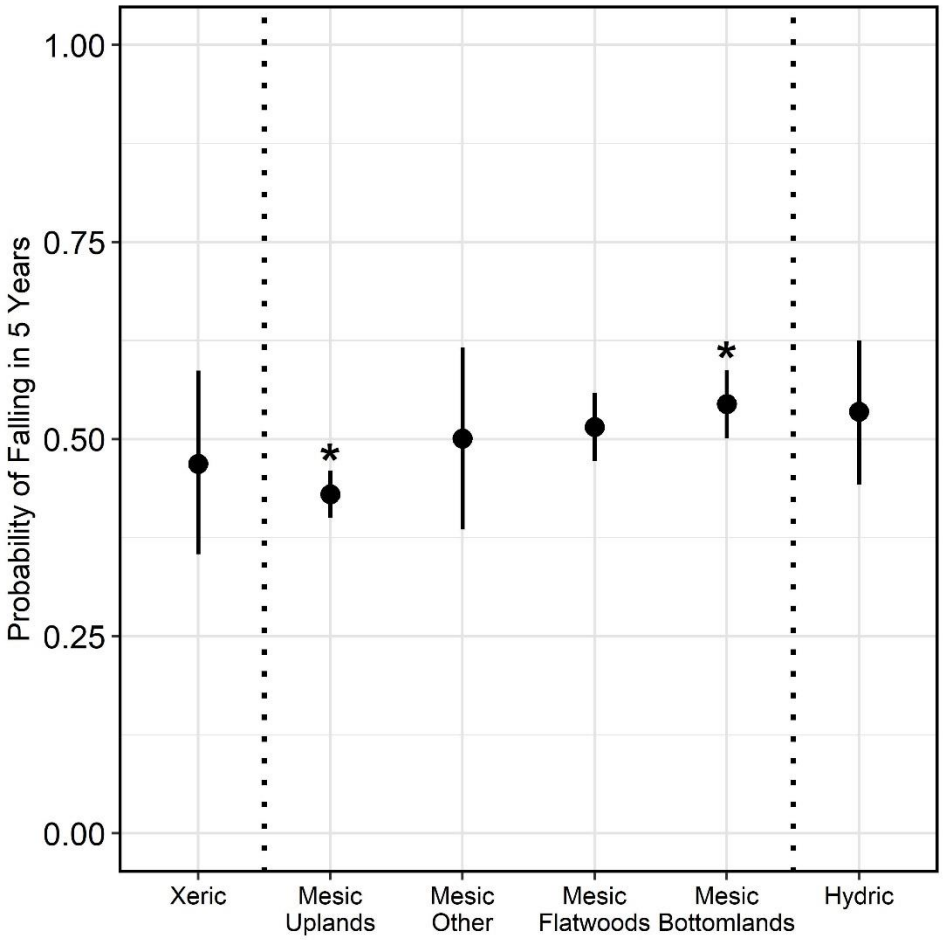

Trends for the selected variables in the snag-fall models are shown in Figure IV.4. The probability of a snag falling in five years generally increased with increasing decay class for both hardwoods and softwoods (holding stem height constant at its median value for softwoods; Figure IV.4A, B). This was most evident for hardwoods but slightly less strong for softwoods. Decay class one and two softwoods followed the same pattern having the lowest probabilities with decay classes four and five following similar patterns and having the highest probabilities. Five-year probabilities of falling for decay class three softwoods were intermediate relative to the other decay classes. Regarding size, the probability of falling in five years followed similar patterns as in the tree-fall models, smaller stems were much more likely to fall than larger stems across all decay classes and for both hardwoods and softwoods (holding stem height constant at its median value for softwoods; Figure IV.4A, B). Smaller softwood stems were more likely to fall than hardwood stems in decay classes one, two, four, and somewhat for three (Appendix C: Figure C.3). Large stems in decay class five hardwoods were more likely to fall after five years than for softwoods (Appendix C: Figure C.3). Large hardwood and softwood stems followed similar patterns for all other decay classes.

Figure IV.4 Predicted probability of snag-fall in five years vs. snag size for A) hardwoods and B) softwoods by decay class. Probabilities were calculated with snag height held constant at the median value.

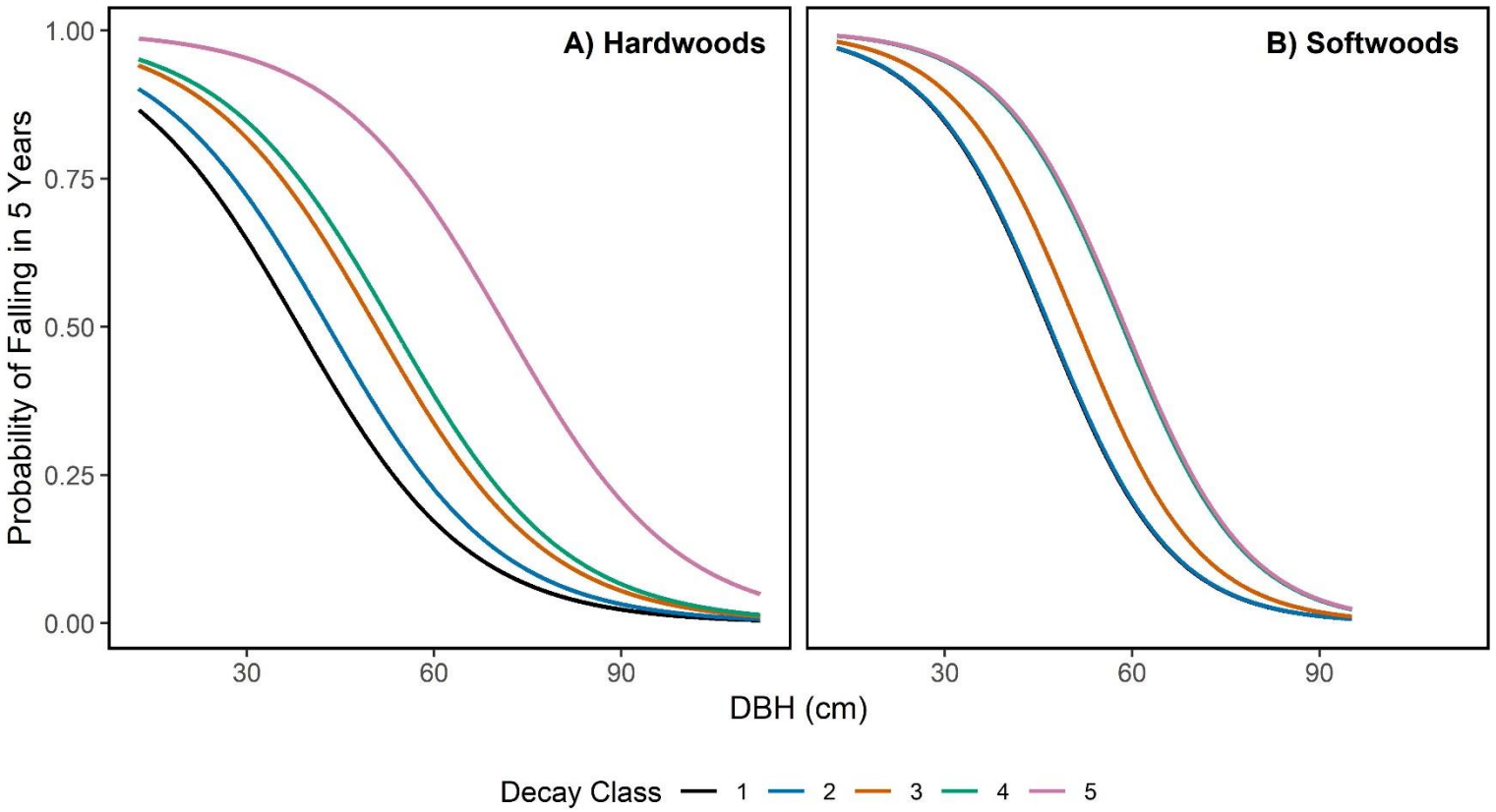

Further examination of DBH for standing and fallen dead tree-fall stems by agent of mortality and estimated year of mortality revealed unique patterns (Figure IV.5A, B). Non-Weather, Other Weather, and 2011 Drought groups all showed that stems remaining standing tended to be significantly larger than fallen stems ($p < 0.05$), indicating that on average smaller stems tended to fall if killed by these agents. However, no significant difference ($p > 0.05$) was found between standing and fallen tree-fall stems in the Hurricane group, indicating that on average there was no difference in the size of stems that fell or remained standing.

Figure IV.5 Mean DBH with standard errors for standing dead and fallen A) hardwoods and B) softwoods from the tree-fall dataset. Groups are based on FIA field crew-assigned agent of mortality and estimated year of mortality. 'Other Weather', '2011 Drought', and 'Hurricane' all correspond to weather-related mortality whereas 'Non-Weather' group corresponds to all other agents excluding harvesting (i.e., insects, diseases, fire, animals, competition, etc.). '2011 Drought' group are all tree-fall stems deemed killed by weather in 2011 and 2012. 'Hurricane' group are all tree-fall stems deemed killed by weather in 2005 and 2008, corresponding to hurricanes Rita and Ike, respectively. Asterisks (*) above bars denote significant differences ($p < 0.05$) between standing and fallen dead tree average DBH for that specific group based on Welch's two-sample t-tests.

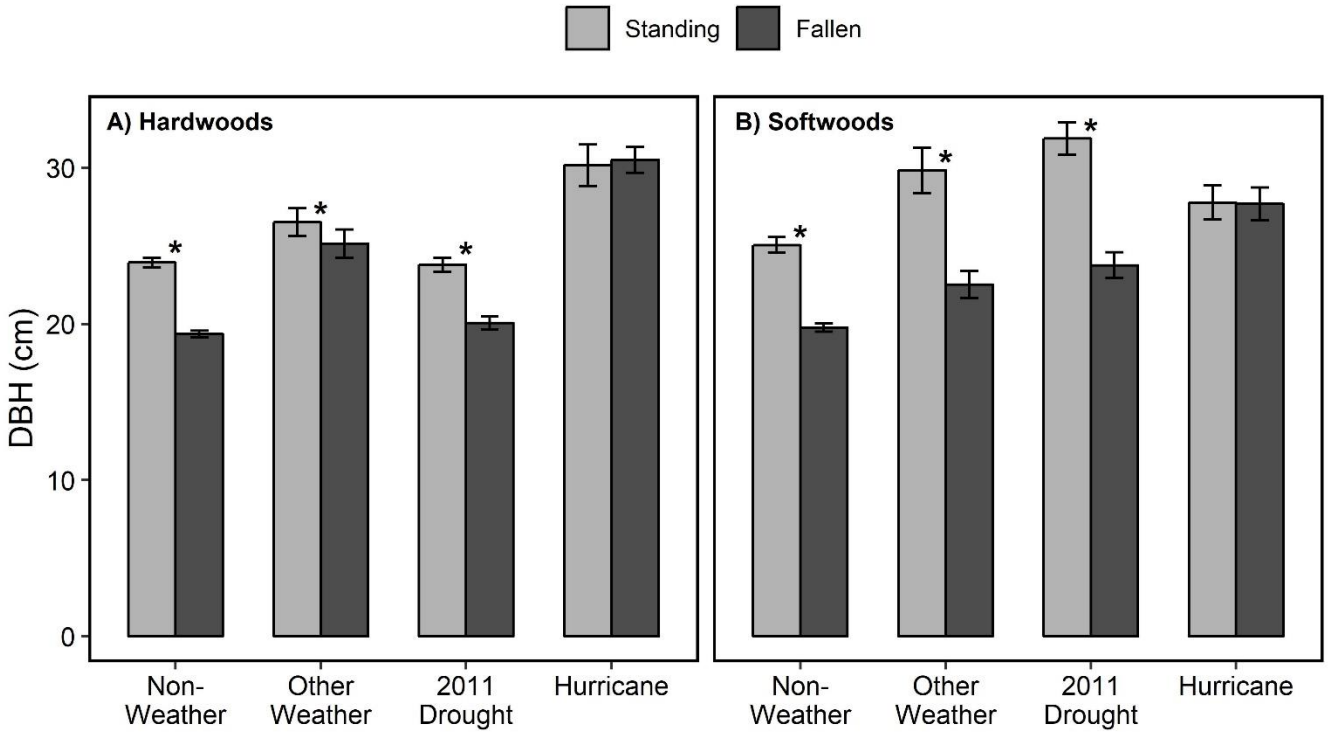

Datasets for the carbon transition simulations contained 455 hardwood snags and 197 softwood snags in total. Results from the Monte Carlo simulations provide predicted estimates of carbon which transitioned from SDT to downed dead wood with initial standing carbon (2012) and remaining standing carbon (2017) shown in Figure IV.6A, B. Simulations indicated that 59.5 and 67.1% of carbon in measured hardwoods and softwoods transitioned from SDT to downed dead wood in five years, respectively (Table IV.3). After aggregating by decay class, between 52.3 and 79.3% of carbon in hardwoods transitioned from standing to downed dead wood (Table IV.3). For softwoods, between 51.6 and 83.4% of carbon transitioned from standing to downed dead wood after accounting for decay class (Table IV.3).

Figure IV.6 Carbon (Mg/ha) contained in standing dead trees inventoried in 2012 (i.e., one year after the 2011 drought) in east Texas (dark gray) and carbon (Mg/ha) contained in those same SDT predicted to remain standing after five years (light gray) with standard deviations, split by A) hardwood and B) softwood species and aggregated by decay class.

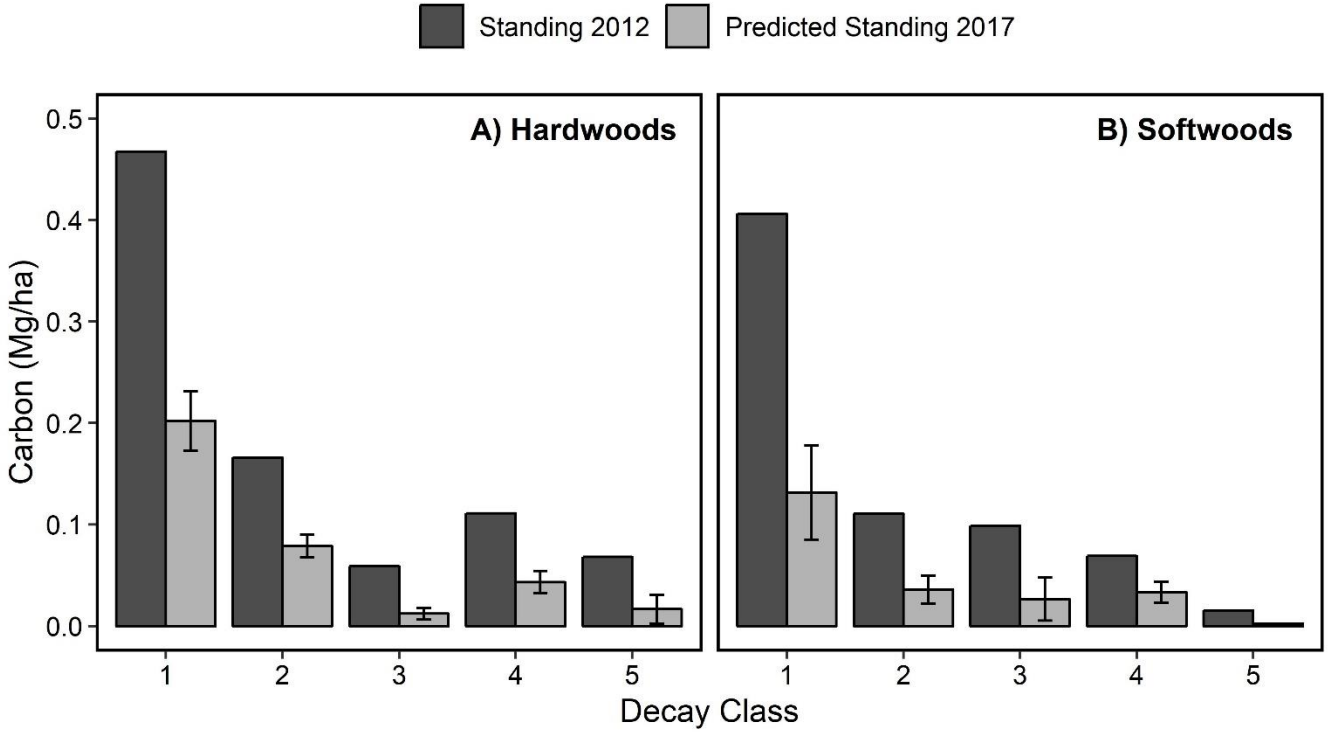

Table IV.3 Carbon (Mg/ha) in hardwood and softwood standing snags for inventory year 2012 plus carbon (Mg/ha) in previously standing snags that were predicted to fall in five years based on Monte Carlo simulations with proportion of carbon in fallen stems. Values in parentheses are standard deviations from Monte Carlo simulations.

	Standing 2012 Carbon (Mg/ha)		Fallen 2017 Carbon (Mg/ha)		% Fallen	
Decay Class	Hardwoods	Softwoods	Hardwoods	Softwoods	Hardwoods	Softwoods
1	0.468	0.406	0.265 (0.030)	0.274 (0.047)	56.7 (6.4)	67.5 (11.6)
2	0.166	0.111	0.087 (0.011)	0.075 (0.014)	52.3 (6.7)	67.5 (12.7)
3	0.059	0.099	0.047 (0.006)	0.072 (0.021)	79.3 (10.2)	73.0 (21.6)
4	0.111	0.069	0.068 (0.011)	0.036 (0.010)	61.0 (10.0)	51.6 (15.1)
5	0.068	0.015	0.051 (0.014)	0.013 (0.004)	75.6 (20.7)	83.4 (23.5)
Total	0.871	0.700	0.518 (0.036)	0.470 (0.052)	59.5 (4.1)	67.1 (7.5)

Discussion

Tree-Fall

Tree-fall trends were similar to patterns found by Vanderwel *et al.* (2006a) and other studies focused on snags (Oberle *et al.*, 2018). In particular, tree size as measured by DBH appeared to be the strongest factor of those examined governing five-year fall probabilities. Smaller stems tended to have the greatest probability of falling in five years, which decreased as stem size increased. Considering trees that died while standing and eventually fell after five years, the effect of stem size has been shown to be a common driver of snag fall in many forest types, including those in the southeastern U.S. (Conner and Saenz, 2005; Zarnoch *et al.*, 2013) generally relating to wood mechanical strength (Oberle *et al.*, 2018). Plot live stem density was an additionally important factor for softwood species. Specifically, five-year probability of tree fall decreased under increasing live tree stem densities. Closely spaced trees have been shown to reduce fall rates and damage (Oberle *et al.*, 2018), presumably by shielding trees and snags from the breaking or uprooting forces of wind (Gardiner *et al.*, 2016). In east Texas, loblolly pine occurs largely in even-aged stands whether as managed plantations or in naturally-regenerated conditions (Edgar and Zehnder, 2015). Subsequently, the canopies of such stands can be relatively uniform and continuous under increasing stem densities potentially helping to buffer against wind damage by reducing the exposure of canopy surface area (i.e., sides of canopies) to wind forces.

Differences in tree fall probabilities between hardwoods and softwoods were evident but relatively slight. Small stems of both wood type classes had similar

probabilities of falling, with softwoods being just slightly greater when held at their median density. However, medium-to-large sized hardwoods appeared to have a greater probability of falling than softwoods under the same scenario. Trees that died and fell at the same time, although undiscernible here, likely do so by two means, snapping along the stem or tipping over at the base/roots. Trees that snap along the main stem experience failure as a result of weak wood mechanical properties. On the other hand, trees that tip over at the base/roots, fail to remain standing as a result of poor rooting ability and weak soil structure. Tree-fall hardwoods tended to follow an increasing trend of fall probability from mesic upland sites to mesic bottomland sites, suggesting weak soil structure and poor rooting may be a potential driver affecting falling of hardwoods. Moorman *et al.* (1999) noted that snags in upland hardwood forests tended to have the greatest longevity at their sites in South Carolina. Moreover, data from the FIA mortality agent and year classifications highlights that hurricanes tend to select for larger fallen trees presumably via wind than trees killed by the other mortality agents, which likely fall after experiencing some decomposition. In fact, Harcombe *et al.* (2009) found that large hardwood species tended to have higher probabilities of damage and death at wetter sites than softwood species following hurricane Rita in east Texas, generally falling in line with our results. They also mention that their results may be confounded slightly by the spatial location of plots relative to the track of the storm. Yet, at a regional scale, wind has been estimated as the second largest driver of carbon turnover behind harvesting within southeastern U.S. forests (Harris *et al.,* 2016). Regardless, results shown here suggest that large hardwoods on wetter sites may be more prone to

falling than those occurring on drier, upland sites in this region, ultimately highlighting a potentially unique process by which particular trees fall over than by typical decomposition agents (e.g., fungi, microbes, insects) that weaken wood.

Snag-Fall

Snag-fall trends generally followed expected patterns as found in studies across multiple regions. As with the tree-fall dataset, snag size as measured by DBH appeared to be a crucial factor governing five-year fall probabilities, similar to other studies (Oberle et al. 2018, Zarnoch et al. 2013, Conner and Saenz 2005). Moreover, decay class also was an important factor describing the probability of snag fall, particularly for hardwoods. Smaller stems in both datasets tended to have the greatest probability of falling in five years (i.e., > 0.75 for the smallest stems) which decreased substantially as stem size increased. The lowest risk of falling in five years was among the least decayed snags and risk increased as decay progressed. Larger diameter trees tend to have greater proportions of decay-resistant heartwood providing stronger structural properties than smaller trees (Conner *et al.*, 1994; Sellin, 1994). It is well documented that wood density in SDT decreases with increasing decay class ultimately reducing structural strength (Harmon *et al.*, 2011). Bark beetles can carry multiple species of fungi which can inoculate the trees and expedite wood decomposition (Barras, 1970; Klepzig and Wilkens, 1997). Moreover, termites are an important part of the biotic decomposer community in east Texas (Zhang et al. 2016), unlike northern and western regions of the U.S., further accelerating decay. In general, hardwood material tends to decay more

quickly than softwood material when in contact with the ground (Weedon *et al.*, 2009; Zell *et al.*, 2009) and this might partially explain the stronger effect of decay class in hardwood snags than softwood snags despite the material being elevated off the ground. Snag stem height was an additionally important factor describing five-year fall probabilities for softwoods but not hardwoods. Specifically, the five-year probability of softwood snag-fall increased as height increased. This effect in softwoods may relate to the excurrent growth form prevalent in softwoods which have a central apical leader and main stem the full length of the tree. Hardwoods, on the other hand, tend to have a decurrent growth form with a weak apical leader which terminates at a fraction of the total tree height. Given this, softwoods would tend to have a higher center of gravity which may increase the susceptibility to falling as the stem weakens with decay (Gardiner *et al.*, 2016).

Carbon Transition Simulations

Quantifying decomposition rates and understanding carbon dynamics in east Texas remains a critical area of research particularly given the frequency of major disturbances in this region over the last few decades (e.g., hurricanes Rita, Ike, and Harvey; 2011 drought) along with the continued threat of similar disturbances. Models produced herein provide critical tools for understanding the turnover of carbon in the SDT pool. Specifically, after applying snag-fall probability predictions to a simple Monte Carlo simulation it was evident that snag-fall decomposition occurs rapidly in east Texas. While the results pertain simply to a single five-year period, over half of the

carbon transitioned from standing dead wood to downed dead wood for both hardwoods and softwoods in five years. Softwoods had a greater proportion of carbon fall within five years, falling in line with other work from this region (Putman *et al.*, 2018). The majority of the carbon was from decay class one SDT which fell after five years. However, nearly all the carbon in the remaining decay classes (i.e., two through five) transitioned to the downed pool after a single five-year period, primarily for softwood species. Results generally align with those from other studies in southeastern U.S. forests which also highlight rapid turnover of snags to downed wood after 4-6 years. Cain (1996) found that hardwoods in Arkansas fell in under 10 years and were fastest for the smallest stems. Moorman *et al.* (1999) found that 95% of all snags measured at their sites in South Carolina fell within six years. Another study in South Carolina found that smaller snags fell faster (4.4-6.9 years) than larger snags (6.0-9.4 years) (Zarnoch *et al.*, 2013). Conner and Saenz (2005) tracked large pine snags (i.e., mean DBH of 49.0 cm) over multiple decades in east Texas and noted loblolly pine had the shortest longevity at six years. Snag fall rates are largely driven by climate factors which speed decomposition (Oberle et al. 2018). The persistent warm, humid conditions in east Texas coupled with a unique biotic decomposer community (i.e., presence of termites) resulted in the rapid turnover of both hardwood and softwood snags after five years. Models and results from this study provide the added understanding of snag-fall dynamics by decay class, which is a commonly used system for classifying decayed stems in forest inventories (Burrill *et al.*, 2018). Future work could model predicted probabilities of SDT remaining standing after five years and their transitions to subsequent decay classes

(e.g., Vanderwel *et al.*, 2006b; Russell *et al.*, 2013) to extend temporal utility of the snag-fall models.

While these results display a simple application, further use of these models could include improving parameterization of dynamic carbon cycle and vegetation models for predicting the effects of future disturbances on regional carbon budgets. Specifically, these models could be coupled with growth-and-yield, mortality rate, and downed dead wood decomposition models under varying silvicultural scenarios and analyzed via simulation to derive decomposition constants and turnover rates of carbon in SDT. Recent studies have employed such methods for other regions (Vanderwel *et al.*, 2006a) and for other dead wood pools (i.e., downed dead wood) (Russell *et al.*, 2013; Russell *et al.*, 2014). Beyond carbon budgets, results can better constrain models predicting fuel loads for understanding wildland fire behavior and risk or inform management activities focused on providing wildlife habitat for cavity-nesting species and reducing falling tree hazards in forests.

CHAPTER V

ALLOMETRY AND STRUCTURAL VOLUME CHANGE OF STANDING DEAD SOUTHERN PINE TREES USING NON-DESTRUCTIVE TERRESTRIAL LIDAR

Introduction

Standing dead trees (SDT) represent a key component of the dead wood pool in forests worldwide (Harmon *et al.*, 1986; Russell *et al.*, 2015). Standing dead trees influence biomass and carbon dynamics (Mobley *et al.*, 2013; Oberle *et al.*, 2018), fuel loads and wildland fire dynamics (Collins *et al.*, 2012; Schoennagel *et al.*, 2012), provide habitat for many wildlife and insect species (Lindhe *et al.*, 2005; Jones *et al.*, 2009), and add to forest structural complexity (Harmon *et al.*, 1986). The National Greenhouse Gas Inventory (NGHGI) administered by the U.S. Environmental Protection Agency classifies dead wood and SDT as a key component of the carbon budget and important for carbon accounting (U.S. EPA 2019). Moreover, the threat of increased large-scale disturbances such as droughts and tree die-off events under a changing climate can cause massive shifts from live-to-dead tree pools (Allen *et al.*, 2015; Young *et al.*, 2017). For example, the state of Texas experienced the worst drought on record in 2011 with approximately 301 million trees killed by 2012 equating to roughly 30 Tg C added to the SDT pool in one year (Moore *et al.*, 2016) with additional trees continuing to die multiple years following the drought (Klockow *et al.*, 2018). Thus, accurately estimating the quantity of SDT at multiple scales is critical for effectively describing

biomass and carbon dynamics, fuel loads, wildlife habitat, falling tree hazards, and forest stand complexity.

Typically, development of individual tree biomass and volume estimates requires laborious destructive sampling of trees in representative sizes and demographics, making development of species and region-specific estimates time-consuming but necessary to achieve appropriate estimates (Weiskittel *et al.*, 2015). Light-detection-and-ranging (LiDAR) is a remote sensing technology with the potential for efficiently estimating tree volume and biomass. LiDAR sensors emit laser pulses from a measuring device and record the distance at which the laser pulses were reflected as well as the subsequent return intensity of the reflected pulses to create three-dimensional representations of objects in space (Lefsky *et al.*, 2002). LiDAR technology has been used and tested successfully via spaceborne, airborne, and ground-based (terrestrial) platforms to develop nondestructive estimates of live tree volume, biomass, and associated inventory metrics at multiple scales (Popescu *et al.*, 2011; Srinivasan *et al.*, 2014; Sheridan *et al.*, 2015; Narine *et al.*, 2019). Terrestrial LiDAR (hereafter, terrestrial laser scanning or TLS) in particular is well-suited for accurately and non-destructively quantifying SDT volume given its ability to scan individual trees within and below the forest canopy at high point densities thus capturing finer morphological attributes of stems and branches without the need for laborious and dangerous destructive sampling (Raumonen *et al.*, 2013; Putman and Popescu, 2018). Many successful efforts have been employed for developing estimates of live tree volume and biomass using TLS approaches (Srinivasan *et al.*, 2014; Stovall *et al.*, 2018). However, only recently has TLS been used to quantify

volume of individual SDT (Putman and Popescu, 2018; Putman *et al.*, 2018). These efforts have shown that TLS along with volume calculation algorithms allow for relatively rapid field data collection and robust volume estimation of SDT in dense and enclosed canopy conditions. Further exploration of these technologies and techniques is necessary to progressively improve estimation and understanding of SDT volume and biomass.

Allometric models statistically relate commonly measured tree parameters such as diameter-at-breast-height (DBH) and tree height to volume or biomass of whole trees and component parts for use in predicting volume and biomass of non-destructively sampled trees. These models are essential for estimating tree volume and biomass at increasingly larger scales beyond the individual tree and remain critical for national forest inventories (NFI) tasked with accurately accounting forest biomass and carbon (U.S. EPA 2019). The NFI for the U.S., the U.S. Forest Service Forest Inventory and Analysis (FIA) program, historically used live tree allometric equations from Jenkins *et al.* (2003) to predict SDT biomass without accounting for density or structural changes inherent in decay classifications (Woudenberg *et al.*, 2010), thus overestimating biomass and carbon (Domke *et al.*, 2011). More recently, correction factors have been created and applied to live tree biomass estimates to account for density and structural changes inherent across decay classes (Harmon *et al.*, 2008; Woodall *et al.*, 2010; Domke *et al.*, 2011; Harmon *et al.*, 2011). Given the plethora of resources developed around reference live tree estimates (e.g., Raile (1982); Jenkins *et al.* (2003); Miles and Smith (2009); Woodall *et al.* (2010)), it is not surprising that allometric equations specifically for SDT

have not been explored more fully. However, if shown to provide strong predictive power, such equations could become efficient tools for estimating volume and biomass of SDT by inherently accounting for structural and density changes across decay classes.

Accounting for density and structural change are critical for accurately predicting SDT volume and biomass as dead wood generally decreases in wood density and volume over time via decomposition (Harmon *et al.*, 2008; Aakala, 2010; Harmon *et al.*, 2011; Fraver *et al.*, 2013). Qualitative descriptions of density and structural changes have been used to define decay classifications often assigned to SDT and downed woody debris (DWD) representing the progression of decomposition for dead wood in many NFI (USDA Forest Service, 2017). Comprehensive studies have been conducted to quantify density reduction by decay class for both DWD and SDT generally showing that density decreases with each successive decay class (Harmon *et al.*, 2008; Harmon *et al.*, 2011). Empirical studies of structural reduction in DWD have shown collectively that large pieces (i.e., logs) generally collapse along the vertical axis in later decay stages, ultimately following a systematic trend in structural reduction across species and forest types (Fraver *et al.*, 2013). For SDT, structural reduction with decay has received very little attention but has been suggested to follow a sigmoidal trend with little change in early decay stages and much greater loss of structural volume in later decay stages (Aakala, 2010). Domke *et al.* (2011) devised theoretical proportions describing the remaining volume of SDT components based on qualitative decay class criteria with the goal of using these proportions to 'correct' live tree volume and biomass estimates to more accurately represent SDT form. Russell *et al.* (2015) noted from a sensitivity

analysis for SDT that density reductions could account for ~20% of carbon change while structural reductions could account for ~60% highlighting the need for empirically-derived understanding of SDT structural change. However, no study has empirically measured SDT volume to examine the proportion of remaining volume in SDT by decay class. Development of estimates of these proportions could be used to verify theoretical estimates and to build further understanding of structural change by decay class in SDT.

Pinus species are common across much of the U.S. and generally have similar morphological growth forms (e.g., excurrent branching structure) amongst themselves and other conifers. Moreover, the decay classification system employed by the U.S. NFI was developed on criteria derived from conifer decay patterns (Cline *et al.*, 1980). Loblolly pine (*Pinus taeda* L.) in particular is an important commercial and ecological species throughout the southeastern United States and east Texas (i.e., focal study area). Thus, loblolly pine is an ideal candidate for developing widely applicable allometric models of SDT volume across decay classes. Following this, the main goal of this study was to quantify and assess empirical volume and structural volume changes in loblolly pine SDT by decay class using TLS and a novel volume calculation algorithm, TreeVolX, from Putman and Popescu (2018). To meet this goal, we addressed three specific objectives, 1) construct empirical volume estimates of SDT by decay class using TLS and the TreeVolX volume calculation algorithm, 2) develop novel allometric relationships of aboveground SDT component volumes by decay class and assess error in models and predictions, and 3) quantify empirical proportion-remaining volume of

SDT TLS-derived components relative to reference live tree predicted component volumes and compare against theoretically-derived estimates from FIA.

Methods

Study Location

Standing dead trees for this study were sampled within the western extent of the Sam Houston National Forest (Figure V.1). The Sam Houston National Forest is located in east Texas approximately 80 km north of the city of Houston, Texas and covers 65,979 ha with flat to gently rolling topography and approximately 70-120 m elevation above sea level. Climate around the national forest consists of hot, humid summers and mild, wet winters. Mean summer (June, July, August) temperature and precipitation is typically 28°C and 277 mm and mean winter (December, January, February) temperature and precipitation is typically 11°C and 284 mm (NOAA 2019). Loblolly pine (*Pinus taeda* L.) is the dominant tree species in the national forest followed by post and water oaks (*Quercus stellata* and *Quercus nigra*, respectively), sweetgum (*Liquidambar styraciflua*), and winged elm (*Ulmus alata*). The understory is composed of many shrubs, often very densely with yaupon (*Ilex vomitoria*).

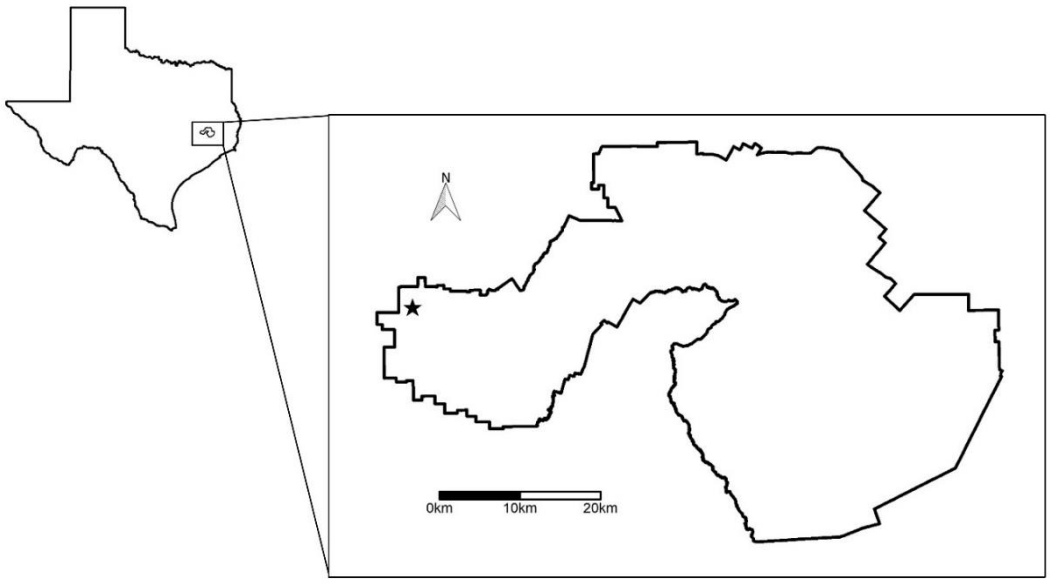

Figure V.1 Sampling area denoted by black star in Sam Houston National Forest, Texas.

Sample Data

Standing dead pine trees were selected for scanning across five decay classes (Table V.1) and a range of diameters (Table V.2) to represent the full range of decay and minimum tree size (i.e., approximately ≥ 12.7 cm) as defined in FIA protocols. Selected SDT were located in pine-dominated stands in both managed and unmanaged conditions. Care was taken to avoid sampling SDT that did not clearly fit into a decay classification (e.g., wind-snapped or substantially fire damaged trees). Field measurements for each tree included DBH, height, genus, percent-remaining bark (estimated visually), and bark thickness at breast height. Scanned SDT (deemed safe to fell) were felled by Texas

A&M Forest Service personnel and wood samples were collected for future, follow up studies on wood density and biomass but were not directly used in results for this chapter. See Appendix D for further details on wood sample collection. Field measurements and sampling, including scanning (discussed in further detail below), took place from December 2016 to May 2017.

Table V.1 Summary of standing dead tree decay classification criteria as outlined by USDA Forest Service (2017).

Decay Class	Description
1	Limbs and branches all present, top pointed, all bark remaining, sapwood intact, heartwood sound, hard, original color
2	Few limbs and no fine branches present, top may be broken, bark variable, sapwood sloughing, heartwood sound at base, incipient decay in outer edge of upper bole, hard, light-to-reddish brown
3	Branches absent with only limb stubs, top broken, bark variable, sapwood sloughing, heartwood with incipient decay at base, advanced decay throughout upper bole, fibrous to cubical, soft, dark, reddish brown
4	Branches absent with few or no stubs, top broken, bark variable, sapwood sloughing, heartwood with advanced decay at base, sloughing from upper bole, fibrous to cubical, soft, dark, reddish brown
5	No limbs or branches, top broken, bark less than 20 percent, sapwood gone, heartwood sloughing, cubical, soft, dark brown, or fibrous, very soft, dark reddish brown, encased in hardened shell

Table V.2 Summary of field data for scanned pine trees (TAS = total above-stump, SB = stem plus bark, TB = tops and branches, and DBH = diameter at breast height). Sample sizes (n) were lower for TB components since many decay class four and all decay class five stems did not have TB material remaining. Stem bark remaining pertains to visually estimated percentage of bark remaining relative to existing upright stem portion (i.e., not original full height of tree). Stem bark remaining is shown as means with standard errors in parentheses.

Decay Class	n (TAS and SB)	n (TB)	DBH (cm)	Height (m)	Stem Bark Remaining (%)
1	10	10	12.5 - 60.1	16.0 - 26.4	67.8 (10.7)
2	10	10	12.7 - 57.2	11.0 - 25.3	53.8 (11.0)
3	10	10	16.6 - 59.4	13.2 - 24.4	40.0 (13.1)
4	12	6	14.8 - 68.0	3.3 - 18.6	62.3 (8.2)
5	7	0	11.9 - 28.6	1.5 - 3.1	82.9 (2.6)
Total	49	36	11.9 - 68.0	1.5 - 26.4	60.1 (4.8)

Scanning

Standing dead pine trees were scanned using a FARO Focus^{3D} X 330 laser scanner (FARO Technologies, Inc., Lake Mary, Florida, USA). The FARO scanner uses phase-based scanning to create a three-dimensional point cloud of objects and operates with relatively fast setup and scanning times. Prior to scanning, the FARO scanner was mounted on a carbon fiber tripod and leveled using the onboard inclinometer. Scanning resolution was set to 3.068 mm at 10 m range (i.e., ½ resolution according to FARO nomenclature) and a quality setting of 2×. Focal SDT or clusters of SDT were scanned from two to seven positions to obtain the most complete point cloud representation possible with minimal occlusion. Additionally, five spherical laser scanning targets (139 mm diameter) were placed on tripods and located around focal SDT for co-registering multiple scans into a single, complete point cloud. Scanning positions were generally

located at equidistant azimuths (e.g., for four scanning positions, scanner locations were ~90° apart with focal SDT as center point or for two positions, scanner locations were ~180° apart) to minimize occlusion of SDT and targets from surrounding vegetation. In some instances, surrounding brush and shrubs which obscured scanning lanes were cleared to provide as clear a view to focal SDT as possible.

Preprocessing and Volume Estimation

Individual scans around focal SDT were co-registered using FARO SCENE software (FARO Scene, 2015) to create a single comprehensive point cloud. Focal SDT were subsequently extracted from each co-registered point cloud using CloudCompare point cloud processing software (Girardeau-Montaut, 2017) such that each extracted point cloud contained only each individual focal SDT (i.e., from base of stump at ground level to branches or stem top) and no ground or neighboring tree points. Extracted individual SDT point clouds contained considerable noise points, a common challenge with phase-based TLS scanners (Aschoff *et al.*, 2004; Pueschel, 2013), particularly in the crooks between branches. Noise points were removed via manual clipping of SDT point clouds as well as through a filtering program, as described in Putman and Popescu (2018), which consisted of a nearest-neighbor point filter and *k*-means intensity cluster filter. In some cases, the *k*-means cluster intensity filter was too aggressive resulting in excessive artificial occlusion, typically at the stem top where return intensity was lower, as compared to the nearest-neighbor filter. Point clouds were examined visually for any gross reductions in points, particularly at the stem top. In total, 28 SDT point clouds

used the nearest-neighbor point filter only and 21 SDT point clouds used both the neareast-neighbor point filter and the *k*-means cluster intensity filter to create the final cleaned point clouds.

The volume calculation algorithm, TreeVolX (Putman and Popescu, 2018), was used to convert filtered and cleaned SDT point clouds into three-dimensional, reconstructed tree models (RTM) using voxels (i.e., virtual cubes of equal side lengths). Briefly, the algorithm accepts a point cloud, voxelizes it into a sparse voxel model, iteratively segments horizontal slices (i.e., of one voxel height) into individual branch and stem segments, and estimates the perimeter of each segment using least-squares ellipse fitting before filling the interior of each segment with remaining voxels. The result is a solid, three-dimensional RTM of each SDT composed of voxels where the volume is simply the number of voxels times the voxel volume (i.e., voxel side-length cubed).

Options are available in TreeVolX for improving the segmentation procedure and the final volume estimate in heavily-occluded point clouds. For segmentation, a proximity-based segmentation method can be used for high quality and high point density point clouds while an incremental ellipse fitting segmentation method can be used for lower quality and lower point density point clouds. Moreover, heavily-occluded point clouds can employ a vertical point cloud resampling (VPCR) technique discussed in full detail in Putman and Popescu (2018). Briefly, the VPCR technique accepts a user-defined voxel side length (i.e., a multiple of 5 mm that is > 5 mm) and, within each horizontal slice of this user-defined side length, condenses the points into a single planar

surface and subsequently voxelizes the condensed layer of points into a slice of 5 mm side-length voxels before expanding the new 5 mm slice vertically to fill the original horizontal slice of user-defined side length with similar layers of 5 mm voxels. Thus, the resulting effect allows for occluded sections of stem and branches to be filled in with voxels based on surrounding point occurrences.

TreeVolX was validated and errors were discussed in detail in Putman and Popescu (2018) generally showing that large branch/stem and fine branch RMSE were 8.45% and 75.92%, respectively (i.e., for incremental ellipse segmentation method). We generally expect similar error in volume estimation given that the trees used in this study were scanned under similar parameters and within the same forest as in Putman and Popescu (2018). For the purposes of this study, the incremental ellipse fitting segmentation was used for all point clouds under the assumption that the quality of fine branches in the upper canopies of less-decayed SDT point clouds was relatively low, precluding the use of the distance-only segmentation method. Moreover, later-decay stage SDT with minimal-to-no branches would not see appreciable change in volume estimates as they were primarily composed of large branch and stem sections which showed similar error under both segmentation methods as discussed in Putman and Popescu (2018). Finally, all SDT volumes were developed using one of two methods, 1) no VPCR with 5 mm voxel side lengths and 2) 1 cm VPCR for comparison. The first method does not account for occlusion while the second accounts for minimal occlusion without producing substantially more error than larger (2 cm - 5 cm) VPCR distances (Putman and Popescu, 2018). Following volume estimation, all SDT RTM were clipped

at approximately 30 cm height to exclude the stump portion and comprise total above-stump volume (TAS). Many stump sections of RTM contained substantial occlusion due to presence of ground-level vegetation and debris that could not always be removed for clear scanning. Where applicable (e.g., early decay stage SDT), TAS sections were further clipped into two main components, 1) main stem plus bark (SB) and 2) tops and branches (TB). All branches were clipped flush with the main stem and tops were clipped from main stems at approximately 10 cm diameter. By definition, TB are most prevalent in early decay class SDT (i.e., decay classes one through three) while later decay class SDT (i.e., decay classes four and five) contain very few-to-none of this material. For all decay class five SDT, TAS volume was equal to SB volume and TB volume was equal to zero.

Data Analysis

Initial examination of DBH as a function of SDT volume suggested that each component generally followed the power model form common to allometric relationships for biomass and volume in live trees. Subsequently, all allometric relationships for TAS, SB, and TB volume estimates were developed using the power model form,

$$Vol = a * X^b \quad \text{(V.1)}$$

where, *Vol* = the response variable volume, *X* = the matrix of covariates (i.e., DBH, height, etc.) and *a* and *b* are the intercept and scaling coefficient parameters to estimate,

respectively. To simplify parameter estimation, the power equation was transformed using the natural logarithm resulting in the log-linear relationship,

$$\ln Vol = \ln a + b * \ln X \quad \text{(V.2)}$$

which can be evaluated simply using least squares estimation for linear regression while also accounting for heteroscedasticity common in biomass and volume data. Models were developed using two continuous covariates, DBH and DBH^2*HT, while also accounting for the effect of decay class. These covariates were selected as they are commonly measured in forest inventories, typically provide strong explanatory power, and are comparable to commonly used live tree allometric relationships in the literature. Decay class was included as a categorical covariate in model development and likelihood ratio tests were used to compare the interaction model (i.e., unequal slopes and intercepts), additive model (i.e., equal slopes and unequal intercepts) and the base model (i.e., single covariate and no effect of decay class) to determine the importance of decay class in predicting volume. Given the three SDT components (TAS, SB, and TB), two voxel sizes (5 mm voxels and 1 cm VPCR), and two main covariates (DBH and DBH^2*HT, a total of 12 allometric models were considered in analyses. Resulting models were evaluated using the coefficient of determination (adjusted R^2), root mean square error (RMSE) as in Stovall *et al.* (2018), and Akaike's Information Criterion (AIC) on log-linear model forms.

Log-linear model forms must be back-transformed to the original power model form to make predictions in desired units of volume and biomass. However, when back-transforming log-linear equations, a correction factor must often be applied to account

for bias when transforming the error term from an additive format to a multiplicative format (Baskerville, 1972). Many correction factors (CF) have been proposed and the importance of each discussed extensively (Clifford *et al.*, 2013) with the suggested method being the 'MM' technique developed by Shen and Zhu (2008), which varies by covariate value as opposed to being constant for all covariate values, as the best CF for back-transforming log-linear model forms. Thus, for this study, the MM correction factor was applied when back-transforming calculated predictions of SDT volume from developed allometric relationships. TLS allometry volume predictions were compared to TLS-derived volumes and assessed using RMSE (as described above) and bias as in Stovall *et al.* (2018).

Proportion-Remaining Volume

Proportion-remaining volume was calculated for each decay class and component by dividing TLS allometry volume and TLS-derived volumes of SDT by a reference live tree volume of the same DBH. Reference live tree volumes were predicted using comprehensive national and regional biomass allometric equations from Jenkins *et al.* (2003) and Gonzalez-Benecke *et al.* (2014), respectively. Jenkins *et al.* (2003) equations were developed using a similar log-linear model form and predictions from these equations were similarly corrected using the MM technique (Shen and Zhu, 2008) as applied to TLS allometry volume predictions. Gonzalez-Benecke *et al.* (2014) equations were modeled using nonlinear regression and, thus, did not require correction. Since the reference live tree equations were developed for biomass, biomass estimates were

converted to volume by dividing by national estimates of component wood density. Stem wood and bark density estimates were taken from Miles and Smith (2009) and converted based on their formulae into a single estimate for combined stem wood and bark. Tops and branches wood density values were taken from Harmon *et al.* (2008) for undecayed fine woody debris and converted to an average, equally-weighted density estimate for all fine woody debris size classes. Finally, for TAS estimates, SB and TB density estimates were combined into a single density estimate by weighting the SB portion as 80% and TB portion as 20% (Jenkins *et al.*, 2003) and summing. Proportion-remaining volumes for TLS allometry volume and TLS-derived volume of SDT and Jenkins *et al.* (2003) and Gonzalez-Benecke *et al.* (2014) reference live tree volumes were summarized by component and decay class and were compared to theoretically-derived proportions from Domke *et al.* (2011) as developed for FIA SDT estimates.

Results

Volume estimates for 49 SDT across five decay classes were successfully developed using TLS point cloud data and the TreeVolX volume calculation algorithm. Between 7-12 SDT were scanned in each decay class with decay class five having the lowest (n_{DC5} = 7) and decay class four having the most (n_{DC4} = 12) stems (Table V.2). TAS and SB sample numbers were the same as for the total number of SDT scanned in each decay class while TB sample numbers were fewer for decay classes four and five (n_{TB_DC4} = 6 and n_{TB_DC5} = 0) (Table V.2). Diameters and heights of scanned SDT ranged from 11.9 cm to 68.0 cm and 1.5 m to 26.4 m, respectively (Table V.2). Decay class five

SDT covered the narrowest range of sizes while the four preceding decay classes all covered similar ranges for DBH and height (Table V.2).

Volume estimates for the different voxel sizes varied by component and were consistently greater in 1 cm VPCR estimates (Table V.3). SB component volumes differed the least (1.6%), followed closely by TAS (3.9%), with TB component volumes differing the most (29.2%) between the two voxel sizes overall. Differences between volume estimates by voxel sizes were greatest for decay class one and generally declined being least in decay class four (i.e., for TB) and decay class five (i.e., for TAS and SB). Percent volume differences between voxel sizes ranged between 0.8-2.2%, 0.8-10.7%, and 17.4-53.1% for SB, TAS, and TB, respectively. By far, SB components comprised the greatest proportion of TAS volumes representing approximately 83% for 5 mm voxels and 77% for 1 cm VPCR of TAS in decay class one and increased to 100% for decay class five. TB components represented roughly 17% for 5 mm voxels and 22% for 1 cm VPCR of TAS volumes in decay class one, the greatest such amount, and decreased in subsequent decay classes to approximately 1% of TAS volume by decay class four, where TB components were still measurable.

Table V.3 Means with standard errors in parentheses for point cloud and volume data for scanned pine trees (TAS = total above-stump, SB = stem plus bark, TB = tops and branches, and DBH = diameter at breast height). NN distance is nearest neighbor distance for points in preprocessed (i.e., registered, filtered) point clouds for total aboveground portion of SDT (i.e., all components including stump portion). Absolute difference values (m^3) are average differences between resampled (1 cm VPCR) and non-resampled (5 mm voxels) volumes. Percent difference values are the percentage increase from resampled (1 cm VPCR) to non-resampled (5 mm voxels) volumes relative to non-resampled volumes.

	Point Cloud	TAS		SB				TB			
Decay Class	NN Distance (cm)	Difference (m^3)	Difference %	Difference (m^3)	Difference %	Proportion Relative to TAS (5 mm)	Proportion Relative to TAS (1 cm VPCR)	Difference (m^3)	Difference %	Proportion Relative to TAS (5 mm)	Proportion Relative to TAS (1 cm VPCR)
1	0.2029 (0.0185)	0.0670 (0.0171)	10.7 (2.2)	0.0241 (0.0105)	2.2 (0.8)	0.829 (0.044)	0.773 (0.050)	0.0429 (0.0088)	53.1 (5.9)	0.171 (0.044)	0.227 (0.050)
2	0.1903 (0.0250)	0.0341 (0.0127)	4.0 (0.7)	0.0216 (0.0096)	1.8 (0.3)	0.902 (0.049)	0.886 (0.051)	0.0122 (0.0034)	40.3 (9.2)	0.098 (0.049)	0.113 (0.052)
3	0.1535 (0.0162)	0.0336 (0.0170)	2.6 (0.5)	0.0279 (0.0167)	1.8 (0.6)	0.942 (0.030)	0.935 (0.030)	0.0056 (0.0012)	28.9 (5.1)	0.058 (0.030)	0.065 (0.030)
4	0.1618 (0.0107)	0.0154 (0.0084)	1.1 (0.3)	0.0148 (0.0082)	1.1 (0.3)	0.986 (0.013)	0.986 (0.013)	0.0006 (0.0004)	17.4 (8.5)	0.014 (0.013)	0.014 (0.013)
5	0.1194 (0.0165)	0.0004 (0.0002)	0.8 (0.2)	0.0004 (0.0002)	0.8 (0.2)	1.000 (0.000)	1.000 (0.000)	-	-	-	-
Total	0.1683 (0.0086)	0.0313 (0.0065)	3.9 (0.7)	0.0187 (0.0049)	1.6 (0.2)	0.930 (0.017)	0.914 (0.019)	0.0125 (0.0030)	29.2 (4.0)	0.070 (0.017)	0.086 (0.019)

A total of 12 allometric models were developed across all SDT component parts (TAS, SB, and TB), each main covariate (DBH and DBH^2*HT) and both voxel sizes (5 mm voxels and 1 cm VPCR) (Table V.4). For all cases, the interaction between the main covariate and decay class did not result in a significantly better model fit than the additive model ($p > 0.05$). For 10 of the 12 allometric models developed, the additive model provided a significantly improved fit over the covariate only model ($p < 0.05$). Notably, the inclusion of height in the main covariate (i.e., DBH^2*HT) for both TAS models provided an improved fit over when decay class was also included. Differences between model parameters and model fits for the two voxel sizes were very minimal at each component and covariate (Table V.4, Figure V.2 and V.3, Appendix D: Figure D.1). Overall, the inclusion of height in the main covariate resulted in improved fits for all TAS and SB models (i.e., higher adjusted R^2, lower RMSE, and lower AIC) but not for TB models. Allometric models for TB contained considerably more variability as adjusted R^2 values were slightly more than half, RMSE values were nearly three-times greater, and AIC values were an order of magnitude greater than those in TAS and SB models (Table V.4). Plots of log-linear models using DBH as the only main covariate showed stratification between each decay class, particularly for decay classes four and five (Figure V.2). The inclusion of height in the main covariate accounted for much of the variability between decay classes resulting in less evident stratification between plotted trends, particularly in TAS and SB models (Figure V.3).

Table V.4 Allometric equation results for log-linear relationships of total and component volumes (TAS = total above-stump, SB = stem plus bark, TB = tops and branches, and SE = standard error). All values and units correspond to log-linear model form: ln(Volume m^3) = a + b*ln(IV), where IV = independent variable. Sample size (n) for TAS and SB included the full dataset, n = 49 while for TB, n = 36 since many decay class four and all decay class five SDT did not have TB material remaining.

Component	Voxel Size	IV	Decay Class	a (SE)	b (SE)	Adj. R^2	RMSE (log units)	AIC
TAS	5 mm	DBH	1	-7.8164 (0.3184)	2.2738 (0.0963)	0.9510	0.2821	29.0512
			2	-7.9948 (0.3262)				
			3	-8.0500 (0.3386)				
			4	-8.4606 (0.3244)				
			5	-9.5476 (0.3002)				
	1 cm	DBH	1	-7.6789 (0.31847)	2.2620 (0.0963)	0.9513	0.2822	29.0731
			2	-7.9179 (0.3263)				
			3	-7.9847 (0.3387)				
			4	-8.4116 (0.3245)				
			5	-9.5056 (0.3003)				
	5 mm	DBH^2*HT	All	-8.8971 (0.1714)	0.8903 (0.0191)	0.9784	0.1960	-14.6656
	1 cm	DBH^2*HT	All	-8.9007 (0.1624)	0.8950 (0.0181)	0.9807	0.1857	-19.9598
SB	5 mm	DBH	1	-8.4750 (0.3700)	2.4180 (0.1118)	0.9372	0.3278	43.7629
			2	-8.5851 (0.3791)				
			3	-8.6016 (0.3935)				
			4	-8.9442 (0.3769)				
			5	-9.9640 (0.3489)				
	1 cm	DBH	1	-8.4979 (0.3708)	2.4320 (0.1121)	0.9376	0.3286	43.9958
			2	-8.6123 (0.3800)				
			3	-8.6315 (0.3944)				
			4	-8.9792 (0.3778)				
			5	-9.9963 (0.3497)				

Table V.4 (Continued)

Component	Voxel Size	IV	Decay Class	a (SE)	b (SE)	Adj. R^2	RMSE (log units)	AIC
SB (cont.)	5 mm	DBH^2*HT	1	-9.9100 (0.3354)	0.9710 (0.0347)	0.9612	0.2576	20.1480
			2	-9.8047 (0.3351)				
			3	-9.7653 (0.3444)				
			4	-9.5514 (0.3124)				
			5	-9.3711 (0.2507)				
	1 cm	DBH^2*HT	1	-9.9433 (0.3341)	0.9769 (0.0346)	0.9619	0.2566	19.7592
			2	-9.8410 (0.3338)				
			3	-9.8040 (0.3430)				
			4	-9.5918 (0.3112)				
			5	-9.4015 (0.2497)				
TB	5 mm	DBH	1	-5.8388 (1.2314)	1.0106 (0.3749)	0.5194	0.9989	114.0875
			2	-6.8714 (1.2621)				
			3	-7.3906 (1.3107)				
			4	-9.3846 (1.3707)				
	1 cm	DBH	1	-5.2730 (1.1323)	0.9641 (0.3447)	0.5815	0.9186	108.0518
			2	-6.4002 (1.1606)				
			3	-6.9868 (1.2053)				
			4	-8.9496 (1.2605)				
	5 mm	DBH^2*HT	1	-6.6585 (1.5081)	0.4294 (0.1573)	0.5217	0.9966	113.9190
			2	-7.6008 (1.5067)				
			3	-8.1032 (1.5492)				
			4	-10.0032 (1.5717)				
	1 cm	DBH^2*HT	1	-6.0876 (1.3835)	0.4131 (0.1443)	0.5854	0.9143	107.7104
			2	-7.1287 (1.3822)				
			3	-7.7002 (1.4212)				
			4	-9.5733 (1.4418)				

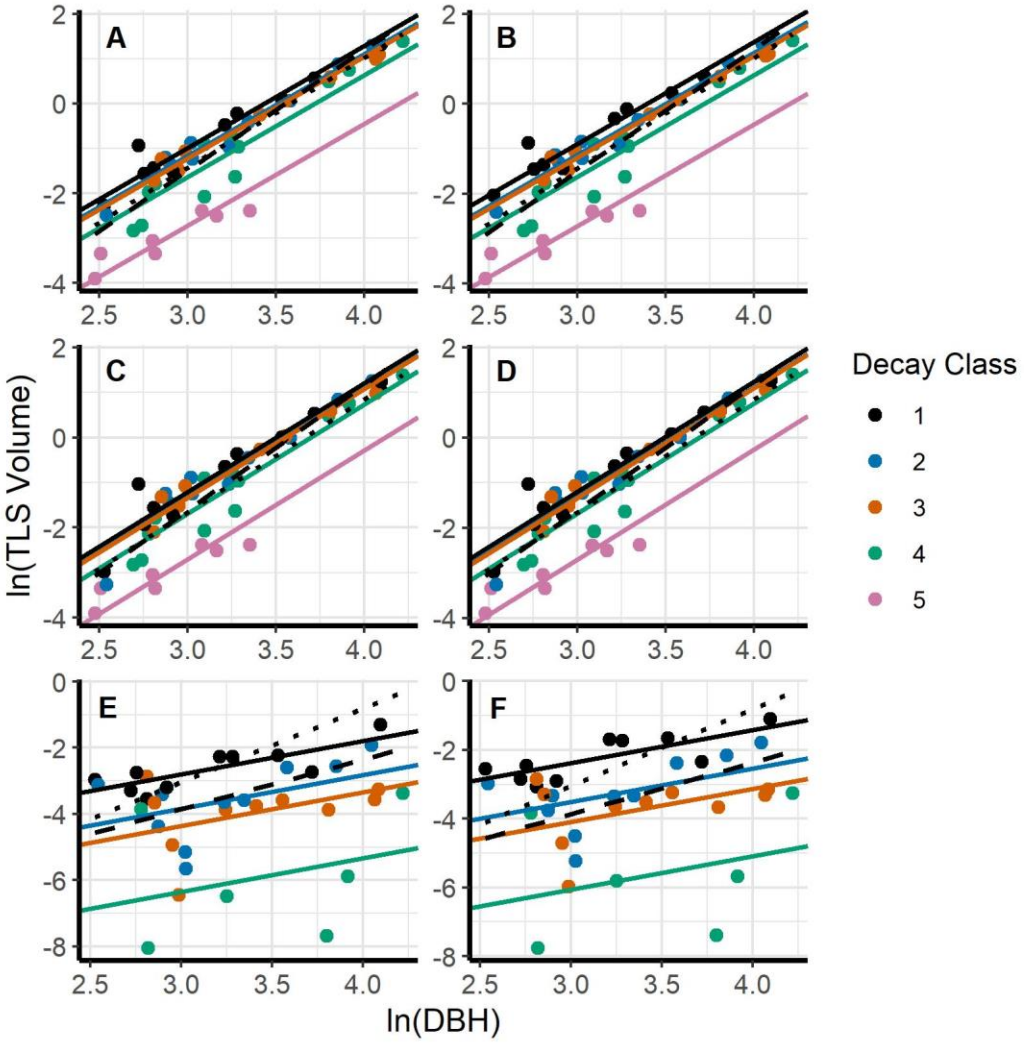

Figure V.2 Allometric relationships of natural logarithm transformed volume (m^3) for A) TAS-5 mm, B) TAS 1-cm VPCR, C) SB-5 mm, D) SB-1 cm VPCR, E) TB-5 mm, and F) TB-1cm VPCR plotted against natural logarithm transformed DBH (cm) by decay class (TAS = total above-stump, SB = stem plus bark, TB = top and branches). Dashed and dotted black lines represent predicted live tree volumes of similar components derived from Gonzalez-Benecke et al. (2014) and Jenkins et al. (2003), respectively.

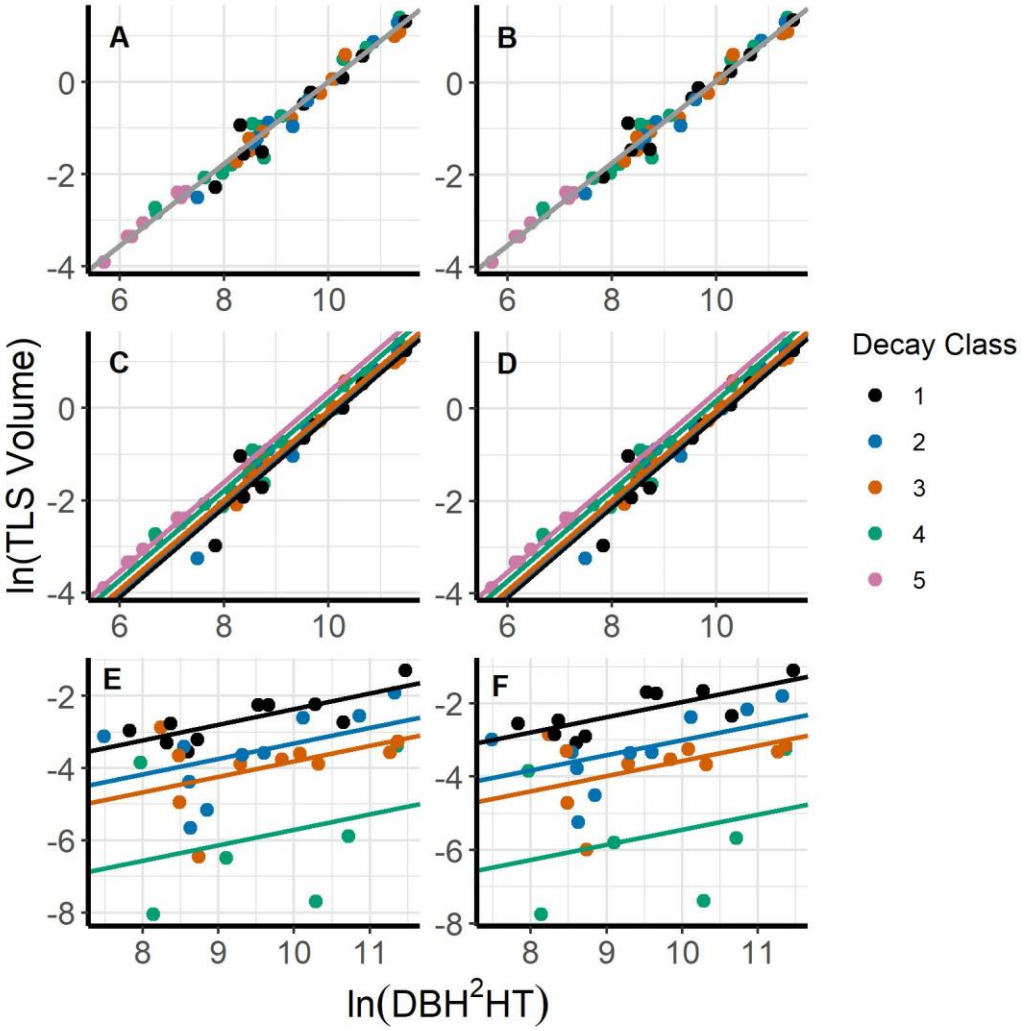

Figure V.3 Allometric relationships of natural logarithm transformed volume (m^3) for A) TAS-5 mm, B) TAS-1 cm VPCR, C) SB-5 mm, D) SB-1 cm VPCR, E) TB-5 mm, and F) TB-1 cm VPCR plotted against natural logarithm transformed DBH^2*HT (cm^2*m) by decay class (TAS = total above-stump, SB = stem plus bark, TB = tops and branches). Predicted live tree component volumes from Gonzalez-Benecke et al. (2014) and Jenkins et al. (2003) were not plotted as they used different model forms for height or did not use height at all, respectively.

TLS allometry volume predictions were back-transformed and corrected from log to original units (volume, m^3) and compared to TLS-derived volume estimates (Figure V.4). Comparisons were made for 5 mm voxel size models only given the similarity between models of both voxel sizes. Predicted TAS TLS allometry volumes matched TLS-derived volumes quite closely for both DBH only and DBH^2*HT models (bias = 0.009 m^3 and -0.0111 m^3, respectively) while SB models tended to slightly overpredict volume (bias = 0.0285 m^3 and 0.0232 m^3, respectively) (Figure V.4). The inclusion of height in the main covariate for TAS and SB models also improved predictions as RMSE was approximately 0.074 and 0.052 m^3 less, respectively, compared to DBH-only models (Figure V.4). Height did not appear to improve allometric model predictions for TB volumes as they compared very similarly to TLS-derived volumes (RMSE ≈ 0.0297 m^3 for both), generally tending to be over predicted (bias ≈ 0.0076 m^3 for both) (Figure V.4).

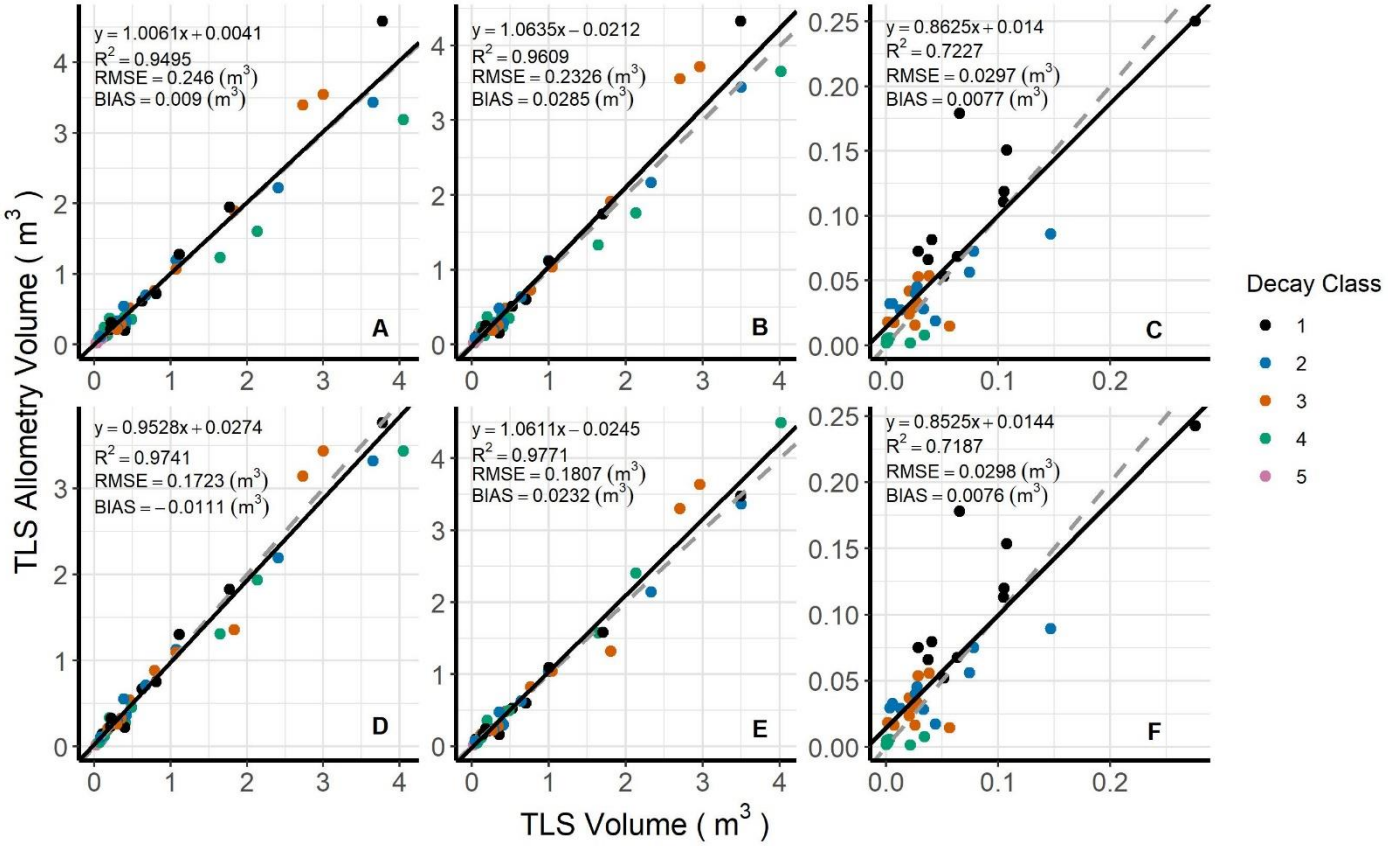

Figure V.4 TLS allometry volume (m^3) from allometric equations vs. TLS-derived volume for A) TAS, B) SB, and C) TB predicted from DBH (cm) and D) TAS, E) SB, and F) TB predicted using DBH^2*HT (cm^2*m). Black lines are fitted regression lines and gray dashed lines are 1:1 lines. TLS allometry volumes were back transformed and corrected from natural logarithm units using the MM correction factor from Shen and Zhu (2008).

Proportion-remaining volume was calculated for each component (TAS, SB, and TB) using both TLS allometry volumes and TLS-derived volumes of SDT while live tree reference values were calculated using allometric models from Gonzalez-Benecke et al. (2014) for loblolly pine (*Pinus taeda*) and from Jenkins et al. (2003) for *Pinus* (Figure V.5, Appendix D: Table D.1). Proportions were calculated and presented for 5 mm voxel size estimates only given the strong similarity with 1 cm VPCR voxel size estimates. Broadly, proportion-remaining volumes suggest that SDT volume estimates were overpredicted relative to generalized national and regional equations for similar species as many proportions are greater than one (Figure V.5, Appendix D: Table D.1), particularly in early decay classes. Both TAS and SB followed nearly identical trends given that TB volumes were the only difference between the two and, ultimately, comprised a much smaller fraction of TAS than the SB material. Proportions for decay class one TB showed considerable variability which stabilized or decreased substantially in the subsequent remaining decay classes (Figure V.5, Appendix D: Table D.1). For TAS and SB, Gonzalez-Benecke et al. (2014)- and Jenkins et al. (2003)-derived proportions in TAS and SB were similar within each decay class while Jenkins et al. (2003)-derived values tended to be lower within each decay class for TB material (Figure V.5, Appendix D: Table D.1). In all cases, proportions decreased as decay class increased with proportions in TB decay class five being zero for both empirical estimates and for theoretical estimates from Domke et al. (2011). Notably, empirical TB proportion estimates were greater but, generally, match closely with theoretical

proportions from Domke et al. (2011), particularly using Jenkins et al. (2003)-derived reference live tree values (Figure V.5, Appendix D: Table D.1).

Figure V.5 Proportion-remaining volume (m^3/m^3) based on 5 mm non-resampled voxels by decay class, live tree reference volume source, and component (TAS = total above-stump, SB = stem and bark, TB = tops and branches) with FIA theoretical values from Domke et al. (2011) as black triangles for TB.The top three figures use TLS-derived volumes for A) TAS, B) SB, and C) TB in the numerator (i.e., black points are outliers) while the bottom three figures use TLS allometry volumes for D) TAS, E) SB, and F) TB in the numerator. TLS allometry volumes and Jenkins et al. (2003) predictions were back transformed from natural logarithm units and corrected using the MM correction factor from Shen and Zhu (2008). Gonzalez-Benecke et al. (2014) predictions did not require correction since models were developed using non-linear regression. Dotted lines represent proportion-remaining volume = 1 where SDT and live tree reference volumes are equal. Decay class five TB are zero for empirical estimates from this study and similarly for theoretical estimates from Domke et al. (2011).

Figure V.5 (continued)

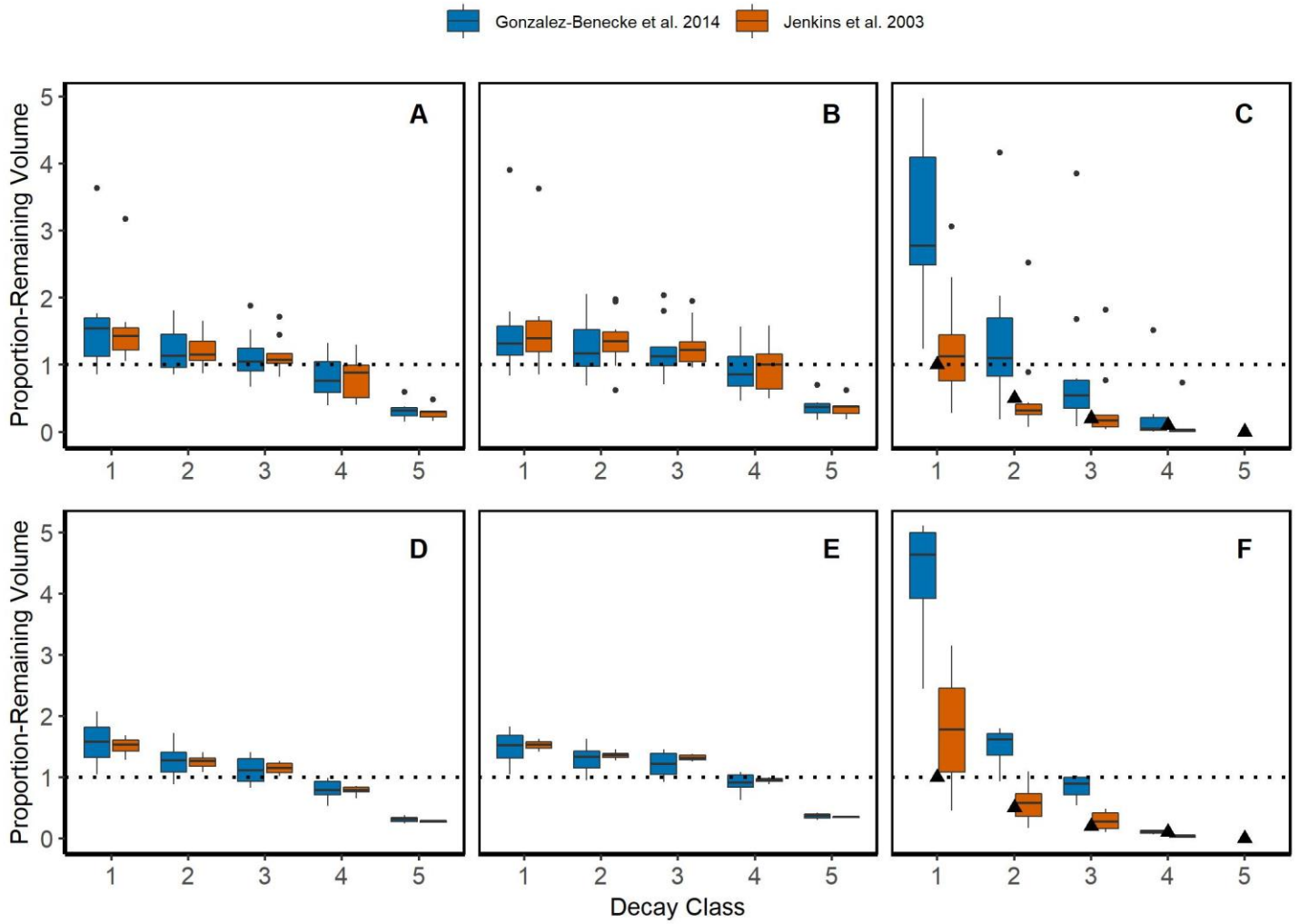

Discussion

Terrestrial LiDAR remote sensing coupled with the TreeVolX volume calculation algorithm allowed for rapid production of loblolly pine SDT component volume estimates across decay classes. Subsequently, these estimates contributed to producing robust allometric models of the same component volumes using commonly measured metrics of DBH, height, and decay class which directly estimate volume of SDT while accounting for volume changes with decay class. Moreover, empirically-derived proportion-remaining volumes of SDT were produced by decay class and component parts using both TLS-derived volumes and TLS allometry volumes. To the authors' knowledge, this is the first such study that produced allometric models of SDT volume using decay class as a covariate as well as calculating empirically-derived proportion-remaining volume of SDT by decay class based on TLS measured volumes. Other studies have, in part, addressed portions of these topics and provided important insight for framing aspects of this study (Aakala, 2010; Domke *et al.*, 2011; Russell and Weiskittel, 2012). Models and results produced herein serve as an attempt to fill a much needed gap in the literature on accurately estimating SDT volume and understanding structural changes in SDT decomposition by employing novel methodologies for estimation. Models can be used to directly estimate volume of SDT by decay class for pine trees in east Texas with possible application in other southern pines in the southeastern U.S.

Volume Estimates and Allometric Relationships

The voxel sizes examined (5mm voxels and 1 cm VPCR) did not appear to result in noticeable differences in volume estimates or allometric model parameters, particularly for TAS and SB components. Differences in TAS volume estimates of similar SDT for the two voxel sizes were all very low (i.e., less than 5% greater in 1 cm VPCR) with the exception of decay class one volumes which were 10.7% greater (Table V.3). Furthermore, model assessment metrics of adjusted R^2, RMSE, and AIC were nearly identical for the two voxel sizes in TAS and SB models of similar covariates. The lack of difference between voxel size estimates and parameters is not surprising for SB components where occlusion tended to be minimal or non-existent. Likewise, the lack of difference might also reflect that choosing 1 cm voxel side lengths for resampling may not have been sufficient to fill in substantial portions of occlusion in SB components. Volume differences between voxel sizes for TAS, for the most part, were of similar magnitude as SB given that greater than 80% of TAS volumes were comprised of SB (Table V.3). However, it was clear the additional tops and branches resulted in greater differences in decay classes one through three compared to SB. In fact, the effect of resampling on TB components alone, even at just 1 cm VPCR, resulted in volume increases of an order of magnitude for all decay classes (i.e., approximately 17-53% greater TB volume, Table V.3) compared to non-resampled 5 mm voxels. Subsequently, these percentages would only increase with larger voxel resampling sizes. This effect of greater differences in TB component volumes with increasing voxel sizes most likely stems from using the incremental ellipse segmentation method for all SDT volume

estimates coupled with occlusion and sparse point densities in the canopy. Putman and Popescu (2018) noted that the incremental ellipse segmentation method could result in up to approximately 75% RMSE of volume estimates in small branches. Erroneous ellipse fitting between sparse points among fine branches likely created artificially increased volumes in TB components at both voxel sizes and was further compounded by resampling.

Allometric models for SDT all followed the power model form commonly used for live tree allometric relationships. In allometric model development, it is important to have a strong relationship between the covariate(s) and response variable. Models produced here, particularly for TAS and SB, highlight that SDT still generally maintained a strong positive exponential relationship with increasing DBH size. In fact, adjusted R^2 values were strong for TAS and SB ranging between approximately 0.93-0.98, comparable to live tree allometric power models of similar species (Gonzalez-Benecke *et al.*, 2014) or those produced via TLS-derived volumes (Olagoke *et al.*, 2016; Stovall *et al.*, 2018), granted these other studies estimated biomass. Decay class five SDT tend to occur rarely on the landscape and this was reflected in the limited DBH size range (11.9-28.6 cm) and sample size for decay class five SDT in our dataset ($n_{DC5} = 7$). Given this, it is difficult to say whether the remaining volume for samples in decay class five would best follow the power model or perhaps a linear model may be more appropriate. Decay class five SDT typically have substantially reduced height, no branches, and little or no remaining bark relative to its past live tree form based on classification criteria (Table V.1). Thus, volume of this decay class is contingent upon

the quantity of any of these remaining attributes. Nevertheless, allometric models of SDT volume appear to follow similar model form and offer similar accuracy as models for live trees.

Inclusion of height as a covariate slightly improved model fits for TAS and SB but not so for TB models. Adjusted R^2 values increased roughly 3% from DBH-only models for TAS and SB while they increased <1% from DBH-only models for TB. Notably, inclusion of height as a covariate in TAS models accounted for the variation across decay classes ultimately by providing a better fit than the model which explicitly included decay class as a factor. However, including both decay class and height together in SB models provided a better fit than excluding either one. These results make logical sense given the general criteria differentiating decay classes in the five-class system employed by FIA, which was used in this study (Table V.1). Remaining canopy volume represents a substantial part of the total volume of a SDT and, following decay class descriptions, generally decreases in volume systematically with increasing decay class. For example, the form of decay class one SDT very closely reflects the form of live trees and by decay classes two and three most of the branches are gone with the top likely broken by decay class three or four. For SB components, bark and the very tops of stems are the portions that can be lost with increasing decay class representing a more gradual reduction in volume than for TAS, especially for decay classes one through three where relatively little change is defined as compared to TAS (Table V.1). Hence, both height and decay class remained important for predicting volume in SB by accounting for changes in height and subtle changes in bark loss. Importantly, these results highlight

that measuring height in inventory situations can provide strong estimation of SDT TAS volume in cases where a decay class was not assigned or a different decay classification system was used, ultimately increasing the applicability and further highlighting the value of SDT allometric equations.

In contrast to TAS and SB components, allometric models of TB provided weaker relationships with DBH, height, and decay class. Approximately 40% less variation was explained via adjusted R^2 values in TB volumes using DBH, height, and decay class than for TAS and SB components (i.e., adjusted R^2 for TB were ~0.52-0.58). Moreover, inclusion of height added no perceivable improvement in model fit than for models with DBH only (i.e., <1% increase in adjusted R^2). This weaker relationship for TB components likely stems in part from the variability in volume estimates produced from the chosen techniques and parameters applied when using TreeVolX, as discussed previously. For example, the TreeVolX algorithm and chosen parameters for volume calculation (i.e., incremental ellipse segmentation method) occasionally will segment sparse points from multiple smaller branches into one segment creating an erroneous overestimate of volume in TB material (e.g., see Putman and Popescu (2018) Figures 19 and 20) which can be compounded by use of resampling. In addition, the weaker relationships for TB component allometric models may also stem in part from the inherent variability in remaining canopy branches with decay class. Decay classifications describing the amount of remaining branches are ambiguous but generally imply that fine branches are lost early in the decay process, followed eventually by medium and large branches in addition to tops (Table V.1). Literature remains sparse on the size-class

proportions of branch material within live or SDT canopies. The reconstructed SDT models derived from TLS point clouds produced herein did not provide sufficient accuracy to consistently and reliably separate branch components by commonly-defined branch size classes. Regardless of branch size class, a SDT in any particular decay class could have variable amounts of branch material remaining yet could still be assigned the same decay classification. For example, a decay class one tree could have all branches intact or could be missing some proportion of branches and yet still potentially be classified as decay class one. Subsequently, inherent variability in the amount of branch material remaining in the canopy for any particular decay class was also compounded at times by the erroneous segmentation and clustering of smaller branch components into overestimates of volume.

Proportion-Remaining Volume

Structural changes in SDT as measured by proportion-remaining volume generally followed expected decreasing patterns with each successive decay class. However, the calculated proportions reflect the large amount of variability in volume estimates of SDT sampled in this study. Moreover, the volume estimates produced herein appear to be overpredicted compared to reference live tree volumes from Jenkins *et al.* (2003) and Gonzalez-Benecke *et al.* (2014). Conceptually, SDT volumes should be less than their respective live tree reference volumes given density and structural losses with decomposition (Domke *et al.*, 2011). Proportions of remaining volume for TAS and SB in decay classes one through three were all greater than or equal to one, indicating

that SDT volume was consistently greater than reference live tree volumes. Despite this, proportions for TB material generally followed the same pattern as devised by Domke *et al.* (2011) and nearly matched their values when using Jenkins *et al.* (2003) for reference values. This trend generally makes sense given the systematic description of changes to tops and branches described in the FIA decay classification criteria (Table V.1). Consequently, the theoretical quantities derived from these criteria by Domke *et al.* (2011) appear to be well founded, particularly for pine species with excurrent branching structure (i.e., dominant apical leader with cone-shaped branching structure). It is worth noting that the reference live tree volumes were derived from biomass estimates and required assumptions about the wood density and proportion of material within a single tree (i.e., proportion of TB or SB to TAS and proportion of branches by size class in TB). Variability in these assumptions also likely affected the variability of proportion-remaining volume estimates.

Conclusions and Applications

TLS provides an effective, rapid, non-destructive means to quantify volume of SDT in field-based, dense or closed canopy forest conditions. This is possible through application of the TreeVolX volume calculation algorithm and the available options for creating reconstructed models of SDT. Importantly, robust allometric models using SDT volumes were produced from these novel, TLS-derived volume estimates using common methods of allometric model development as for live tree volume or biomass. Allometric models of SDT volume generally differed by decay class in intercept only and not slope.

Inclusion of height as a covariate in SDT allometric models for TAS precluded the need for including decay class as an additional covariate. Importantly, this means that TAS volume estimates can still be derived for SDT measured in forest inventories with dissimilar decay classification schemes or where no decay class was assigned. The choice of the incremental ellipse segmentation method in TreeVolX volume reconstruction created large amounts of variability and erroneous estimates of volume among fine branches of early decay class SDT. The choice of 1 cm VPCR increased volume estimates relative to non-resampled 5 mm voxel sizes yet did not substantially differ in estimates for TAS and SB and in allometric models. Given this, it is recommended to use the allometric models developed with non-resampled 5 mm voxels for predicting volume of SDT loblolly pine. Empirically-derived proportion-remaining volume by SDT component showed expected decreasing trends as decay class increased and, for TB material, appeared to match theoretically-derived estimates fairly closely. Further refining of volume reconstruction options will be necessary to reduce error in associated estimates, particularly TB material. Future work should include development of allometric relationships for more species and growth forms (e.g., trees with decurrent growth structure).

Application of allometric models developed herein could include for direct estimation of SDT southern pine volume in east Texas and possibly in other regions where loblolly pine occurs, notably, without the need to account for volume reduction with decay. Specifically, estimates could directly determine volume of SDT as wildlife habitat, volume of standing fuels for wildfire or prescribed fire or falling tree risk

assessment, as well as volume of SDT following major disturbance. Models could be coupled with component wood density and carbon/nutrient estimates to produce above stump and component biomass or carbon/nutrient estimates of SDT where needed. Direct prediction of SDT resources and improved understanding of volume change with decay class remain critical areas of research with the continued threat of future disturbances and need for accurately quantifying forest resources for a variety of ecosystem services.

CHAPTER VI

SUMMARY AND CONCLUSIONS

East Texas is unique within the south-central U.S. in that it is important both ecologically and economically in regards to its forests. This region comprises the western range margin of West Gulf Coastal Plain forests and the southwestern extent of many eastern tree species, both angiosperms and gymnosperms. In particular, east Texas is a notable producer of timber and wood products with substantial proportions of the landscape comprised of intensively managed plantations. Four national forests are located in this region, managed for multiple uses including wildlife habitat, recreation, threatened and endangered species, and grazing among others. Moreover, many forested hectares are owned by small-scale, private landowners seeking to make a small profit from wood products or provide habitat and healthy forests for future generations.

As climate changes globally, the impacts of future disturbances on forest ecosystems will become increasingly apparent. The extreme and record drought that occurred in east Texas and the south-central U.S. in 2011 is one example of a potential extreme disturbance that could become more common in the next few decades. The effects of extreme drought could have far-reaching implications on the forest ecosystem services and local communities in east Texas. However, little is known about the impacts of extreme droughts in forests especially with regard to species mortality responses, management, and dead wood dynamics. Subsequently, this dissertation aimed to address the following questions: What was the temporal mortality response of different species

in east Texas multiple years after the 2011 drought and did pests play a role in driving lagged mortality? What impact did management have on the mortality response of important southern pine species following the 2011 drought? What are the dynamics of trees and snags transitioning from the standing dead pool to the downed pool in a region characterized by rapid decomposition? Finally, how effective are estimates of SDT volume, derived from non-destructive LiDAR measurements, at quantifying and characterizing structural volume changes in standing dead pines across decay classes?

Tree species showed variation in their mortality response and ability to tolerate water stress under the extreme, acute drought conditions throughout 2011. Oaks were most negatively affected and endured immediate and substantial mortality. The 2011 drought appeared to surpass a threshold by which oak species could not continue transpiration. Pine species, on the other hand, appeared to tolerate the drought conditions quite well having the lowest mortality of all species examined. Albeit, mortality did increase two years post-drought suggesting that pines were not completely immune to the water stress. Tree species employ differing strategies for coping with water stress including deep rooting, regulating stomata, and leaf abcission, among others. The ability of trees to successfully employ these strategies depends also on the nature of the water stress such as timing, intensity, and duration. It appears that, despite the intense and acute nature of the extreme 2011 drought, some tree species in east Texas, such as pines, were able to utilize their strategies to overcome mortality. Put another way, the extreme drought conditions did not result in indiscriminate and substantial mortality regardless of species. Pests also appeared to play a role in driving continued mortality beyond the

drought event yet were not as substantial a driver as the drought conditions alone. Pest mortality trends were similar as with drought-specific mortality for pines (lower mortality) and oaks (greater mortality). In particular, southern red oak was most affected by pest mortality falling in line with trends seen in red oak species affected by the red oak borer in Arkansas and Missouri.

A critical finding from this dissertation was that pines in east Texas were inherently resistant to mortality from the extreme drought conditions. In particular, the effect of management appeared to play an important role in reducing mortality in loblolly pine. Specifically, planted loblolly pine increased in mortality rate by only 10% under extreme drought conditions whereas, drought exposed naturally-regenerated loblolly pine and shortleaf pine increased mortality rates by >20%. Common management practices that maintain stands at low densities to reduce competition and harvesting moderate tree sizes were important for reducing the risk of drought mortality in planted pines. Interestingly, greater overstory species diversity in naturally-regenerated loblolly stands appeared to be an important factor for reducing drought mortality. Unfortunately, little information was gleaned for shortleaf pine response to extreme drought. As expected, shortleaf pine mortality was generally greater than loblolly pine yet the limited sample size in the dataset precluded any meaningful management recommendations. Importantly, maintenance of loblolly pine within common management targets for stand density and stem size appeared to be sufficient for avoiding excessive mortality from extreme drought.

Following mortality, decomposition generally governs the rate at which SDT transition to downed dead wood. This dissertation has shown that the rate at which trees and snags transition from standing to downed is rapid in east Texas. Two separate groups of standing trees were defined based on inherent processes and nuances of inventory re-measurements, tree-fall and snag-fall. The tree-fall group included live trees which died and fell at the same time or died, remained standing for a short period, and fell within five years. The snag-fall group included SDT which fell after five years. As expected for both groups, stem size was a critical factor determining the probability of falling in a five-year period. Stem size generally correlates positively with wood durability and, subsequently, larger stems require greater forces to snap and take longer to decompose. For trees that die and fall simultaneously, large hardwoods on wet sites had a slightly greater chance of falling. This result highlights a unique process by which bottomland species may be more susceptible to wind disturbance such as hurricanes. Ultimately, models produced in this dissertation for predicting tree- and snag-fall probabilities provide key quantitative tools for managers and modelers seeking to provide appropriate wildlife habitat, predict falling tree hazards, understand wildland fire behavior and risk, and parameterize carbon models.

Understanding structural volume changes in SDT remains an important area of development for improving volume, biomass, and carbon estimates across multiple scales. Terrestrial LiDAR and the TreeVolX volume calculation algorithm were shown to be effective tools for efficient, non-destructive estimation of standing dead pine tree volumes. Most notably, these estimates produced robust allometric models for predicting

SDT volume by decay class, a first such attempt. These allometric models directly and inherently account for structural volume changes with progressive decay. In fact, models appeared to differ in intercept and not slope suggesting uniform differences between decay classes regardless of the predictive covariates of DBH or height. Moreover, the addition of height precluded the need for decay class as a predictor altogether for total above-stump volume estimates. These results highlight that, while decay classifications are subjective, quantitative and systematic trends can be gleaned from their use for improving biomass and carbon estimates of SDT. Further refinement of volume estimates is needed, however, for reducing overestimation of volume in remaining canopy materials (i.e., tops and branches). Volume estimates of SDT provided an opportunity to examine trends in proportion of remaining volume relative to reference live tree estimates by decay class, another first such attempt using TLS-derived SDT volumes. Estimated proportions of remaining volume followed expected decreasing trends with decay class, however, further refinement of volume estimates for both SDT and reference live trees will subsequently enhance understanding of these structural changes.

Overall, this dissertation provided a regional scale assessment of the impacts of extreme drought and subsequent decomposition dynamics in West Gulf Coastal Plain forests, a uniquely situated region characterized by both managed and unmanaged forests at the western extent of their range. Pine forests, particularly managed pine forests, appeared resistant to the record heat and water stress imposed by the 2011 drought. On the other hand, oak species appeared quite vulnerable to the drought and, if

similar drought conditions become more frequent, as climate predictions suggest, some species may not be able to persist into the future. Future work should continue to examine the specific management techniques and physiological traits by which pines and oaks survive and succumb to extreme water stress. Subsequent decomposition of SDT in these forests was found to be quite rapid with nuances in regards to stem size, wood type, and stage of decay. In general, the rapid fall-rate of SDT is largely due to the warm, moist climate and unique decomposer community that includes termites. As future disturbances are predicted to become more frequent and severe, managers and scientists will require the quantitative tools for tree- and snag-fall and SDT volume prediction developed herein to ensure they provide sufficient habitat for cavity-nesting species, quantify and predict fuel loads and fire risk, and accurately constrain biomass and carbon models for accounting and inventory. Continued refinement of these tools will improve estimation and, ultimately, enhance management actions and advance modeling efforts for predicting future impacts of extreme disturbances.

An implied goal of this dissertation was to inform understanding of future extreme droughts with an application to forest resources of east Texas. The findings summarized above provide a broad perspective to the impacts of extreme drought. Management-oriented objectives will still need to be devised by local managers and stakeholders for the specific forested stands which they oversee. However, the broad-scale findings and tools produced here can provide an important starting point for devising these objectives where, previously, little was known about response of east Texas forests to extreme drought. Importantly, basic management actions such as

thinning could go a long way toward reducing mortality risk of loblolly pine. Planting young loblolly at lower densities could help reduce mortality as the stand initiates. Moderate stem sizes had very low mortality thus, harvesting stems at merchantable sizes before they reach large size classes could help provide economic returns and reduce losses from drought mortality. If managing stands of naturally-regenerated loblolly pine, it may be worthwhile to reduce loblolly densities and allow other hardwoods to establish. In this scenario, objectives may need to shift from pure loblolly-focused economic returns to multiple objectives providing merchantable hardwoods or improving wildlife habitat.

In terms of dead wood resources, the tools developed in this dissertation can help managers better understand and manipulate dead wood on their land base. As carbon markets develop, the SDT allometric models could simplify estimation of dead wood pools and, coupled with the tree- and snag-fall models, could be used to predict turnover of dead wood resources over time. Beyond carbon, these tools could be used in a similar manner to better estimate and predict fuel amounts and dynamics where prescribed fire or wildfire is a major focal point. Similarly, tree- and snag-fall models can be applied to SDT which pose a falling risk to humans allowing managers to predict when SDT might fall and target those for removal. Finally, these models can, once again, be applied to better estimate SDT resources to provide sufficient habitat for cavity-nesting species on a particular land base. The utility of results and tools from this dissertation is broad yet, offers a key starting point for managers concerned about future extreme droughts and managing dead wood resources.

REFERENCES

Aakala, T., 2010. Coarse woody debris in late-successional Picea abies forests in northern Europe: Variability in quantities and models of decay class dynamics. Forest Ecology and Management 260, 770-779.

Aakala, T., 2011. Temporal Variability of Deadwood Volume and Quality in Boreal Old-Growth Forests. Silva Fennica 45, 969-981.

Aakala, T., Kuuluvainen, T., Gauthier, S., De Grandpré, L., 2008. Standing dead trees and their decay-class dynamics in the northeastern boreal old-growth forests of Quebec. Forest Ecology and Management 255, 410-420.

Abrams, M.D., 1990. Adaptions and responses to drought in *Quercus* species of North America. Tree Physiology 7, 227-238.

Adams, H.D., Zeppel, M.J.B., Anderegg, W.R.L., Hartmann, H., Landhäusser, S.M., et al., 2017. A multi-species synthesis of physiological mechanisms in drought-induced tree mortality. Nature Ecology & Evolution 1, 1285-1291.

Agresti, A., 2013. Categorical Data Analysis, 3rd Edn. John Wiley & Sons, Hoboken, New Jersey, USA.

Allen, C.D., Breshears, D.D., McDowell, N.G., 2015. On underestimation of global vulnerability to tree mortality and forest die-off from hotter drought in the Anthropocene. Ecosphere 6, 1-55.

Allen, C.D., Macalady, A.K., Chenchouni, H., Bachelet, D., McDowell, N., et al., 2010. A global overview of drought and heat-induced tree mortality reveals emerging climate change risks for forests. Forest Ecology and Management 259, 660-684.

Anderegg, W.R.L., Hicke, J.A., Fisher, R.A., Allen, C.D., Aukema, J., et al., 2015. Tree mortality from drought, insects, and their interactions in a changing climate. New Phytologist 208, 674-683.

Anderegg, W.R.L., Kane, J.M., Anderegg, L.D.L., 2013a. Consequences of widespread tree mortality triggered by drought and temperature stress. Nature Climate Change 3, 30-36.

Anderegg, W.R.L., Klein, T., Bartlett, M., Sack, L., Pellegrini, A.F., et al., 2016. Meta-analysis reveals that hydraulic traits explain cross-species patterns of drought-induced tree mortality across the globe. Proceedings of the National Academy of Sciences, USA 113, 5024-5029.

Anderegg, W.R.L., Plavcova, L., Anderegg, L.D.L., Hacke, U.G., Berry, J.A., et al., 2013b. Drought's legacy: multiyear hydraulic deterioration underlies widespread aspen forest die-off and portends increased future risk. Global Change Biology 19, 1188-1196.

Angers, V.A., Drapeau, P., Bergeron, Y., 2012. Mineralization rates and factors influencing snag decay in four North American boreal tree species. Canadian Journal of Forest Research 42, 157-166.

Angers, V.A., Gauthier, S., Drapeau, P., Jayen, K., Bergeron, Y., 2011. Tree mortality and snag dynamics in North American boreal tree species after a wildfire: a long-term study. International Journal of Wildland Fire 20, 751-763.

Asaro, C., Nowak, J.T., Elledge, A., 2017. Why have southern pine beetle outbreaks declined in the southeastern US with the expansion of intensive pine silviculture? A brief review of hypotheses. Forest Ecology and Management 391, 338-348.

Aschoff, T., Thies, M., Spiecker, H., 2004. Describing forest stands using terrestrial laser-scanning. International Archives of Photogrammetry, Remote Sensing and Spatial Information Sciences 35, 237-241.

Barras, S.J., 1970. Antagonism between Dendroctonus frontalis and the fungus Ceratocystis minor. Annals of the Entomological Society of America 63, 1187-1190.

Barrett, J.W., 1995. Regional silviculture of the United States. John Wiley & Sons, New York.

Baskerville, G., 1972. Use of logarithmic regression in the estimation of plant biomass. Canadian Journal of Forest Research 2, 49-53.

Bates, D., Maechler, M., Bolker, B., Walker, S., 2015. Fitting Linear Mixed-Effects Models Using lme4. Journal of Statistical Software 67, 1-48.

Bechtold, W.A., Patterson, P.L., 2005. The enhanced Forest Inventory and Analysis program – national sampling design and estimation procedures. Gen. Tech. Rep. SRS-80. Asheville, NC: U.S. Department of Agriculture, Forest Service, Southern Research Station., 85.

Bennett, A.C., McDowell, N.G., Allen, C.D., Anderson-Teixeira, K.J., 2015. Larger trees suffer most during drought in forests worldwide. Nature Plants 1, 15139.

Berdanier, A.B., Clark, J.S., 2016. Multiyear drought-induced morbidity preceding tree death in southeastern U.S. forests. Ecological Applications 26, 17-23.

Bigler, C., Gavin, D.G., Gunning, C., Veblen, T.T., 2007. Drought induces lagged tree mortality in a subalpine forest in the Rocky Mountains. Oikos 116, 1983-1994.

Bottero, A., D'Amato, A.W., Palik, B.J., Bradford, J.B., Fraver, S., et al., 2017. Density-dependent vulnerability of forest ecosystems to drought. Journal of Applied Ecology 54, 1605-1614.

Bracho, R., Vogel, J.G., Will, R.E., Noormets, A., Samuelson, L.J., et al., 2018. Carbon accumulation in loblolly pine plantations is increased by fertilization across a soil moisture availability gradient. Forest Ecology and Management 424, 39-52.

Breshears, D.D., Allen, C.D., 2002. The importance of rapid, disturbance-induced losses in carbon management and sequestration. Global Ecology and Biogeography 11, 1-5.

Breshears, D.D., Cobb, N.S., Rich, P.M., Price, K.P., Allen, C.D., et al., 2005. Regional vegetation die-off in response to global-change-type drought. Proceedings of the National Academy of Sciences, USA 102, 15144-15148.

Burns, R.M., Honkala, B.H., 1990. Silvics of North America. Vol. 1 and 2. Washington, DC: U.S. Department of Agriculture, Forest Service, Agriculture Handbook 654.

Burrill, E.A., Wilson, A.M., Turner, J.A., Pugh, S.A., Menlove, J., et al., 2018. The Forest Inventory and Analysis Database: database description and user guide version 8.0 for Phase 2. U.S. Department of Agriculture, Forest Service., 946.

Cailleret, M., Jansen, S., Robert, E.M.R., Desoto, L., Aakala, T., et al., 2017. A synthesis of radial growth patterns preceding tree mortality. Global Change Biology 23, 1675-1690.

Cain, M.D., 1996. Hardwood snag fragmentation in a pine-oak forest of southeastern Arkansas. American Midland Naturalist, 72-83.

Cavin, L., Mountford, E.P., Peterken, G.F., Jump, A.S., 2013. Extreme drought alters competitive dominance within and between tree species in a mixed forest stand. Functional Ecology 27, 1424-1435.

Chen, G., Pan, S., Hayes, D.J., Tian, H., 2017. Spatial and temporal patterns of plantation forests in the United States since the 1930s: an annual and gridded data set for regional Earth system modeling. Earth System Science Data 9, 545-556.

Clark, J.S., Iverson, L., Woodall, C.W., Allen, C.D., Bell, D.M., et al., 2016. The impacts of increasing drought on forest dynamics, structure, and biodiversity in the United States. Global Change Biology, 1-24.

Clifford, D., Cressie, N., England, J.R., Roxburgh, S.H., Paul, K.I., 2013. Correction factors for unbiased, efficient estimation and prediction of biomass from log-log allometric models. Forest Ecology and Management 310, 375-381.

Cline, S.P., Berg, A.B., Wight, H.M., 1980. Snag characteristics and dynamics in Douglas-fir forests, western Oregon. The Journal of Wildlife Management 44, 773-786.

Collins, B., Rhoades, C., Battaglia, M., Hubbard, R., 2012. The effects of bark beetle outbreaks on forest development, fuel loads and potential fire behavior in salvage

logged and untreated lodgepole pine forests. Forest Ecology and Management 284, 260-268.

Conner, R.N., Rudolph, D.C., Saenz, D., Schaefer, R.R., 1994. Heartwood, sapwood, and fungal decay associated with red-cockaded woodpecker cavity trees. The Journal of Wildlife Management 106, 728-734.

Conner, R.N., Saenz, D., 2005. The longevity of large pine snags in eastern Texas. Wildlife Society Bulletin 33, 700-705.

Crecente-Campo, F., Pasalodos-Tato, M., Alberdi, I., Hernández, L., Ibañez, J.J., et al., 2016. Assessing and modelling the status and dynamics of deadwood through national forest inventory data in Spain. Forest Ecology and Management 360, 297-310.

D'Amato, A.W., Bradford, J.B., Fraver, S., Palik, B.J., 2013. Effects of thinning on drought vulnerability and climate response in north temperate forest ecosystems. Ecological Applications 23, 1735-1742.

Dassot, M., Constant, T., Fournier, M., 2011. The use of terrestrial LiDAR technology in forest science: Application fields, benefits and challenges. Annals of Forest Science 68, 959-974.

Desprez-Loustau, M.L., Marcais, B., Nageleisen, L.M., Piou, D., Vannini, A., 2006. Interactive effects of drought and pathogens in forest trees. Annals of Forest Science 63, 597-612.

Dietze, M.C., Moorcroft, P.R., 2011. Tree mortality in the eastern and central United States: Patterns and drivers. Global Change Biology 17, 3312-3326.

Dipesh, K., Will, R.E., Lynch, T.B., Heinemann, R., Holeman, R., 2015. Comparison of loblolly, shortleaf, and pitch X loblolly pine plantations growing in Oklahoma. Forest Science 61, 540-547.

Domec, J.-C., King, J.S., Ward, E., Oishi, A.C., Palmroth, S., et al., 2015. Conversion of natural forests to managed forest plantations decreases tree resistance to prolonged droughts. Forest Ecology and Management 355, 58-71.

Domke, G.M., Woodall, C.W., Smith, J.E., 2011. Accounting for density reduction and structural loss in standing dead trees: Implications for forest biomass and carbon stock estimates in the United States. Carbon Balance and Management 6, 14.

Ducey, M.J., Knapp, R.A., 2010. A stand density index for complex mixed species forests in the northeastern United States. Forest Ecology and Management 260, 1613-1622.

Edgar, C.B., Westfall, J.A., Klockow, P.A., Vogel, J.G., Moore, G.W., 2019. Interpreting effects of multiple, large-scale disturbances using national forest inventory data: A case study of standing dead trees in east Texas, USA. Forest Ecology and Management 437, 27-40.

Edgar, C.B., Zehnder, R., 2015. East Texas Forestlands, 2015. Forest Resource Reports, College Station, TX: Texas A&M Forest Service, 6.

Esperon-Rodriguez, M., Barradas, V.L., 2015. Ecophysiological vulnerability to climate change: water stress responses in four tree species from the central mountain region of Veracruz, Mexico. Regional Environmental Change 15, 93-108.

Fan, Z., Fan, X., Crosby, M.K., Moser, W.K., He, H., et al., 2012. Spatio-temporal trends of oak decline and mortality under periodic regional drought in the Ozark Highlands of Arkansas and Missouri. Forests 3, 614-631.

Fan, Z., Kabrick, J.M., Shifley, S.R., 2006. Classification and regression tree based survival analysis in oak-dominated forests of Missouri's Ozark Highlands. Canadian Journal of Forest Research 36, 1740-1748.

Fan, Z., Kabrick, J.M., Spetich, M.A., Shifley, S.R., Jensen, R.G., 2008. Oak mortality associated with crown dieback and oak borer attack in the Ozark Highlands. Forest Ecology and Management 255, 2297-2305.

FARO Scene (Version 5.5). 2015. [Computer Software]. FARO Technologies, Inc., Lake Mary, Florida, USA.

Fasth, B., Harmon, M.E., Woodall, C.W., Sexton, J., 2010. Evaluation of techniques for determining the density of fine woody debris. Research Paper NRS-11. Newtown

Square, PA: U.S. Department of Agriculture, Forest Service, Northern Research Station, 18.

Flewelling, J.W., Monserud, R.A., 2002. Comparing Methods for Modelling Tree Mortality. In: Crookston, Nicholas L.; Havis, Robert N., comps. 2002. Second Forest Vegetation Simulator Conference; 2002 February 12-14; Fort Collins, CO. Proc. RMRS-P-25. Ogden, UT: U.S. Department of Agriculture, Forest Service, Rocky Mountain Research Station., 168-177.

Floyd, M.L., Clifford, M., Cobb, N.S., Hanna, D., Delph, R., et al., 2009. Relationship of stand characteristics to drought-induced mortality in three Southwestern piñon - Juniper woodlands. Ecological Applications 19, 1223-1230.

Forrester, D.I., 2014. The spatial and temporal dynamics of species interactions in mixed-species forests: From pattern to process. Forest Ecology and Management 312, 282-292.

Foster, D.R., Knight, D.H., Franklin, J.F., 1998. Landscape patterns and legacies resulting from large, infrequent forest disturbances. Ecosystems 1, 497-510.

Fox, T.R., Jokela, E.J., Allen, H.L., 2007. The development of pine plantation silviculture in the southern United States. Journal of Forestry 105, 337-347.

Franklin, J.F., Shugart, H.H., Harmon, M.E., 1987. Tree Death as an Ecological Process: The causes, consequences, and variability of tree mortality. Bioscience 37, 550-556.

Fraver, S., Milo, A.M., Bradford, J.B., D'Amato, A.W., Kenefic, L., et al., 2013. Woody Debris Volume Depletion Through Decay: Implications for Biomass and Carbon Accounting. Ecosystems 16, 1262-1272.

Fraver, S., Ringvall, A., Jonsson, B.G., 2007. Refining volume estimates of down woody debris. Canadian Journal of Forest Research 37, 627-633.

Ganey, J.L., Vojta, S.C., 2011. Tree mortality in drought-stressed mixed-conifer and ponderosa pine forests, Arizona, USA. Forest Ecology and Management 261, 162-168.

Garbarino, M., Marzano, R., Shaw, J.D., Long, J.N., Arbarino, M.G., et al., 2015. Environmental drivers of deadwood dynamics in woodlands and forests. Ecosphere 6, 30.

Gardiner, B., Berry, P., Moulia, B., 2016. Wind impacts on plant growth, mechanics and damage. Plant Science 245, 94-118.

Gaylord, M.L., Kolb, T.E., Pockman, W.T., Plaut, J.A., Yepez, E.A., et al., 2013. Drought predisposes piñon-juniper woodlands to insect attacks and mortality. New Phytologist 198, 567-578.

Gelman, A., Rubin, D.B., 1992. Inference from iterative simulation using multiple sequences. Statistical science 7, 457-472.

Girardeau-Montaut, D. (Version 2.9.1). 2017. [Computer Software]. GPL Software, http://www.cloudcompare.org/.

Giuggiola, A., Bugmann, H., Zingg, A., Dobbertin, M., Rigling, A., 2013. Reduction of stand density increases drought resistance in xeric Scots pine forests. Forest Ecology and Management 310, 827-835.

Gleason, K.E., Bradford, J.B., Bottero, A., D'Amato, A.W., Fraver, S., et al., 2017. Competition amplifies drought stress in forests across broad climatic and compositional gradients. Ecosphere 8, 1-16.

Gobakken, T., Næsset, E., Nelson, R., Martin, O., Gregoire, T.G., et al., 2012. Remote Sensing of Environment Estimating biomass in Hedmark County , Norway using national forest inventory fi eld plots and airborne laser scanning. Remote Sensing of Environment 123, 443-456.

Gonzalez-Benecke, C.A., Gezan, S.A., Albaugh, T.J., Allen, H.L., Burkhart, H.E., et al., 2014. Local and general above-stump biomass functions for loblolly pine and slash pine trees. Forest Ecology and Management 334, 254-276.

Green, M.J., Medley, G.F., Browne, W.J., 2009. Use of posterior predictive assessments to evaluate model fit in multilevel logistic regression. Veterinary Research 40, 10.

Guldin, J.M., Hallgren, S., Crooks, J.S., 2015. Outlook for Mid-South forests: a subregional report from the Southern Forest Futures Project. Gen. Tech. Report SRS-206. Asheville, NC: U.S. Department of Agriculture Forest Service, Southern Research Station., 70.

Haavik, L.J., Jones, J.S., Galligan, L.D., Guldin, J.M., Stephen, F.M., 2012. Oak decline and red oak borer outbreak: impact in upland oak-hickory forests of Arkansas, USA. Forestry 84, 341-351.

Hamilton Jr., D.A., Edwards, B.M., 1976. Modeling the probability of individual tree mortality. USDA Forest Service Intermountain Research Station Research Paper INT-185, 22.

Harcombe, P.A., Leipzig, L.E.M., Elsik, I.S., 2009. Effects of Hurricane Rita on Three Long-Term Forest Study Plots in East Texas, USA. Wetlands 29, 88-100.

Harmon, M.E., Franklin, J.F., Swanson, F.J., Sollins, P., Gregory, S.V., et al., 1986. Ecology of Coarse Woody Debris in Temperate Ecosystems. Advances in Ecological Research 15, 133-302.

Harmon, M.E., Woodall, C.W., Fasth, B., Sexton, J., 2008. Woody Detritus Density and Density Reduction Factors for Tree Species in the United States: A Synthesis. USDA General Technical Report NRS-29. USDA Forest Service Northern Research Station, 84.

Harmon, M.E., Woodall, C.W., Fasth, B., Sexton, J., Yatkov, M., 2011. Differences between standing and downed dead tree wood density reduction factors: A comparison across decay classes and tree species. Research Paper NRS-15. Newtown Square, PA: U.S. Department of Agriculture, Forest Service, Northern Research Station., 40.

Harris, N.L., Hagen, S.C., Saatchi, S.S., Pearson, T.R.H., Woodall, C.W., et al., 2016. Attribution of net carbon change by disturbance type across forest lands of the conterminous United States. Carbon Balance and Management 11, 24.

Hartmann, H., Moura, C.F., Anderegg, W.R.L., Ruehr, N.K., Salmon, Y., et al., 2018. Research frontiers for improving our understanding of drought-induced tree and forest mortality. New Phytologist 218, 15-28.

Hauglin, M., Astrup, R., Gobakken, T., Naesset, E., 2013. Estimating single-tree branch biomass of Norway spruce with terrestrial laser scanning using voxel-based and crown dimension features. Scandinavian Journal of Forest Research 28, 456-469.

Hobbs, N.T., Hooten, M.B., 2015. Bayesian models: a statistical primer for ecologists. Princeton University Press, Princeton, NJ.

Hoerling, M., Kumar, A., Dole, R., Nielsen-Gammon, J.W., Eischeid, J., et al., 2013. Anatomy of an extreme event. Journal of Climate 26, 2811-2832.

Hoffmann, W.A., Marchin, R.M., Abit, P., Lau, O.L., 2011. Hydraulic failure and tree dieback are associated with high wood density in a temperate forest under extreme drought. Global Change Biology 17, 2731-2742.

Hooper, M.C., Arii, K., Lechowicz, M.J., 2001. Impact of a major ice storm on an old-growth hardwood forest. Canadian Journal of Botany-Revue Canadienne De Botanique 79, 70-75.

IPCC [Intergovernmental Panel on Climate Change], 2013. Climate Change 2013: The Physical Science Basis. Contribution of Working Group I to the Fifth Assessment Report of the Intergovernmental Panel on Climate Change. In, Cambridge, United Kingdom and New York, New York, USA, p. 1535.

Jenkins, J., Chojnacky, D., Heath, L., Birdsey, R., 2003. National scale biomass estimates for United States tree species. Forest Science 49, 12-32.

Johnson, D.M., Domec, J.C., Berry, Z.C., Schwantes, A.M., McCulloh, K.A., et al., 2018. Co-occurring woody species have diverse hydraulic strategies and mortality rates during an extreme drought. Plant Cell and Environment 41, 576-588.

Jones, P.D., Hanberry, B., Demarais, S., 2009. Stand-level wildlife habitat features and biodiversity in Southern pine forests: a review. Journal of Forestry 107, 398-404.

Joyce, L.A., Running, S.W., Breshears, D.D., Dale, V.H., Malmsheimer, R.W., et al., 2014. Ch. 7: Forests. In: Melillo, J.M., Richmond, T.T.C., Yohe, G.W. (Eds.), Climate Change Impacts in the United States: The Third National Climate Assessment. U.S. Global Change Research Program, pp. 175-194.

Kankare, V., Holopainen, M., Vastaranta, M., Puttonen, E., Yu, X., et al., 2013. Individual tree biomass estimation using terrestrial laser scanning. ISPRS Journal of Photogrammetry and Remote Sensing 75, 64-75.

Klein, T., 2014. The variability of stomatal sensitivity to leaf water potential across tree species indicates a continuum between isohydric and anisohydric behaviours. Functional Ecology 28, 1313-1320.

Klepzig, K., Shelfer, R., Choice, Z., 2014. Outlook for Coastal Plain forests: a subregional report from the Southern Forest Futures Project. Gen. Tech. Report SRS-196. Asheville, NC: U.S. Department of Agriculture Forest Service, Southern Research Station., 68.

Klepzig, K.D., Wilkens, R.T., 1997. Competitive interactions among symbiotic fungi of the southern pine beetle. Applied and Environmental Microbiology 63, 621-627.

Klockow, P.A., Vogel, J.G., Edgar, C.B., Moore, G.W., 2018. Lagged mortality among tree species four years after an exceptional drought in east Texas. Ecosphere 9, e02455.

Klos, R.J., Wang, G.G., Bauerle, W.L., Rieck, J.R., 2009. Drought impact on forest growth and mortality in the southeast USA: an analysis using Forest Health and Monitoring data. Ecological Applications 19, 699-708.

Kolb, T.E., Fettig, C.J., Ayres, M.P., Bentz, B.J., Hicke, J.A., et al., 2016. Observed and anticipated impacts of drought on forest insects and diseases in the United States. Forest Ecology and Management 380, 321-334.

Kramer, I., Holscher, D., 2010. Soil water dynamics along a tree diversity gradient in a deciduous forest in Central Germany. Ecohydrology 3, 262-271.

Kruys, N., Jonsson, B.G., Ståhl, G., 2002. A Stage-Based Matrix Model for Decay-Class Dynamics of Woody Debris. Ecological Applications 12, 773-781.

Kukowski, K.R., Schwinning, S., Schwartz, B.F., 2013. Hydraulic responses to extreme drought conditions in three co-dominant tree species in shallow soil over bedrock. Oecologia 171, 819-830.

Laiho, R., Prescott, C.E., 2004. Decay and nutrient dynamics of coarse woody debris in northern coniferous forests: a synthesis. Canadian Journal of Forest Research 34, 763-777.

Lee, P., 1998. Dynamics of snags in aspen-dominated midboreal forests. Forest Ecology and Management 105, 263-272.

Lefsky, M.A., Cohen, W.B., Parker, G.G., Harding, D.J., 2002. Lidar Remote Sensing for Ecosystem Studies. Bioscience 52, 19-30.

Lindenmayer, D.B., Laurance, W.F., Franklin, J.F., 2012. Global Decline in Large Old Trees. Science 338, 1305-1306.

Lindhe, A., Lindelöw, Å., Åsenblad, N., 2005. Saproxylic beetles in standing dead wood density in relation to substrate sun-exposure and diameter. Biodiversity & Conservation 14, 3033-3053.

Lines, E.R., Coomes, D.a., Purves, D.W., 2010. Influences of Forest Structure, Climate and Species Composition on Tree Mortality across the Eastern US. Plos One 5, e13212.

Lohr, S.L., 1999. Sampling: design and analysis. Duxbury Press, Pacific Grove, California, USA.

Maggard, A., Will, R., Wilson, D., Meek, C., 2016. Response of mid-rotation loblolly pine (*Pinus taeda* L.) physiology and productivity to sustained, moderate drought on the western edge of the range. Forests 7, 1-19.

Maggard, A.O., Will, R.E., Wilson, D.S., Meek, C.R., Vogel, J.G., 2017. Fertilization can compensate for decreased water availability by increasing the efficiency of stem volume production per unit of leaf area for loblolly pine (Pinus taeda) stands. Canadian Journal of Forest Research 47, 445-457.

Manion, P.D., 1981. Tree Disease Concepts. Prentice Hall, Englewood Cliffs, New Jersey, USA.

Maser, C., Tarrant, R.F., Trappe, J.M., Franklin, J.F., 1988. From the forest to the sea : a story of fallen trees. Gen. Tech. Rep. PNW-GTR-229. Portland, OR: U.S. Department of Agriculture, Forest Service, Pacific Northwest Research Station., 153.

Masuda, M.M., Stone, R.P., 2015. Bayesian logistic mixed-effects modelling of transect data: relating red tree coral presence to habitat characteristics. ICES Journal of Marine Science 72, 2674-2683.

Mattoon, W.R., 1915. Life history of shortleaf pine. US Dept. of Agriculture.

McDowell, N.G., Allen, C.D., 2015. Darcy's law predicts widespread forest mortality under climate warming. Nature Climate Change 5, 669-672.

McDowell, N.G., Coops, N.C., Beck, P.S.A., Chambers, J.Q., Gangodagamage, C., et al., 2015. Global satellite monitoring of climate-induced vegetation disturbances. Trends in Plant Science 20, 114-123.

McDowell, N.G., Michaletz, S.T., Bennett, K.E., Solander, K.C., Xu, C.G., et al., 2018. Predicting chronic climate-driven disturbances and their mitigation. Trends in Ecology & Evolution 33, 15-27.

McDowell, N.G., Pockman, W.T., Allen, C.D., Breshears, D.D., Cobb, N., et al., 2008. Mechanisms of plant survival and mortality during drought: Why do some plants survive while others succumb to drought? New Phytologist 178, 719-739.

McNulty, S.G., Boggs, J.L., Sun, G., 2014. The rise of the mediocre forest: why chronically stressed trees may better survive extreme episodic climate variability. New forests 45, 403-415.

Michaelian, M., Hogg, E.H., Hall, R.J., Arsenault, E., 2011. Massive mortality of aspen following severe drought along the southern edge of the Canadian boreal forest. Global Change Biology 17, 2084-2094.

Miles, P.D., Smith, W.B., 2009. Specific gravity and other properties of wood and bark for 156 tree species found in North America. Res. Note. NRS-38. Newtown Square, PA: U.S. Department of Agriculture, Forest Service, Northern Research Station., 35.

Mobley, M.L., Richter, D.d., Heine, P.R., 2013. Accumulation and decay of woody detritus in a humid subtropical secondary pine forest. Canadian Journal of Forest Research 43, 109-118.

Moore, G.W., Edgar, C.B., Vogel, J.G., Washington-Allen, R.A., March, R.G., et al., 2016. Tree mortality from an exceptional drought spanning mesic to semiarid ecoregions. Ecological Applications 26, 602-611.

Moorman, C.E., Russell, K.R., Sabin, G.R., Guynn, D.C., 1999. Snag dynamics and cavity occurrence in the South Carolina Piedmont. Forest Ecology and Management 118, 37-48.

Morrison, M.L., Raphael, M.G., 1993. Modeling the dynamics of snags. Ecological Applications 3, 322-330.

Narine, L.L., Popescu, S., Neuenschwander, A., Zhou, T., Srinivasan, S., et al., 2019. Estimating aboveground biomass and forest canopy cover with simulated ICESat-2 data. Remote Sensing of Environment 224, 1-11.

Nelson, A.S., Bragg, D.C., 2016. Multidecadal response of naturally regenerated southern pine to early competition control and commercial thinning. Forest Science 62, 115-124.

Nielsen-Gammon, J.W., 2012. The 2011 Texas Drought. The Texas Water Journal 3, 59-95.

NOAA [National Oceanic and Atmospheric Administration]. 2018. National Centers for Environmental Information, Climate at a Glance: Divisional Time Series. Published July 2018. Accessed on July 26, 2018. https://www.ncdc.noaa.gov/cag/

NOAA [National Oceanic and Atmospheric Administration]. 2019. National Centers for Environmental Information, Climate at a Glance: Divisional Time Series. Published March 2019. Accessed on April 12, 2019. https://www.ncdc.noaa.gov/cag/

Norman, S.P., Koch, F.H., Hargrove, W.W., 2016. Review of broad-scale drought monitoring of forests: Toward an integrated data mining approach. Forest Ecology and Management 380, 346-358.

Oberle, B., Ogle, K., Zanne, A.E., Woodall, C.W., 2018. When a tree falls: Controls on wood decay predict standing dead tree fall and new risks in changing forests. Plos One 13, e0196712.

Olagoke, A., Proisy, C., Féret, J.-B., Blanchard, E., Fromard, F., et al., 2016. Extended biomass allometric equations for large mangrove trees from terrestrial LiDAR data. Trees 30, 935-947.

Palmer, W.C., 1965. Meteorological drought. US Department of Commerce, Weather Bureau Washington, DC.

Pataki, D.E., Oren, R., 2003. Species differences in stomatal control of water loss at the canopy scale in a mature bottomland deciduous forest. Advances in Water Resources 26, 1267-1278.

Peet, R.K., Christensen, N.L., 1987. Competition and Tree Death. Bioscience 37, 586-595.

Peng, C., Ma, Z., Lei, X., Zhu, Q., Chen, H., et al., 2011. A drought-induced pervasive increase in tree mortality across Canada's boreal forests. Nature Climate Change 1, 467-471.

Penner, M., Penttilä, T., Hökkä, H., 1995. A method for using random parameters in analyzing permanent sample plots. Silva Fennica 29, 287-296.

Pezeshki, S.R., Chambers, J.L., 1986. Stomatal and photosynthetic response of drought-stressed cherrybark oak (*Quercus falcata* var. *pagodaefolia*) and sweet gum (*Liquidambar styraciflua*). Canadian Journal of Forest Research 16, 841-846.

Pfeifer, E.M., Hicke, J.A., Meddens, A.J.H., 2011. Observations and modeling of aboveground tree carbon stocks and fluxes following a bark beetle outbreak in the western United States. Global Change Biology 17, 339-350.

Popescu, S.C., Zhao, K., Neuenschwander, A., Lin, C., 2011. Satellite lidar vs. small footprint airborne lidar: Comparing the accuracy of aboveground biomass estimates and forest structure metrics at footprint level. Remote Sensing of Environment 115, 2786-2797.

Poulos, H.M., 2014. Tree mortality from a short-duration freezing event and global-change-type drought in a Southwestern piñon-juniper woodland, USA. PeerJ 2, e404.

Pretzsch, H., Schutze, G., Uhl, E., 2013. Resistance of European tree species to drought stress in mixed versus pure forests: evidence of stress release by inter-specific facilitation. Plant Biology 15, 483-495.

Pueschel, P., 2013. The influence of scanner parameters on the extraction of tree metrics from FARO Photon 120 terrestrial laser scans. ISPRS Journal of Photogrammetry and Remote Sensing 78, 58-68.

Puettmann, K.J., 2011. Silvicultural Challenges and Options in the Context of Global Change: "Simple" Fixes and Opportunities for New Management Approaches. Journal of Forestry 109, 321-331.

Putman, E.B., Popescu, S.C., 2018. Automated Estimation of Standing Dead Tree Volume Using Voxelized Terrestrial Lidar Data. IEEE Transactions on Geoscience and Remote Sensing 56, 6484-6503.

Putman, E.B., Popescu, S.C., Eriksson, M., Zhou, T., Klockow, P., et al., 2018. Detecting and quantifying standing dead tree structural loss with reconstructed tree models using voxelized terrestrial lidar data. Remote Sensing of Environment 209, 52-65.

R Core Team 2016. R: A langauge and environment for statistical computing. R Foundation for Statistical Computing, Vienna, Austria.

R Core Team 2018. R: A language and environment for statistical computing. R Foundation for Statistical Computing, Vienna, Austria.

Radtke, P.J., Amateis, R.L., Prisley, S.P., Copenheaver, C.A., Chojnacky, D.C., et al., 2009. Modeling production and decay of coarse woody debris in loblolly pine plantations. Forest Ecology and Management 257, 790-799.

Raffa, K.F., Aukema, B.H., Bentz, B.J., Carroll, A.L., Hicke, J.A., et al., 2008. Cross-scale drivers of natural disturbances prone to anthropogenic amplification: The dynamics of bark beetle eruptions. Bioscience 58, 501-517.

Raile, G.K., 1982. Estimating stump volume. Res. Pap. NC-224. St. Paul, MN: U.S. Department of Agriculture, Forest Service, North Central Forest Experiment Station., 4.

Raumonen, P., Kaasalainen, M., Åkerblom, M., Kaasalainen, S., Kaartinen, H., et al., 2013. Fast automatic precision tree models from terrestrial laser scanner data. Remote Sensing 5, 491-520.

Rehm, E.M., Olivas, P., Stroud, J., Feeley, K.J., 2015. Losing your edge: climate change and the conservation value of range-edge populations. Ecology and Evolution 5, 4315-4326.

Roberts, J., Cabral, O.M.R., Aguiar, L.F.d., 1990. Stomatal and Boundary-Layer Conductances in an Amazonian Terra Firme Rain Forest. Journal of Applied Ecology 27, 336-353.

Rodríguez-Calcerrada, J., Sancho-Knapik, D., Martin-StPaul, N.K., Limousin, J.-M., McDowell, N.G., et al., 2017. Drought-induced oak decline – factors involved, physiological dysfunctions, and potential attenuation by forestry practices. In, Oaks Physiological Ecology. Exploring the Functional Diversity of Genus Quercus L. Springer, Cham, eBook Collection (EBSCOhost), pp. 419-451.

Russell, M.B., Fraver, S., Aakala, T., Gove, J.H., Woodall, C.W., et al., 2015. Quantifying carbon stores and decomposition in dead wood: A review. Forest Ecology and Management 350, 107-128.

Russell, M.B., Weiskittel, A.R., 2012. Assessing and modeling snag survival and decay dynamics for the primary species in the Acadian forest of Maine, USA. Forest Ecology and Management 284, 230-240.

Russell, M.B., Woodall, C.W., Fraver, S., D'Amato, A.W., 2013. Estimates of downed woody debris decay class transitions for forests across the eastern United States. Ecological Modelling 251, 22-31.

Russell, M.B., Woodall, C.W., Fraver, S., D'Amato, A.W., Domke, G.M., et al., 2014. Residence Times and Decay Rates of Downed Woody Debris Biomass/Carbon in Eastern US Forests. Ecosystems 17, 765-777.

Ryan, M.G., 2015. Tree mortality: Large trees losing out to drought. Nature Plants 1, 15150.

Schoennagel, T., Veblen, T.T., Negron, J.F., Smith, J.M., 2012. Effects of Mountain Pine Beetle on Fuels and Expected Fire Behavior in Lodgepole Pine Forests, Colorado, USA. Plos One 7, e30002.

Schwantes, A.M., Swenson, J.J., Gonzalez-Roglich, M., Johnson, D.M., Domec, J.C., et al., 2017. Measuring canopy loss and climatic thresholds from an extreme drought along a fivefold precipitation gradient across Texas. Global Change Biology 23, 5120-5135.

Schwantes, A.M., Swenson, J.J., Jackson, R.B., 2016. Quantifying drought-induced tree mortality in the open canopy woodlands of central Texas. Remote Sensing of Environment 181, 54-64.

Sellin, A., 1994. Sapwood–heartwood proportion related to tree diameter, age, and growth rate in Picea abies. Canadian Journal of Forest Research 24, 1022-1028.

Shaw, J.D., Steed, B.E., DeBlander, L.T., 2005. Forest Inventory and Analysis (FIA) annual inventory answers the question: What is happening to pinyon-juniper woodlands? Journal of Forestry 103, 280-285.

Shen, H.P., Zhu, Z.Y., 2008. Efficient mean estimation in log-normal linear models. Journal of Statistical Planning and Inference 138, 552-567.

Sheridan, R., Popescu, S., Gatziolis, D., Morgan, C., Ku, N.-W., 2015. Modeling forest aboveground biomass and volume using airborne LiDAR metrics and forest inventory and analysis data in the Pacific Northwest. Remote Sensing 7, 229-255.

Srinivasan, S., Popescu, S.C., Eriksson, M., Sheridan, R.D., Ku, N.W., 2014. Multi-temporal terrestrial laser scanning for modeling tree biomass change. Forest Ecology and Management 318, 304-317.

Stan Development Team (R package version 2.16.2). 2017. RStan: the R interface to Stan.

Storaunet, K.O., Rolstad, J., 2004. How long do Norway spruce snags stand? Evaluating four estimation methods. Canadian Journal of Forest Research 34, 376-383.

Stovall, A.E., Anderson-Teixeira, K.J., Shugart, H.H., 2018. Assessing terrestrial laser scanning for developing non-destructive biomass allometry. Forest Ecology and Management 427, 217-229.

Thrippleton, T., Bugmann, H., Folini, M., Snell, R.S., 2018. Overstorey-Understorey Interactions Intensify After Drought-Induced Forest Die-Off: Long-Term Effects for Forest Structure and Composition. Ecosystems 21, 723-739.

Twidwell, D., Wonkka, C.L., Taylor, C.A., Zou, C.B., Twidwell, J.J., et al., 2014. Drought-induced woody plant mortality in an encroached semi-arid savanna depends on topoedaphic factors and land management. Applied Vegetation Science 17, 42-52.

U.S. Environmental Protection Agency, 2019. Inventory of U.S. Greenhouse Gas Emissions and Sinks: 1990-2017, Ch. 6: Land Use, Land-Use Change, and Forestry. In, Washington, D.C., p. 126.

USDA Forest Service, 2017. Forest inventory and analysis national core field guide. Volume 1: Field data collection procedures for Phase 2 plots. Version 7.2. U.S. Department of Agriculture, Forest Service, Washington D.C., U.S.A.

USDA NRCS [U.S. Department of Agriculture, Natural Resources Conservation Service], 2006. Land resource regions and major land resource areas of the United States, the Caribbean, and the Pacific Basin. In, Washington, DC, USA, p. 669.

van Mantgem, P.J., Stephenson, N.L., Byrne, J.C., Daniels, L.D., Franklin, J.F., et al., 2009. Widespread increase of tree mortality rates in the western United States. Science 323, 521-524.

Vanderwel, M.C., Caspersen, J.P., Woods, M.E., 2006a. Snag dynamics in partially harvested and unmanaged northern hardwood forests. Canadian Journal of Forest Research 36, 2769-2779.

Vanderwel, M.C., Malcolm, J.R., Smith, S.M., 2006b. An integrated model for snag and downed woody debris decay class transitions. Forest Ecology and Management 234, 48-59.

Vogt, J.T., Smith, W.B., 2017. Forest Inventory and Analysis Fiscal Year 2016 Business Report. In, Washington, DC, USA, p. 84.

Vose, J.M., Clark, J.S., Luce, C.H., Patel-Weynand, T., 2016. Effects of drought on forests and rangelands in the United States: a comprehensive science synthesis. Gen. Tech. Rep. WO-93b. Washington, DC: U.S. Department of Agriculture, Forest Service, Washington Office., 289.

Wang, W., Peng, C., Kneeshaw, D.D., Larocque, G.R., Luo, Z., 2012. Drought-induced tree mortality: ecological consequences, causes, and modeling. Environmental Reviews 20, 109-121.

Ward, E.J., Domec, J.-C., Laviner, M.A., Fox, T.R., Sun, G., et al., 2015. Fertilization intensifies drought stress: Water use and stomatal conductance of Pinus taeda in a midrotation fertilization and throughfall reduction experiment. Forest Ecology and Management 355, 72-82.

Waring, E.F., Schwilk, D.W., 2014. Plant dieback under exceptional drought driven by elevation, not by plant traits, in Big Bend National Park, Texas, USA. PeerJ 2, e477.

Weedon, J.T., Cornwell, W.K., Cornelissen, J.H.C., Zanne, A.E., Wirth, C., et al., 2009. Global meta-analysis of wood decomposition rates: a role for trait variation among tree species? Ecology Letters 12, 45-56.

Weiskittel, A.R., MacFarlane, D.W., Radtke, P.J., Affleck, D.L.R., Temesgen, H., et al., 2015. A Call to Improve Methods for Estimating Tree Biomass for Regional and National Assessments. Journal of Forestry 113, 414-424.

Will, R.E., Wilson, S.M., Zou, C.B., Hennessey, T.C., 2013. Increased vapor pressure deficit due to higher temperature leads to greater transpiration and faster mortality during drought for tree seedlings common to the forest-grassland ecotone. New Phytologist 200, 366-374.

Woodall, C.W., Heath, L.S., Domke, G.M., Nichols, M.C., 2010. Methods and equations for estimating aboveground volume, biomass, and carbon for trees in the U.S. forest inventory. Gen. Tech. Rep. NRS-88. Newtown Square, PA: U.S. Department of Agriculture, Forest Service, Northern Research Station., 30.

Woodall, C.W., Oswalt, C.M., Westfall, J.A., Perry, C.H., Nelson, M.D., et al., 2009. An indicator of tree migration in forests of the eastern United States. Forest Ecology and Management 257, 1434-1444.

Woudenberg, S.W., Conkling, B.L., O'Connell, B.M., LaPoint, E.B., Turner, J.A., et al., 2010. The Forest Inventory and Analysis Database: Database description and users manual version 4.0 for Phase 2. Gen. Tech. Rep. RMRS-GTR-245. Fort Collins, CO: US Department of Agriculture, Forest Service, Rocky Mountain Research Station. 336 p. 245.

Yatskov, M.A., Harmon, M.E., Barrett, T.M., Dobelbower, K.R., 2019. Carbon pools and biomass stores in the forests of Coastal Alaska: Uncertainty of estimates and impact of disturbance. Forest Ecology and Management 434, 303-317.

Young, D.J.N., Stevens, J.T., Earles, J.M., Moore, J., Ellis, A., et al., 2017. Long-term climate and competition explain forest mortality patterns under extreme drought. Ecology Letters 20, 78-86.

Zarnoch, S.J., Blake, J.I., Parresol, B.R., 2014. Are prescribed fire and thinning dominant processes affecting snag occurrence at a landscape scale? Forest Ecology and Management 331, 144-152.

Zarnoch, S.J., Vukovich, M.A., Kilgo, J.C., Blake, J.I., 2013. Snag characteristics and dynamics following natural and artificially induced mortality in a managed loblolly pine forest. Canadian Journal of Forest Research 43, 817-825.

Zell, J., Kändler, G., Hanewinkel, M., 2009. Predicting constant decay rates of coarse woody debris-A meta-analysis approach with a mixed model. Ecological Modelling 220, 904-912.

Zhang, Y., Vogel, J.G., Meek, C., Will, R., Wilson, D., et al., 2016. Wood decomposition by microbes and macroinvertebrates, and soil CO2 efflux vary in

response to throughfall reduction and fertilization in a loblolly pine (*Pinus taeda* L.) plantation. Forest Ecology and Management 382, 10-20.

Zhang, Y.J., Meinzer, F.C., Hao, G.Y., Scholz, F.G., Bucci, S.J., et al., 2009. Size-dependent mortality in a Neotropical savanna tree: the role of height-related adjustments in hydraulic architecture and carbon allocation. Plant Cell and Environment 32, 1456-1466.

APPENDIX A

SUPPLEMENTARY TABLES AND FIGURES FOR CHAPTER II

Table A.1. Coefficient estimates from logistic regression of weather mortality in plots across east Texas. Reprinted with permission from Klockow *et al.*, (2018).

Coefficient	Estimate	SE	*p*-value	95% CI
Intercept (PITA:2011)	-5.2601	0.2047	<<0.001***	(-5.6897, -4.8839)
PIEC	0.7253	0.4940	0.1420	(-0.3668, 1.6121)
QUST	-0.5978	1.0215	0.5584	(-3.4829, 0.9602)
QUNI	2.2365	0.2958	<<0.001***	(1.6519, 2.8188)
QUFA	0.6384	0.6152	0.2994	(-0.8025, 1.6966)
LIST	0.2307	0.4579	0.6143	(-0.7646, 1.0637)
ULAL	1.1911	0.5442	0.0286*	(-0.0395, 2.1517)
2012	0.3295	0.2896	0.2551	(-0.2418, 0.9008)
2013	0.9832	0.2408	<<0.001***	(0.5255, 1.4739)
2014	0.6273	0.2644	0.0177*	(0.1150, 1.1574)
2015	0.1764	0.2895	0.5424	(-0.3948, 0.7475)
PIEC:2012	-0.1078	0.7898	0.8914	(-1.7866, 1.4142)
QUST:2012	2.9758	1.0624	0.0051**	(1.2947, 5.9006)
QUNI:2012	0.3184	0.4088	0.4361	(-0.4826, 1.1248)
QUFA:2012	2.9906	0.6725	<<0.001***	(1.7962, 4.5131)
LIST:2012	1.2803	0.5559	0.0213*	(0.2302, 2.4362)
ULAL:2012	-0.6973	0.9187	0.4479	(-2.7481, 1.0426)
PIEC:2013	0.3958	0.5670	0.4851	(-0.6629, 1.5998)
QUST:2013	2.0613	1.0506	0.0498*	(0.4126, 4.9744)
QUNI:2013	-0.5123	0.3632	0.1584	(-1.2279, 0.2005)
QUFA:2013	1.5502	0.6593	0.0187*	(0.3823, 3.0520)
LIST:2013	1.0959	0.4991	0.0281*	(0.1708, 2.1574)
ULAL:2013	0.2119	0.6119	0.7291	(-0.9124, 1.5419)
PIEC:2014	0.6266	0.6131	0.3068	(-0.5442, 1.9012)
QUST:2014	2.0699	1.0644	0.0518	(0.3792, 4.9963)
QUNI:2014	-0.1968	0.3824	0.6069	(-0.9480, 0.5555)
QUFA:2014	1.3252	0.6949	0.0565	(0.0676, 2.8766)
LIST:2014	0.9119	0.5297	0.0852	(-0.0814, 2.0235)
ULAL:2014	0.5096	0.6366	0.4234	(-0.6735, 1.8770)
PIEC:2015	0.7000	0.6233	0.2615	(-0.4902, 1.9935)
QUST:2015	2.7504	1.0668	0.0099**	(1.0551, 5.6794)
QUNI:2015	-1.2730	0.5240	0.0151*	(-2.3546, 0.2801)
QUFA:2015	1.3913	0.7247	0.0549	(0.0591, 2.9849)
LIST:2015	0.1778	0.6146	0.7723	(-1.0231, 1.4218)
ULAL:2015	-0.2970	0.7693	0.6995	(-1.8496, 1.2556)

Notes: Covariates included species, measurement year, and their interaction. SE refers to the standard error and CI refers to the 95% confidence interval for each estimate. Deviance and Akaike Information Criterion (AIC) metrics for this model were 3511.6 (on 5192 degrees of freedom) and 4223, respectively. Species codes are as follows: *PITA = Pinus taeda*, *PIEC = Pinus echinata*, *QUST = Quercus stellata*, *QUNI = Quercus nigra*, *QUFA = Quercus falcata*, *LIST = Liquidambar styraciflua*, *ULAL = Ulmus alata*.; *$p < 0.05$, **$p < 0.01$, ***$p < 0.001$

Table A.2. Coefficient estimates from logistic regression of pest mortality in plots across east Texas. Reprinted with permission from Klockow *et al.*, (2018).

Coefficient	Estimate	SE	*p*-value	95% CI
Intercept (*PITA*:2011)	-5.6346	0.1549	<<0.001***	(-5.9482, -5.3403)
PIEC	1.7164	0.1797	<<0.001***	(1.3564, 2.0627)
QUST	1.5830	0.1822	<<0.001***	(1.2175, 1.9334)
QUNI	1.3090	0.1877	<<0.001***	(0.9311, 1.6691)
QUFA	2.3780	0.1690	<<0.001***	(2.0418, 2.7057)
LIST	1.1805	0.1621	<<0.001***	(0.8588, 1.4954)
ULAL	0.7450	0.2968	0.0121*	(0.1155, 1.2892)
2012	-0.1430	0.2113	0.4986	(-0.5659, 0.2652)
2013	0.4109	0.1664	0.0135*	(0.0874, 0.7409)
2014	0.4837	0.1699	0.0044**	(0.1526, 0.8199)
2015	0.5492	0.1658	0.0009***	(0.2270, 0.8782)

Notes: Covariates included species and measurement year. The interaction between species and measurement year did not add significantly to the model ($p < 0.05$, likelihood ratio test). SE refers to the standard error and CI refers to the 95% confidence interval for each estimate. Deviance and Akaike Information Criterion (AIC) metrics for this model were 2237.7 (on 5192 degrees of freedom) and 2672.4, respectively. Species codes are as follows: *PITA = Pinus taeda, PIEC = Pinus echinata, QUST = Quercus stellata, QUNI = Quercus nigra, QUFA = Quercus falcata, LIST = Liquidambar styraciflua, ULAL = Ulmus alata*.; *$p < 0.05$, **$p < 0.01$, ***$p < 0.001$

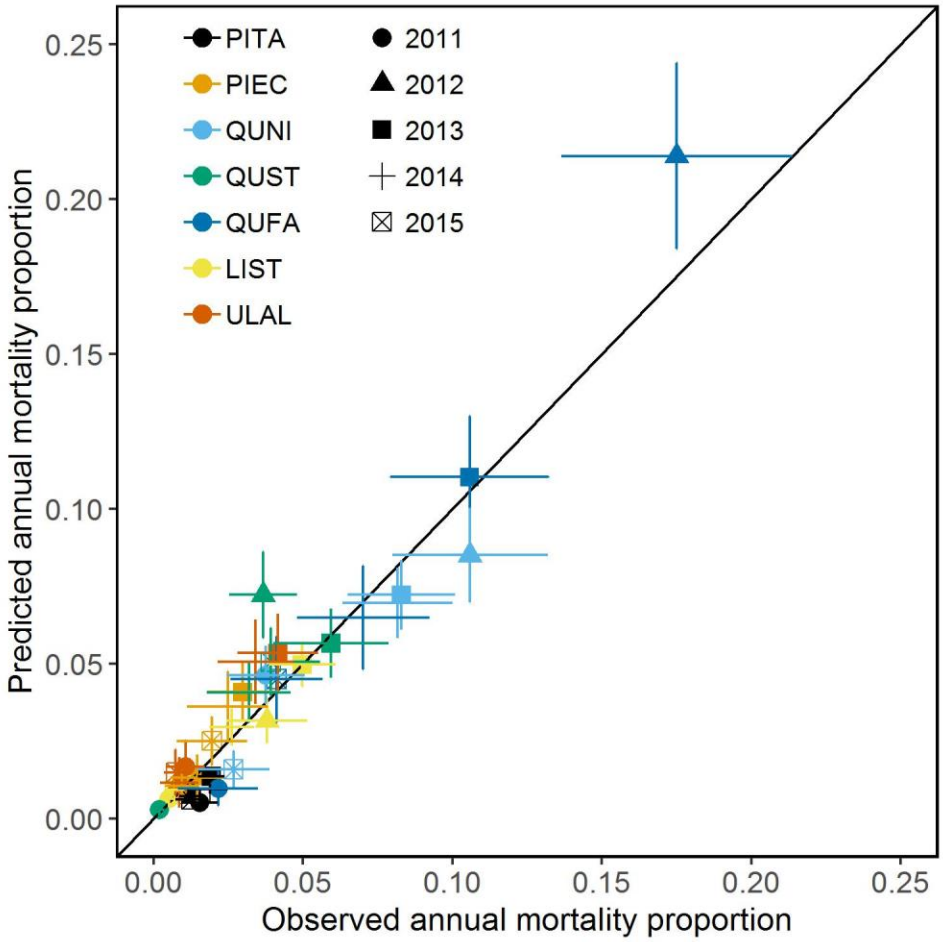

Figure A.1. Predicted vs. observed mean annual probability of weather mortality in a plot for each species and measurement year across east Texas derived from logistic regression results. Vertical and horizontal bars at each point denote standard errors for each estimate. The solid black, diagonal line represents a 1:1 line. Species codes are as follows: *PITA = Pinus taeda*, *PIEC = Pinus echinata*, *QUNI = Quercus nigra*, *QUST = Quercus stellata*, *QUFA = Quercus falcata*, *LIST = Liquidambar styraciflua*, *ULAL = Ulmus alata*. Reprinted with permission from Klockow *et al.*, (2018).

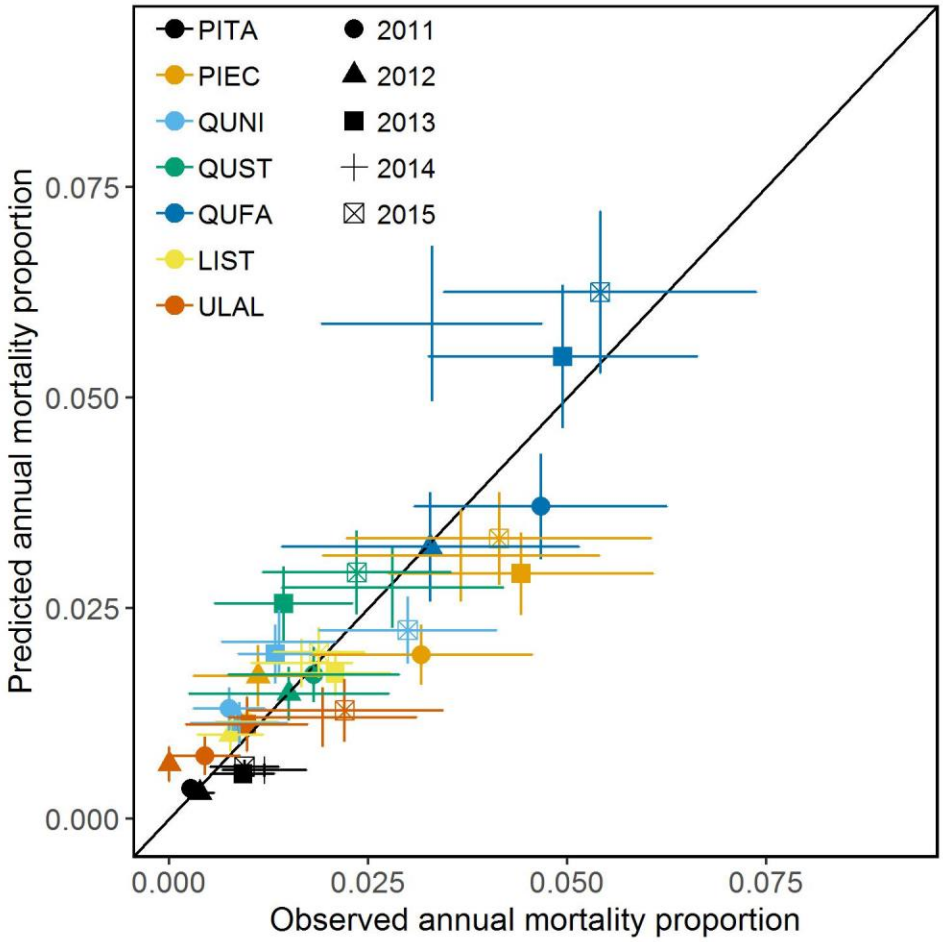

Figure A.2. Predicted vs. observed mean annual probability of pest mortality in a plot for each species and measurement year across east Texas derived from logistic regression results. Vertical and horizontal bars at each point denote standard errors for each estimate. The solid black, diagonal line represents a 1:1 line. Species codes are as follows: *PITA = Pinus taeda*, *PIEC = Pinus echinata*, *QUNI = Quercus nigra*, *QUST = Quercus stellata*, *QUFA = Quercus falcata*, *LIST = Liquidambar styraciflua*, *ULAL = Ulmus alata*. Reprinted with permission from Klockow *et al.*, (2018).

APPENDIX B

SUPPLEMENTARY TABLES AND FIGURES FOR CHAPTER III

Table B.1. Model results pertaining to pine group mortality rates for each measurement period presented as log odds of mortality and converted to probability of mortality. Plot RE SD is the estimated standard deviation due to the random effect of plots. Different letters next to estimates indicate significant differences (i.e., 95% credible intervals do not overlap). The R^2 for the mixed predictive assessment was 0.09. Prediction accuracy of live and dead trees was 0.999 and 0.132 for observed vs. predicted responses and 0.916 and 0.097 for replicated vs. predicted responses, respectively.

Pine Group	Period	Mortality (Log Odds)	Mortality (Probability)
Planted Loblolly	Pre	-5.231[a] (-5.521, -4.954)	0.00532[a] (0.00399, 0.00701)
	Drought	-5.138[a] (-5.361, -4.926)	0.00584[a] (0.00468, 0.00720)
Naturally-regenerated Loblolly	Pre	-4.487[b] (-4.679, -4.299)	0.01113[b] (0.00920, 0.01340)
	Drought	-4.250[bc] (-4.413, -4.101)	0.01406[bc] (0.01197, 0.01628)
Shortleaf	Pre	-4.138[bc] (-4.448, -3.847)	0.01570[bc] (0.01156, 0.02089)
	Drought	-3.953[c] (-4.196, -3.708)	0.01884[c] (0.01483, 0.02394)
Plot RE SD	-	-1.132 (-1.227, -1.042)	0.244 (0.227, 0.261)

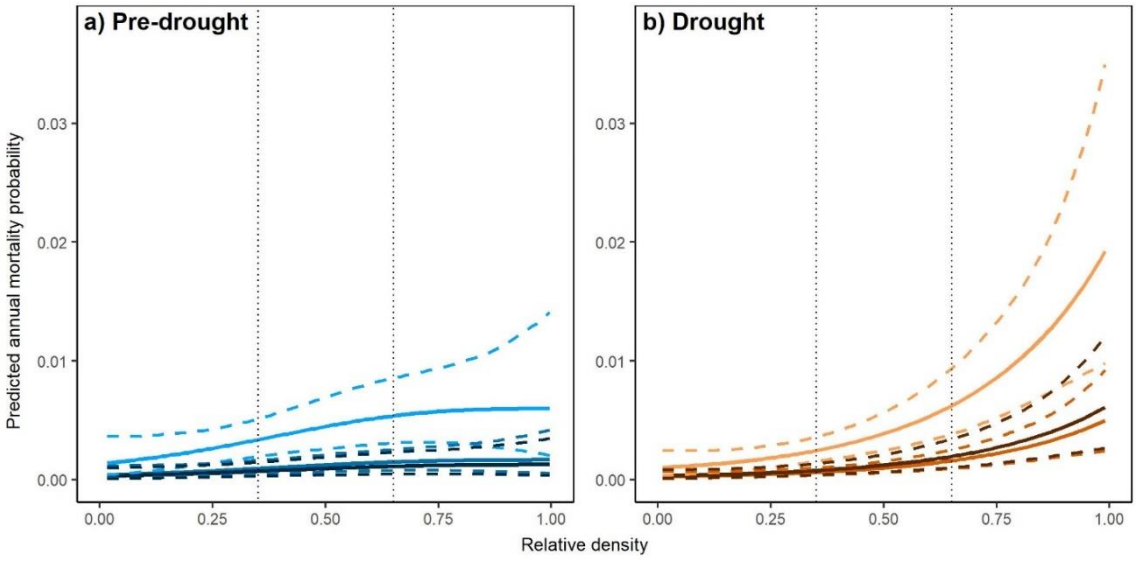

Figure B.1. Predicted annual mortality probability curves (solid lines) for planted loblolly and relative density (RD) with 95% credible intervals (dashed lines). Diameter at breast height (DBH) is held constant at merchantable size classes (15 cm = light blue, light orange; 25 cm = medium blue, medium orange; and 35 cm = dark blue, dark orange) while species dominance is held constant at its median values (~90%, see Table III.1). Dotted lines highlight lower (35%) and upper (65%) limits of fully-stocked conditions.

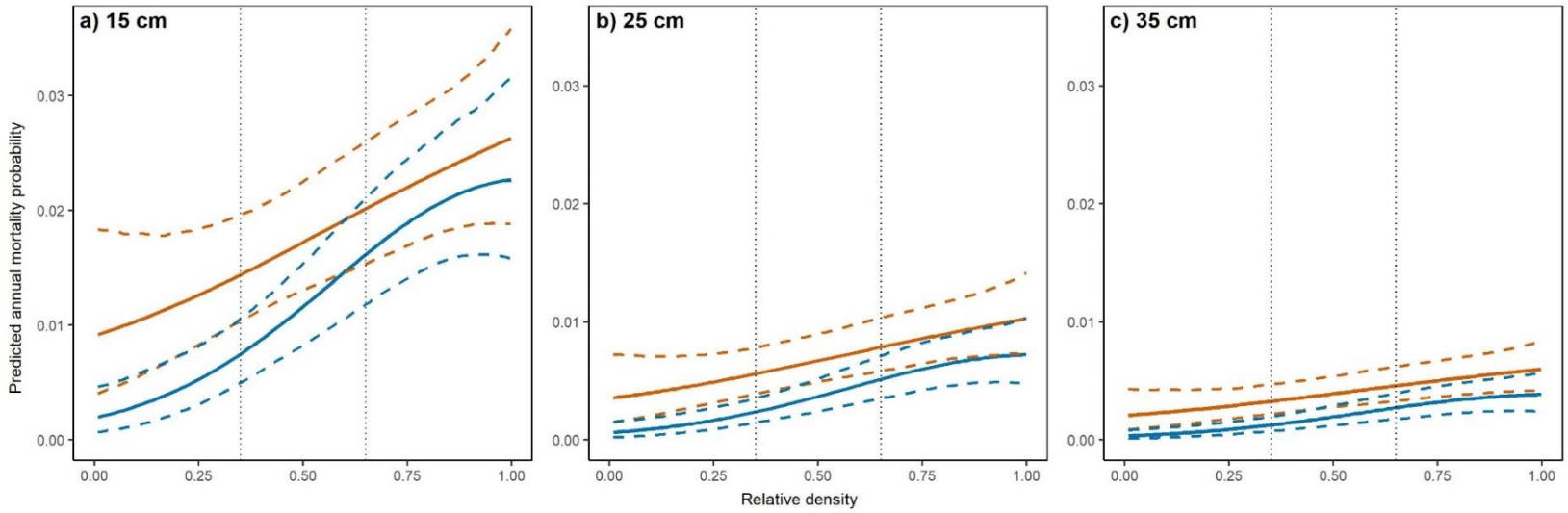

Figure B.2. Predicted annual mortality probability curves (solid lines) for naturally-regenerated loblolly and relative density (RD) with 95% credible intervals (dashed lines) (blue = pre-drought, orange = drought). Diameter at breast height (DBH) is held constant at merchantable size classes (15, 25, and 35 cm) while species dominance is held constant at its median values (~60%, see Table III.1). Dotted lines highlight lower (35%) and upper (65%) limits of fully-stocked conditions.

APPENDIX C

SUPPLEMENTARY TABLES AND FIGURES FOR CHAPTER IV

Table C.1. Summary of parameter estimates from chosen models based on covariates in original units (i.e., non-standardized).

Parameter	Tree-Fall		Snag-Fall	
	Hardwoods	Softwoods	Hardwoods	Softwoods
Intercept	0.645	1.667	na	na
DBH	-0.025	-0.053	-0.073	-0.102
Height	ns	ns	ns	0.059
Plot Density	ns	-0.001	ns	ns
Decay Class 1	na	na	2.788	4.125
Decay Class 2	na	na	3.132	4.143
Decay Class 3	na	na	3.687	4.597
Decay Class 4	na	na	3.890	5.338
Decay Class 5	na	na	5.196	5.374

*na = not applicable to specific model
*ns = variable tested but no significant effect added to model via likelihood ratio tests ($p > 0.05$)

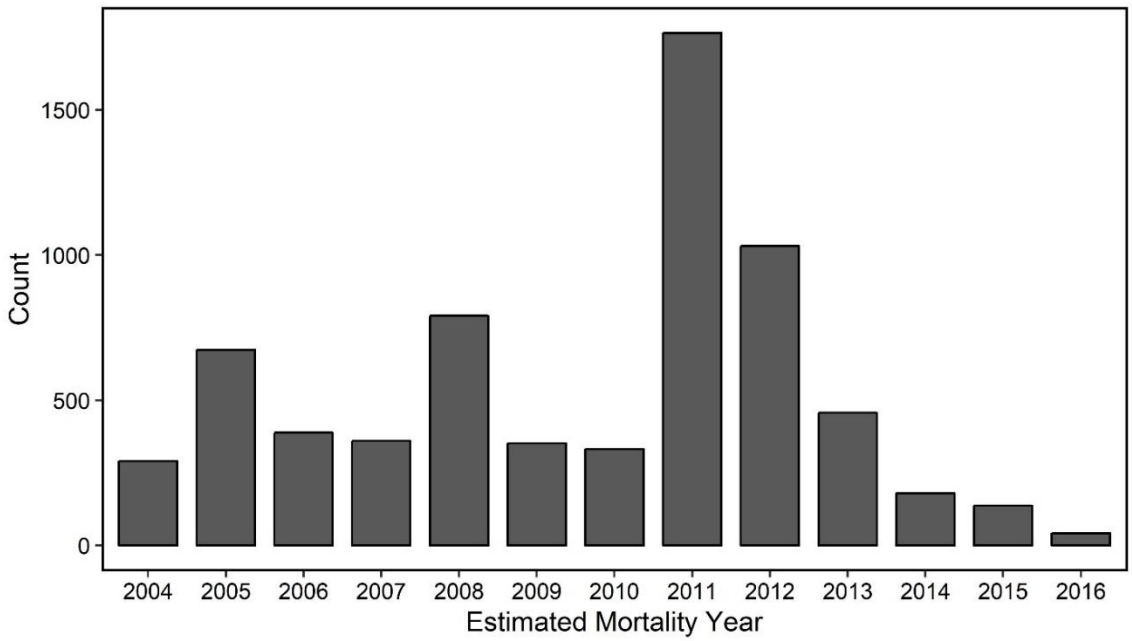

Figure C.1. Histogram of dead stems in the tree-fall dataset with field-crew-estimated year of mortality.

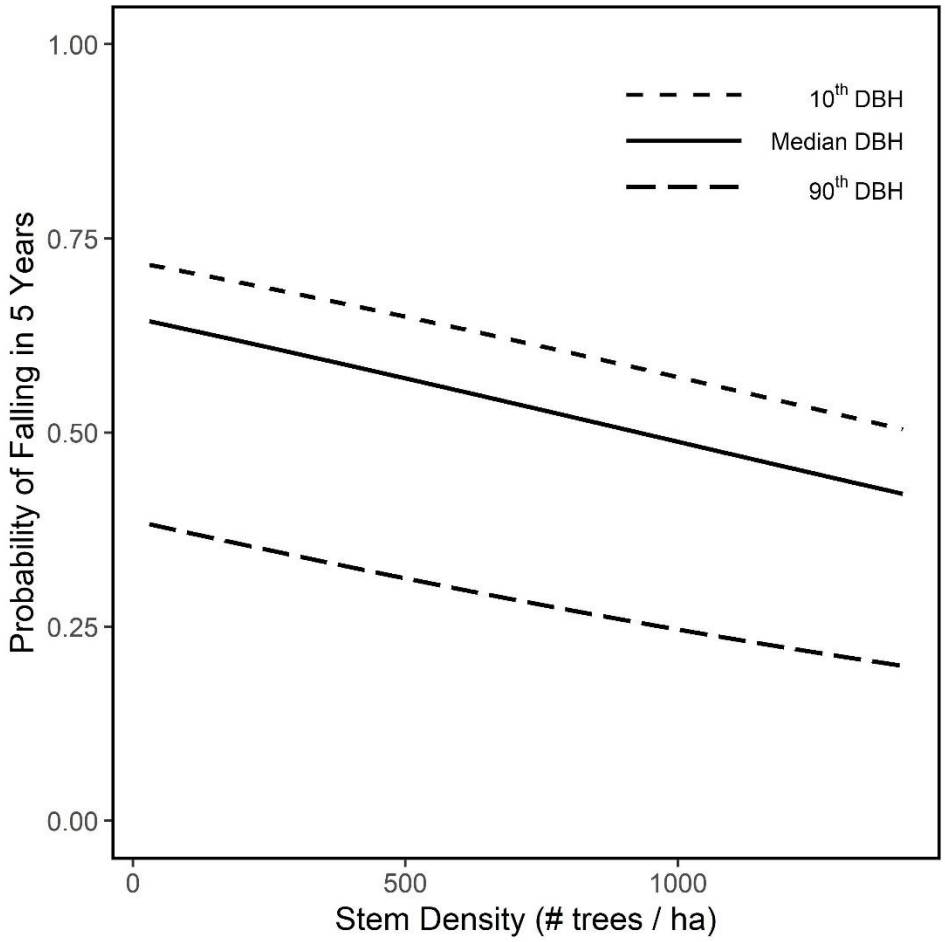

Figure C.2. Predicted probability of tree-fall in five years vs. plot live tree density for softwoods by decay class. Probabilities were calculated with diameter-at-breast-height (DBH) held constant at the median value (solid line), 10th percentile of DBH (short dashed line), and 90th percentile of DBH (long dashed line).

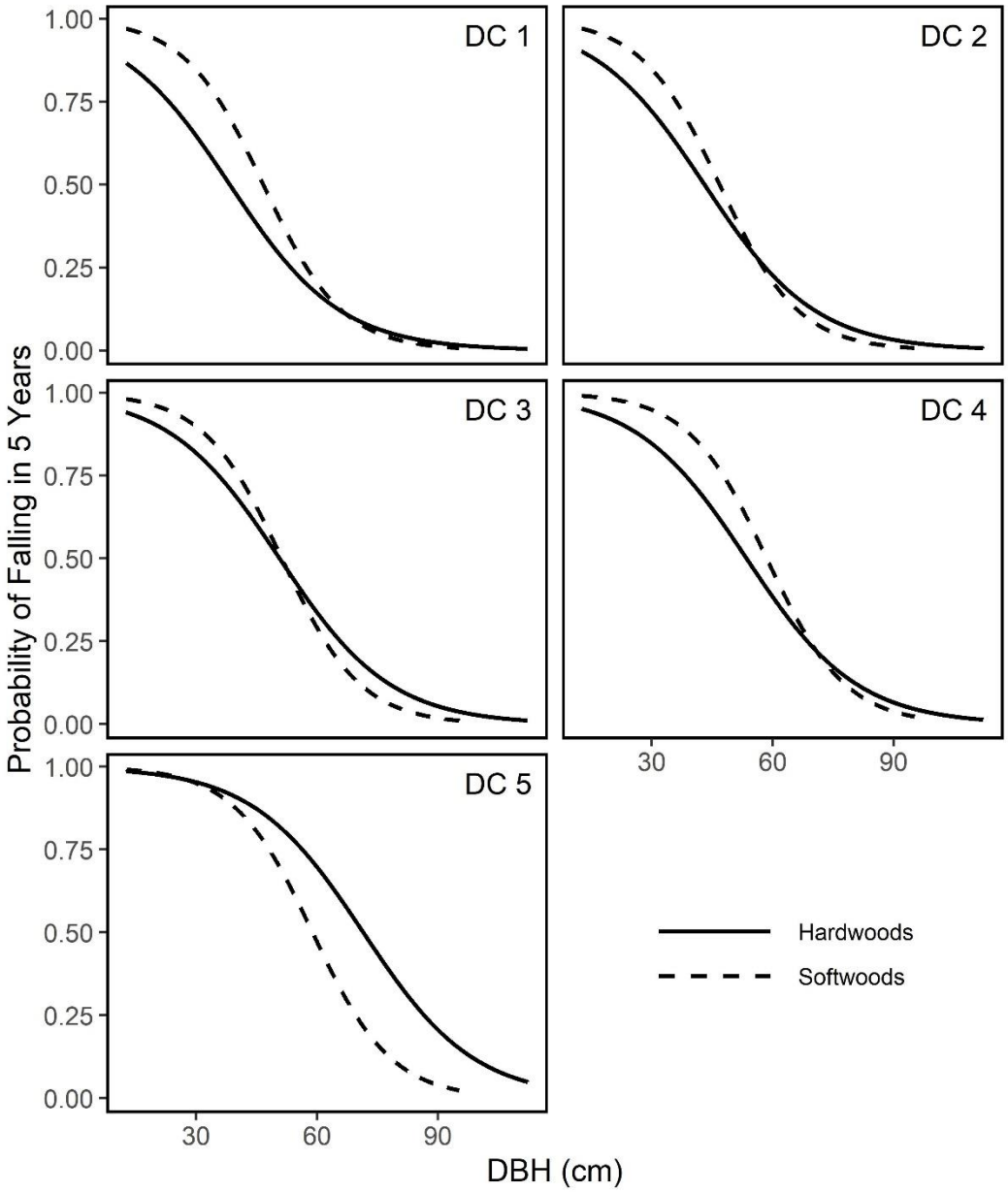

Figure C.3. Predicted probability of snag-fall in five years vs. snag size for hardwoods (solid line) and softwoods (dashed line) by decay class (DC). Predicted probabilities for softwood were calculated with tree height held constant at the median value.

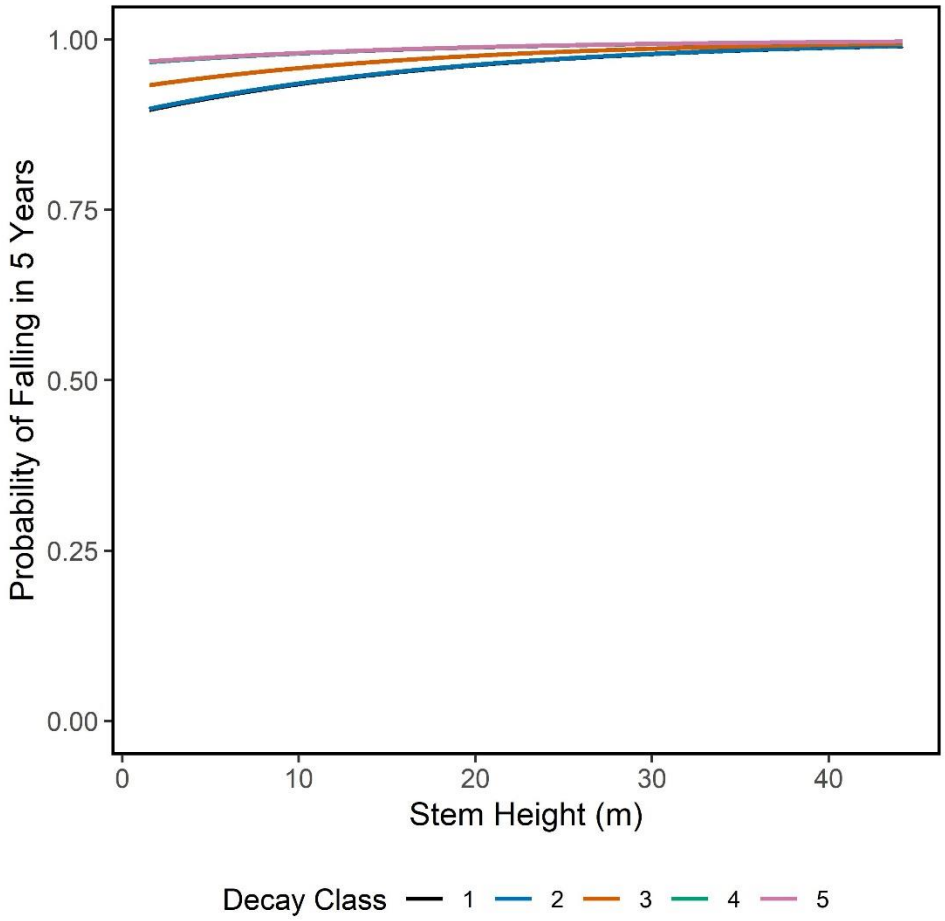

Figure C.4. Predicted probability of snag-fall in five years vs. stem height for softwoods by decay class. Probabilities were calculated with diameter-at-breast-height (DBH) held constant at the median value.

APPENDIX D

SUPPLEMENTARY TABLES AND FIGURES FOR CHAPTER V

Following scanning of SDT for volume estimation, the same SDT which were scanned were subsequently felled by Texas A&M Forest Service personnel such that wood samples could be collected for future analyses of wood density and biomass estimation. Only 41 of the 49 scanned trees were deemed safe to fell and were subsequently sampled for wood discs. SDT were felled just above breast height. Between 1-3 wood discs were collected for each SDT depending on the length between breast height and a ~10 cm top. All stems had a wood disc cut at ~1.5 m height (just above the fell cut point; BASE). A second, top wood disc was cut at ~10 cm diameter for stems which were still in tact and tapered to this diameter (TOP). If the distance between the base disc and top disc was > 10 m in length, a third wood disc was cut from the mid-point between the base and top discs (MID). The position of the top and mid-point discs were recorded and corrected to height values by adding 1.5 m (height of stem below base wood disc) and are presented as 'Bole Sample Height (m)' in table D.2.

After felling, branches were harvested from those SDT which still retained branches. Branches were collected from SDT in decay classes 1-3 and split according to three different size classes of fine woody debris (FWD) as defined in FIA protocols (i.e., <7.62 to ≥2.54 cm (LARGE), <2.54 to ≥0.63 cm (MEDIUM), and <0.63 cm (SMALL) diameters). Branches were sampled along the stem where they were still present and sufficient to fill up to one large paper grocery bag for each size class which was still present along the stem.

All wood samples were returned to the laboratory after collection in the field. Wood disc sample dimensions were measured immediately prior to placing in the drying oven. Specifically, diameters and thicknesses were measured at four approximately equidistant locations along the circumference of each end of the discs. The four diameter measurements at each end and the four thickness measurements around the circumference were averaged to determine mean values for each of the two end diameters and overall thickness of each disc. From these mean values, volume of each disc was calculated using the formula for a truncated cone and is presented as 'Bole Sample Volume (cm^3)' in table D.2. After measurements were collected for each wood disc, the samples were placed in a drying oven at 65°C and weighed periodically until a constant mass was reached. The constant oven-dried mass was then recorded and is presented as 'Bole Sample Weight (g)' in table D.2. Wood density of wood disc samples was calculated by dividing Bole Sample Weight (g) by Bole Sample Volume (cm^3) and is presented as 'Bole Sample Density ($g\ cm^{-3}$)' in table D.2.

Branch samples were placed in drying ovens upon arrival in the laboratory and dried similarly to wood disc samples. Once a constant mass was reached, this value was recorded and is presented as 'Branch Sample Weight (g)' in table D.3. Branch volumes were determined using volumetric displacement in water following methods outlined in (Fasth *et al.*, 2010). Very briefly, each oven-dried sample was soaked in water for 15 minutes prior to volume displacement measurements. Soaked samples were placed in an empty plastic bucket of known volume (i.e., either 2 or 5 gallons) and sealed with a lid. A similar bucket of equal volume was filled with water to the top and subsequently

siphoned into the bucket containing the branch samples until it was filled to the same level. The remaining water in the non-branch sample bucket was weighed and converted to volume using the specific gravity of room temperature and atmospheric pressure water. The resulting volume was presumed to be the volume of the branch sample. This procedure was repeated three times in immediate succession for each branch sample. For six branch samples (5 smallest size class and 1 medium size class of FWD), only a small amount of sample could be collected resulting in just a few grams of branches (i.e., <40 g). For these six samples, volume was determined by soaking each sample for 15 minutes and subsequently placing the soaked sample into a graduated cylinder with known volume of water and immersing the branch samples into the cylinder. The resulting difference in water volume measurement (after correcting for a lid/bung which allowed for complete immersion of the sample) produced the volume of the branch sample. This procedure was conducted once for each of the six branch samples. For branch samples measured three times, the three branch volume measurements for each sample were averaged to determine a mean volume. All branch sample volumes are presented as 'Branch Sample Mean Volume (cm^3)' in table D.3. Wood density of each branch sample was subsequently calculated by dividing Branch Sample Weight (g) by Branch Sample Mean Volume (cm^3) and is presented as 'Branch Sample Density ($g\ cm^{-3}$)' in table D.3.

Table D.1. Proportion-remaining volume (m^3/m^3) calculated from TLS-derived volumes using 5 mm non-resampled voxels and reference live tree volumes from Gonzalez-Benecke et al. (2014) (i.e., GB) and Jenkins et al. (2003) (i.e, Jenkins). Theoretical values from Domke et al. (2011) (i.e., Domke) are listed for TB material.

	TAS		SB		TB		
Decay Class	GB	Jenkins	GB	Jenkins	GB	Jenkins	Domke
1	1.61 (0.25)	1.54 (0.19)	1.55 (0.28)	1.58 (0.24)	3.15 (0.38)	1.29 (0.27)	1.00
2	1.23 (0.10)	1.22 (0.08)	1.29 (0.14)	1.36 (0.13)	1.39 (0.36)	0.55 (0.23)	0.50
3	1.12 (0.12)	1.14 (0.08)	1.21 (0.13)	1.30 (0.10)	0.92 (0.35)	0.36 (0.18)	0.20
4	0.80 (0.09)	0.81 (0.08)	0.91 (0.10)	0.97 (0.0999)	0.32 (0.24)	0.14 (0.12)	0.10
5	0.32 (0.05)	0.29 (0.04)	0.38 (0.06)	0.36 (0.05)	0.00	0.00	0.00

Table D.2. Bole sample volumes, weights, and calculated wood densities.

Tree ID	Decay Class	Bole Location	DBH (cm)	Total Tree Height (m)	Bole Sample Height (m)	Bole Sample Weight (g)	Bole Sample Volume (cm^3)	Bole Sample Density ($g\ cm^{-3}$)
1095	1	BASE	12.5	16.0	1.5	247.4	528.5	0.4681
1167	1	BASE	15.2	17.6	1.5	569.2	1307.1	0.4355
1195	1	BASE	15.7	17.4	1.5	502.9	1066.8	0.4714
1074	1	BASE	16.6	19.6	1.5	486.6	938.2	0.5186
1207	1	BASE	18.5	17.9	1.5	453.5	1195.1	0.3795
1062	1	BASE	24.8	22.3	1.5	1210.0	2581.3	0.4688
1216	1	BASE	34.2	24.7	1.5	3120.0	6672.6	0.4676
1127	1	BASE	41.2	24.9	1.5	4700.0	11642.1	0.4037
1123	1	BASE	60.1	26.4	1.5	9080.0	19158.8	0.4739
1095	1	MID	12.5	16.0	5.0	468.9	1266.8	0.3701
1167	1	MID	15.2	17.6	8.0	276.7	698.4	0.3962
1195	1	MID	15.7	17.4	9.0	277.8	598.0	0.4645
1074	1	MID	16.6	19.6	9.0	228.8	463.0	0.4942
1207	1	MID	18.5	17.9	5.5	416.3	1232.5	0.3378
1062	1	MID	24.8	22.3	9.0	669.0	1556.2	0.4299
1216	1	MID	34.2	24.7	12.0	1740.0	4198.8	0.4144
1127	1	MID	41.2	24.9	11.5	2220.0	6208.9	0.3575
1123	1	MID	60.1	26.4	12.5	4280.0	10286.9	0.4161
1095	1	TOP	12.5	16.0	8.5	362.6	719.5	0.5039
1167	1	TOP	15.2	17.6	13.0	197.2	469.6	0.4199
1195	1	TOP	15.7	17.4	13.0	211.5	424.8	0.4979
1074	1	TOP	16.6	19.6	15.5	720.1	1653.3	0.4356
1207	1	TOP	18.5	17.9	11.5	369.2	934.9	0.3949
1062	1	TOP	24.8	22.3	18.0	186.3	536.1	0.3475
1216	1	TOP	34.2	24.7	23.0	403.2	1128.5	0.3573
1127	1	TOP	41.2	24.9	22.5	540.8	1480.7	0.3652
1123	1	TOP	60.1	26.4	27.2	295.1	802.6	0.3677
1211	2	BASE	12.7	11.0	1.5	526.4	1063.8	0.4948
1187	2	BASE	17.7	17.5	1.5	880.0	2049.9	0.4293
1199	2	BASE	18.1	15.6	1.5	611.2	1781.0	0.3432
1175	2	BASE	20.5	16.5	1.5	1110.0	2451.2	0.4528
1131	2	BASE	20.6	13.1	1.5	728.1	2290.0	0.3179
1191	2	BASE	25.4	17.1	1.5	990.0	2544.4	0.3891
1078	2	BASE	28.4	18.2	1.5	2330.0	7465.8	0.3121
1018	2	BASE	35.9	19.1	1.5	1670.0	4783.4	0.3491
1054	2	BASE	47.2	23.3	1.5	5500.0	14168.5	0.3882
1187	2	MID	17.7	17.5	10.0	368.5	991.3	0.3717
1199	2	MID	18.1	15.6	8.0	360.2	1141.0	0.3157
1175	2	MID	20.5	16.5	9.0	667.9	1600.0	0.4174
1131	2	MID	20.6	13.1	6.5	508.2	1867.4	0.2721
1191	2	MID	25.4	17.1	7.5	470.0	1563.7	0.3006
1078	2	MID	28.4	18.2	8.0	693.8	2745.6	0.2527
1018	2	MID	35.9	19.1	7.0	950.0	3960.7	0.2399
1054	2	MID	47.2	23.3	12.0	3040.0	8932.6	0.3403
1211	2	TOP	12.7	11.0	7.0	149.9	476.7	0.3145
1187	2	TOP	17.7	17.5	16.0	181.5	787.9	0.2304
1199	2	TOP	18.1	15.6	14.0	219.6	506.0	0.4340
1175	2	TOP	20.5	16.5	17.0	110.5	497.5	0.2221
1131	2	TOP	20.6	13.1	13.0	245.3	933.0	0.2629

Table D.2. (continued)

Tree ID	Decay Class	Bole Location	DBH (cm)	Total Tree Height (m)	Bole Sample Height (m)	Bole Sample Weight (g)	Bole Sample Volume (cm^3)	Bole Sample Density ($g\ cm^{-3}$)
1191	2	TOP	25.4	17.1	14.0	183.8	748.7	0.2455
1078	2	TOP	28.4	18.2	17.5	190.0	774.4	0.2454
1018	2	TOP	35.9	19.1	14.0	249.7	1110.8	0.2248
1054	2	TOP	47.2	23.3	21.0	830.0	3765.5	0.2204
1163	3	BASE	16.6	13.7	1.5	830.0	1503.5	0.5520
1203	3	BASE	17.3	16.0	1.5	700.2	1553.7	0.4507
1135	3	BASE	19.1	13.2	1.5	770.0	1607.4	0.4790
1179	3	BASE	19.8	15.8	1.5	820.0	1925.9	0.4258
1038	3	BASE	25.6	16.4	1.5	1120.0	3073.0	0.3645
1058	3	BASE	45.1	14.9	1.5	5740.0	13172.7	0.4357
1163	3	MID	16.6	13.7	5.0	420.9	1329.8	0.3165
1203	3	MID	17.3	16.0	10.0	312.5	1029.3	0.3036
1135	3	MID	19.1	13.2	7.0	408.3	1318.6	0.3097
1038	3	MID	25.6	16.4	8.0	734.7	2074.4	0.3542
1058	3	MID	45.1	14.9	8.0	3740.0	10130.2	0.3692
1163	3	TOP	16.6	13.7	11.0	141.3	396.9	0.3560
1203	3	TOP	17.3	16.0	18.0	111.8	593.3	0.1884
1135	3	TOP	19.1	13.2	14.0	150.8	604.9	0.2493
1179	3	TOP	19.8	15.8	4.0	497.5	1647.8	0.3019
1038	3	TOP	25.6	16.4	15.5	187.3	676.6	0.2768
1058	3	TOP	45.1	14.9	11.0	4300.0	13784.3	0.3119
1147	4	BASE	14.8	3.7	1.5	860.0	2596.1	0.3313
1171	4	BASE	15.5	3.3	1.5	711.5	1914.2	0.3717
1087	4	BASE	16.1	11.1	1.5	261.4	917.4	0.2849
1091	4	BASE	16.7	12.2	1.5	356.9	1151.3	0.3100
1151	4	BASE	22.1	10.5	1.5	940.0	2333.6	0.4028
1183	4	BASE	22.1	4.2	1.5	1110.0	2232.4	0.4972
1103	4	BASE	25.8	13.4	1.5	890.0	3349.6	0.2657
1155	4	BASE	26.3	9.2	1.5	1790.0	4032.6	0.4439
1022	4	BASE	26.8	8.2	1.5	1110.0	2863.5	0.3876
1046	4	BASE	44.7	14.6	1.5	2680.0	7419.4	0.3612
1087	4	MID	16.1	11.1	6.0	274.0	874.2	0.3134
1091	4	MID	16.7	12.2	6.0	596.5	2013.2	0.2963
1151	4	MID	22.1	10.5	5.5	940.0	3155.7	0.2979
1183	4	MID	22.1	4.2	9.0	644.9	1445.7	0.4461
1103	4	MID	25.8	13.4	7.1	780.5	3601.2	0.2167
1046	4	MID	44.7	14.6	7.5	2600.0	6381.6	0.4074
1171	4	TOP	15.5	3.3	3.3	221.8	1212.7	0.1829
1087	4	TOP	16.1	11.1	12.0	229.1	832.0	0.2754
1091	4	TOP	16.7	12.2	12.0	180.0	1139.0	0.1580
1151	4	TOP	22.1	10.5	11.0	391.0	2264.8	0.1726
1183	4	TOP	22.1	4.2	15.0	138.9	658.5	0.2109
1103	4	TOP	25.8	13.4	14.6	436.8	2239.7	0.1950
1022	4	TOP	26.8	8.2	10.0	486.2	2395.2	0.2030
1046	4	TOP	44.7	14.6	14.5	1470.0	5673.6	0.2591
1083	5	BASE	11.9	2.1	1.5	586.8	1816.9	0.3230
1139	5	BASE	12.3	3.1	1.5	565.7	1788.9	0.3162
1143	5	BASE	16.5	2.3	1.5	850.0	3006.2	0.2827
1099	5	BASE	16.7	1.8	1.5	306.0	997.5	0.3068

Table D.2 (continued)

Tree ID	Decay Class	Bole Location	DBH (cm)	Total Tree Height (m)	Bole Sample Height (m)	Bole Sample Weight (g)	Bole Sample Volume (cm^3)	Bole Sample Density ($g\ cm^{-3}$)
1159	5	BASE	21.8	3.0	1.5	1490.0	3803.7	0.3917
1107	5	BASE	23.7	2.3	1.5	2380.0	6148.8	0.3871
1034	5	BASE	28.6	1.5	1.5	723.2	3649.0	0.1982

Table D.3. Branch sample volumes, weights, and calculated wood densities.

Tree ID	Decay Class	Branch Size Class	DBH (cm)	Total Tree Height (m)	Branch Sample Weight (g)	Branch Sample Mean Volume (cm^3)	Branch Sample Density (g cm^{-3})
1095	1	LARGE	12.5	16.0	840.0	1960.0	0.4286
1167	1	LARGE	15.2	17.6	2220.0	5160.0	0.4302
1195	1	LARGE	15.7	17.4	1451.0	3203.3	0.4530
1074	1	LARGE	16.6	19.6	2610.0	6396.6	0.4080
1207	1	LARGE	18.5	17.9	1720.0	4780.0	0.3598
1062	1	LARGE	24.8	22.3	1350.0	3400.0	0.3971
1216	1	LARGE	34.2	24.7	2160.0	5676.6	0.3805
1127	1	LARGE	41.2	24.9	2360.0	6233.3	0.3786
1123	1	LARGE	60.1	26.4	2250.0	5503.3	0.4088
1095	1	MEDIUM	12.5	16.0	840.0	1835.3	0.4577
1167	1	MEDIUM	15.2	17.6	678.4	1392.0	0.4873
1195	1	MEDIUM	15.7	17.4	1150.0	2308.6	0.4981
1074	1	MEDIUM	16.6	19.6	520.6	1255.4	0.4147
1207	1	MEDIUM	18.5	17.9	719.9	1865.4	0.3859
1062	1	MEDIUM	24.8	22.3	621.8	1485.3	0.4186
1216	1	MEDIUM	34.2	24.7	738.6	1868.6	0.3953
1127	1	MEDIUM	41.2	24.9	551.1	1492.0	0.3694
1123	1	MEDIUM	60.1	26.4	1040.0	2335.3	0.4453
1095	1	SMALL	12.5	16.0	160.5	355.2	0.4519
1167	1	SMALL	15.2	17.6	12.6	20.0	0.6300
1195	1	SMALL	15.7	17.4	186.2	391.9	0.4752
1074	1	SMALL	16.6	19.6	42.4	113.51	0.3735
1207	1	SMALL	18.5	17.9	34.4	70.0	0.4914
1062	1	SMALL	24.8	22.3	96.8	255.2	0.3793
1216	1	SMALL	34.2	24.7	245.8	581.9	0.4224
1127	1	SMALL	41.2	24.9	26.5	65.0	0.4077
1123	1	SMALL	60.1	26.4	138.0	325.2	0.4244
1211	2	LARGE	12.7	11.0	810.0	3676.6	0.2203
1187	2	LARGE	17.7	17.5	450.4	1540.0	0.2925
1199	2	LARGE	18.1	15.6	510.9	1750.0	0.2920
1175	2	LARGE	20.5	16.5	288.1	1000.0	0.2881
1131	2	LARGE	20.6	13.1	672.4	2443.3	0.2752
1191	2	LARGE	25.4	17.1	1023.0	4496.6	0.2275
1078	2	LARGE	28.4	18.2	810.0	3310.0	0.2447
1018	2	LARGE	35.9	19.1	1590.0	4763.3	0.3338
1054	2	LARGE	47.2	23.3	2470.0	7363.3	0.3354
1211	2	MEDIUM	12.7	11.0	621.2	2215.4	0.2804
1187	2	MEDIUM	17.7	17.5	434.6	1095.4	0.3968
1199	2	MEDIUM	18.1	15.6	88.7	348.6	0.2544
1175	2	MEDIUM	20.5	16.5	153.0	432.0	0.3541
1131	2	MEDIUM	20.6	13.1	41.7	158.6	0.2629
1191	2	MEDIUM	25.4	17.1	625.8	2095.2	0.2987
1078	2	MEDIUM	28.4	18.2	98.7	348.6	0.2831
1018	2	MEDIUM	35.9	19.1	328.0	912.0	0.3597
1078	2	SMALL	28.4	18.2	5.0	10.0	0.5000
1163	3	LARGE	16.6	13.7	536.0	2043.3	0.2623
1179	3	LARGE	19.8	15.8	344.2	1166.6	0.2950
1038	3	LARGE	25.6	16.4	495.1	1350.0	0.3667
1038	3	MEDIUM	25.6	16.4	26.9	95.0	0.2832

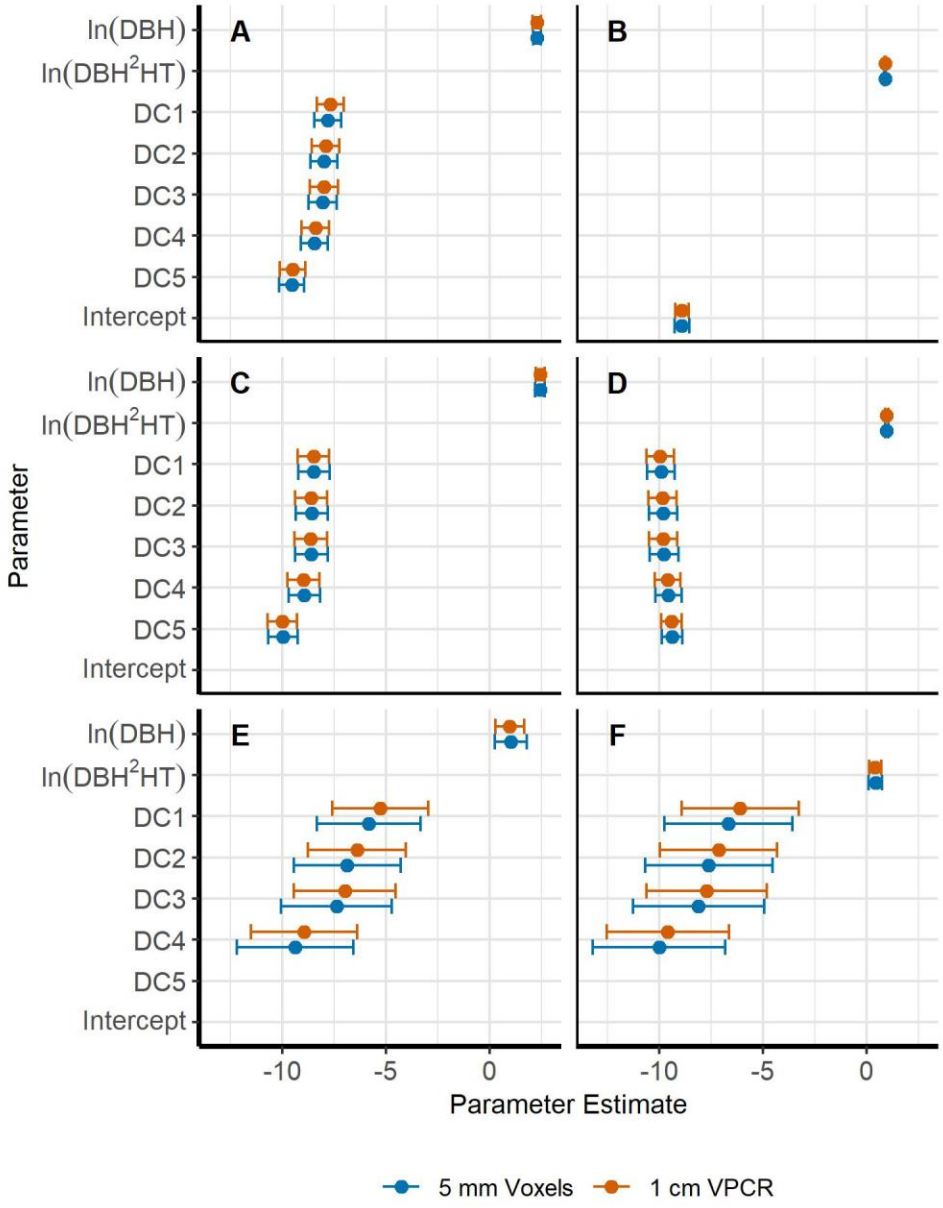

Figure D.1. Allometric model parameter estimates and 95% confidence intervals for log-linear relationships of A and B) TAS, C and D) SB, and E and F) TB total and component volumes (TAS = total above-stump, SB = stem plus bark, and TB = tops and branches). Labels along the y-axes correspond to the parameter estimate for the corresponding label where DC# refers to intercepts for decay classes 1-5 and 'Intercept' refers to the single, common intercept for TAS-DBH^2*HT models.